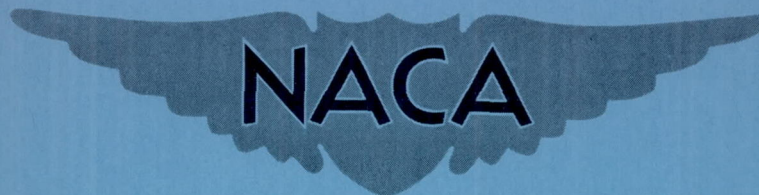RM E52L16

NACA

RESEARCH MEMORANDUM

COMPONENT AND OVER-ALL PERFORMANCE EVALUATION OF A

J47-GE-25 TURBOJET ENGINE OVER A RANGE OF

ENGINE-INLET REYNOLDS NUMBER INDICES

By Curtis L. Walker, Willis M. Braithwaite
and David B. Fenn

Lewis Flight Propulsion Laboratory
Cleveland, Ohio

NATIONAL ADVISORY COMMITTEE
FOR AERONAUTICS
WASHINGTON

September 29, 1953
Declassified August 19, 1960

2717

NATIONAL ADVISORY COMMITTEE FOR AERONAUTICS

RESEARCH MEMORANDUM

COMPONENT AND OVER-ALL PERFORMANCE EVALUATION OF A J47-GE-25 TURBOJET

ENGINE OVER A RANGE OF ENGINE-INLET REYNOLDS NUMBER INDICES

By Curtis L. Walker, Willis M. Braithwaite, and
David B. Fenn

SUMMARY

An investigation was conducted in an altitude test chamber to evaluate the performance of an axial-flow turbojet engine over a range of engine-inlet Reynolds number indices. The range of Reynolds number indices investigated provided data which were applicable over a range of flight conditions, for example, altitudes from 15,000 to 55,000 feet at a flight Mach number of 0.7.

Secondary effects of exhaust-nozzle flow coefficient, air-flow leakage, and inlet temperature which should be considered before analyzing the effect of variations in engine-inlet Reynolds number index are presented. In general, the effect of reducing Reynolds number index was to lower compressor efficiency and air flow with a resultant shift in the compressor map and rematching of compressor with turbine. There was only a slight effect of Reynolds number index variation on the turbine performance.

Several minor design modifications proposed by the manufacturer (designated as a block change) did not produce any measurable improvement in engine performance.

INTRODUCTION

Previous altitude investigations of turbojet engines made at the NACA Lewis laboratory have indicated that failure of the performance variables to generalize for all altitudes and flight Mach numbers, over the range of engine speeds where sonic flow exists in the exhaust nozzle, has been a result of either a Reynolds number effect or a variation in combustion efficiency (ref. 1). An investigation was therefore conducted in a Lewis laboratory altitude chamber to evaluate the component and over-all performance of the J47-GE-25 turbojet engine over a range of Reynolds number indices which corresponds to a wide range of altitude conditions. For example, at a flight Mach number of 0.7, the data are applicable over a range of altitudes from 15,000 to 55,000 feet. Fewer data are required by this method and departures from established generalizations may be investigated directly. The data of this investigation were presented in a preliminary data release (ref. 2). Subsequent refinements in calculation procedures have resulted in minor changes in the static sea-level thrust and in the scale thrust at high altitudes that are contained herein.

Also included in this investigation are the effects on performance of several minor design modifications to the compressor, the combustor, and the turbine shroud ring which were proposed by the engine manufacturer as a tentative block change in the production engine. The effect of inlet temperature is substantiated by additional data obtained on a J47-GE-17 engine which has a power section similar to that of the J47-GE-25.

Compressor, combustor, turbine, and over-all performance data are presented in tabular and graphical form over the range of Reynolds number indices investigated. The trends of over-all engine performance are discussed with relation to component performance variations. The effect of the block changes on performance is presented in graphical form.

APPARATUS

Engine

A schematic sketch of the J47-GE-25 turbojet engine as it was installed in the NACA Lewis 10-foot-diameter altitude test chamber is shown in figure 1. The test chamber is described in reference 3. This engine had a 12-stage axial-flow compressor, eight tubular combustion chambers, and a single-stage turbine. The maximum diameter (turbine flange) was 37 inches and the over-all length excluding tail pipe and exhaust nozzle was 144 inches. The approximate dry weight of the engine was 2653 pounds. At rated engine speed, 7950 rpm, and rated turbine-outlet temperature, 1250° F (1710° R), the manufacturer's guaranteed sea-level static thrust was 5970 pounds. At rated engine speed and sea-level static conditions, the compressor-inlet air flow was approximately 104.5 pounds per second, the compressor pressure ratio was approximately 5.3, and a conical exhaust nozzle with an area of 2.073 square feet produced a turbine-outlet temperature of 1280° F (1740° R) based on NACA instrumentation. This exhaust nozzle had an exit to inlet area ratio of 0.87 and a half-cone angle of $7\frac{1}{2}°$.

The fuel used in this investigation was MIL-F-5624A grade JP-4. The hydrogen-carbon ratio was 0.17 and the lower heat of combustion was 18,700 Btu per pound.

Instrumentation

Instrumentation was located at the stations shown in figure 1. There was no instrumentation at station 2, which was a calculation station. Details of the instrumentation at each station are illustrated in figure 2, except for station 3b. There was a wall-static probe installed in each of two combustors in the plane of the cross-over tubes at station 3b.

Thrust was measured by means of balanced-diaphragm pneumatic thrust cell connected to the thrust bed, as shown schematically in figure 1.

Engine Modifications

After calibration of the standard engine configuration was completed, modified engine parts were installed in the J47-GE-25 turbojet engine in the manner proposed by the manufacturer as a block change to the production engine. These modifications were incorporated in two additional configurations as shown in figure 3 and described in the following table:

Configuration	Engine modifications incorporated	Exhaust-nozzle area, sq ft
A (standard)	Standard engine as supplied by manufacturer with additional instrumentation installed	2.073
B	New twelfth-stage compressor seal New combustor liners, postless transition pieces Floating turbine shroud	2.106
C	New parts as installed for configuration B Shrouded fuel-spray nozzles	[a]2.124

[a]Nozzle area for configuration C was too small to obtain rated engine speed without exceeding rated temperature.

The new twelfth-stage compressor seal (fig. 3(a)) consisted of a slant-toothed labyrinth seal instead of the V-tooth design; the minimum clearance was maintained the same but the maximum clearance was reduced by increasing the minimum dimension of diameter "D" as shown in the figure. The combustor liner was modified to induct more air into the primary combustion zone by adding three rings of air-inlet holes near the dome on the liner. The center posts in the transition pieces were removed. The location of these posts is indicated in figure 1. The proposed method of installing the floating turbine shroud ring is shown in figure 3(c). In the installation as provided, the shim extended into the space between the shroud ring and the nozzle diaphragm. Furthermore, clearances marked a, b, and c (fig. 3(b)) were not great enough to provide a free-floating shroud as evidenced by gall marks on the shim and tail cone in this area. These clearances were proposed to prevent seizing of the shroud ring on the nozzle diaphragm. For configuration C, shrouded fuel nozzles (fig. 3(c)) were installed in addition to the configuration B modifications. The purpose of the shroud around the fuel nozzle was to induct air into the combustor at the origin of the spray pattern by ejector action. These shrouded fuel nozzles are standard installation equipment on the J47-GE-17 engine.

2717

PROCEDURE

Sizing Exhaust Nozzle and Determining Sea-Level Static Thrust

Prior to obtaining performance data, an attempt was made to size the exhaust nozzle to produce an exhaust-gas temperature of 1250° F (1710° R) at rated engine speed and static sea-level conditions. Since it is impossible to operate the altitude chamber at static conditions, the nozzle size was based on the extrapolation of data obtained at low altitudes and flight Mach numbers from 0.2 to 0.8. A review of the complete performance data indicated that the nozzle used in this investigation (area, 2.073 sq ft) would have actually produced an exhaust-gas temperature of about 1280° F (1740° R) based on NACA instrumentation at these conditions.

Thrust is dependent on exhaust-gas temperature and exhaust-gas temperature is a function of exhaust-nozzle area. In this investigation, the exhaust-gas temperature was measured by the engine manufacturer's four-probe and five-probe thermocouple harnesses as well as by the 25 NACA thermocouples. The readings of these different sets of instrumentation differ with the result that the sea-level static thrust would vary, depending on which temperature readings were used in sizing the exhaust nozzle. It was assumed that the NACA instrumentation (corrected for thermocouple recovery) indicated the true gas temperature, and jet thrust calculated from this temperature corresponded to scale jet thrust. Because the engine is normally rated by the manufacturer for an exhaust-gas temperature based on the thermocouple reading obtained from the four- or five-probe thermocouple harnesses, static sea-level thrust values have been included in the following table for a thermocouple reading of 1250° F (1710° R) obtained from the four- and five-probe systems with the corresponding gas temperatures included. The sea-level thrust of 6070 pounds at an exhaust-gas temperature of 1280° F (1740° R) for the exhaust nozzle used in this investigation was slightly above the manufacturer's guarantee (5970 lb) and provides a point of reference for the performance data presented herein.

Basis of performance rating	Engine speed, rpm	Engine manufacturer's exhaust-gas thermocouple reading, $T_{9,i}$, $^\circ R$		Exhaust-gas total temperature based on NACA instrumentation, T_9, $^\circ R$	Static sea-level thrust, lb
		Four-probe harness	Five-probe harness		
Exhaust-gas total temperature of 1740° R (obtained with exhaust nozzle used in this investigation)	7950	1684	1690	1740	6070
Exhaust-gas total temperature of 1710° R	7950	1653	1658	1710	5960
Engine manufacturer's five-probe thermocouple harness	7950	1704	1710	1760	6135
Engine manufacturer's four-probe thermocouple harness	7950	1710	1717	1766	6160

Obtaining Performance Data at Various Reynolds Number Indices

Engine inlet total pressure and temperature were varied to correspond to Reynolds number indices from 0.8 to 0.15. For a given set of inlet conditions, exhaust pressure was reduced to the minimum of the exhaust system with the engine operating at rated speed. The inlet temperature and pressure and the exhaust pressure were then maintained constant while data were taken over a range of engine speeds from rated speed to approximately the speed at which the exhaust nozzle became unchoked. A summary of the operating conditions covered in the investigation is given in the following table:

Reynolds number index	Inlet total temperature, $^\circ R$	Inlet total pressure, $\dfrac{lb}{sq\ ft}$	Ram pressure ratio
0.8	530	1740	1.70
.6	467	1108	2.14
.5	467	923	1.95
.4	467	739	1.35
.425	437	718	1.41
.4	410	620	1.70
.3	410	465	1.70
.3	410	465	1.34
.25	410	387	1.64
.2	410	315	1.48
.15	410	232	1.19

As shown in the table, three ram pressure ratios P_1/p_0 were used at a Reynolds number index of 0.4 and two at 0.3 to verify the generalization with variations in ram pressure ratio. At a Reynolds number index of about 0.4, three sets of inlet conditions were used to determine whether there were any effects of temperature and pressure other than those of Reynolds number index. (The variation of the performance parameters from 0.4 to 0.425 Reynolds number index is considered small enough that they may all three be considered a Reynolds number index of about 0.4.)

All symbols are defined in appendix A, and the methods of calculation are described in appendix B.

RESULTS AND DISCUSSION

The performance evaluation of an axial-flow turbojet engine over a range of Reynolds number indices provides data which are applicable over a range of flight conditions. However, the performance investigation of the J47-GE-25 turbojet engine has shown that several factors producing secondary performance variations should be recognized if effective use is to be made of the performance data in its application to flight conditions. These secondary effects are discussed and evaluated in the following paragraphs.

Secondary Effects

Effect of nozzle flow coefficient. - As engine ram pressure ratio, and consequently nozzle pressure ratio, was increased at a constant corrected engine speed, the exhaust-nozzle flow coefficient C_d

increased. The increase in nozzle flow coefficient with increasing pressure ratio is illustrated in figure 4(a) which, although obtained directly from reference 4, was assumed applicable to this nozzle, which has the same cone angle and area ratio. This flow coefficient was nearly constant above a nozzle pressure ratio of about 2.3, which is 25 percent higher than that required to produce sonic velocity in the exhaust nozzle. The effect of nozzle flow coefficient was typical of conical exhaust nozzles. The magnitude of this effect depends on the nozzle configuration.

During the process of sizing the nozzle, as described in PROCEDURE, the effect of varying ram pressure ratio at corrected engine speeds near rated was investigated with three different nozzle areas. The results of this investigation are presented in figure 4(b), which illustrates a decrease in corrected exhaust-gas temperature of about 40° R accompanying an increase in ram pressure ratio from 1.0 to 1.25 (which corresponds to flight Mach numbers from 0 to 0.575).

The corresponding variation in the ratio of net thrust at actual corrected exhaust-gas temperature to net thrust at constant corrected exhaust-gas temperature is shown in figure 4(c). A thrust loss of about 3 percent is incurred because of the increase in effective exhaust-nozzle flow area and accompanying decrease in corrected exhaust-gas total temperature.

Generalization of performance parameters presented in this investigation requires that there be no effect of ram pressure ratio on engine component performance. Since a nozzle pressure ratio greater than 25 percent above that required for choked flow results in a nearly constant flow coefficient, there is no effect of ram pressure ratio above a value 25 percent higher than that required to produce choked flow in the exhaust nozzle. The solid line and data points on figure 5 illustrate the relation of corrected engine speed and flight Mach number required for choked flow in the exhaust nozzle. The dashed line of figure 5 represents flight Mach numbers corresponding to ram pressure ratios 25 percent greater than those required to produce choked flow in the exhaust nozzle. However, it should be noted that if an exhaust nozzle having a smaller cone angle were used, the data would be applicable to lower flight Mach numbers. The performance data presented herein may be applied directly to flight conditions above this dashed curve. However, when the performance data are applied to lower ram pressure ratios at which the exhaust-nozzle flow coefficient varies, the trends shown in figure 4(a) should be used in conjunction with the pumping characteristics, which are presented in a following section entitled "Effect of Engine-Inlet Reynolds Number Index."

Effect of air flow leakage. - The engine as originally received had approximately 5 to 7 percent air flow leakage downstream of the inlet measuring station 1. This leakage occurred around sheet-metal parts

between station 1 and the compressor inlet, through open bolt holes at
the compressor inlet, and through the gaskets on the high pressure deicing-
air lines. The leakage was reduced to about 3.3 percent of station 1
air flow by using gaskets on the sheet-metal joints and sheet-metal screws
instead of spring-type fasteners, plugging the open bolt holes, and using
soft-aluminum gaskets on the deicing-air lines. For the performance
calculations all the leakage except compressor seal leakage was assumed
to occur ahead of the compressor, and compressor air flow was calculated
based on measurements of gas flow at the exhaust nozzle as explained in
appendix B. Both station 1 and compressor inlet (station 2) air flow
are presented in table I for the data of this investigation.

In aircraft installations, the magnitude of the leakage would be a
function of nacelle pressure as well as of whatever steps were taken to
seal the points of leakage. The result of leakage ahead of the com-
pressor is to increase ram drag and decrease net thrust. Therefore, in
calculating net thrust, the air flow at station 1 should be used in the
ram drag term.

Effect of inlet temperature. - Although a previous investigation of
a similar engine (ref. 3) indicated no effect on performance of different
inlet temperatures, a check was made in the present investigation at a
Reynolds number index of about 0.4 for three engine-inlet temperatures
from 7° to -50° F. These data (fig. 6) showed a definite, though minor,
increase in the corrected jet-thrust parameter, exhaust-gas total tempera-
ture, and ideal corrected fuel-air ratio with increase in inlet tempera-
ture. (The ideal fuel-air ratio is the fuel-air ratio that would be
required if combustion efficiency were 1.00.) The effect was not expli-
cable by the conventional correction factors for a Reynolds number effect.

Examination of other variables for these conditions definitely
established that the effect was not due to a change in pumping character-
istics, compressor efficiency, combustor-pressure loss, or exhaust-nozzle
flow coefficient. However, because of experimental scatter and possible
swirl effects on the turbine-outlet total-pressure probes, it was impos-
sible to establish whether there was a change in turbine efficiency or
tail-pipe pressure losses. A study of factors likely to cause a change
in turbine-outlet gas swirl indicated that a change in corrected turbine
work would be required. Further examination of the engine data revealed
that the corrected compressor leakage did not generalize with variations
in engine-inlet temperature (corrected leakage increased with temperature
increase) and a small increase in turbine work (fig. 7) and swirl
with increase in inlet temperature was therefore indicated. The increased
turbine-outlet gas swirl would produce a small increase in the tail-pipe
pressure loss. The increased pressure loss accompanied by no change in
pumping characteristics (as measured at the exhaust-nozzle inlet) results
in increased corrected exhaust-gas temperature and corrected jet-thrust
parameter. There was a slight increase in compressor efficiency with
increases in inlet temperature, which resulted in generalization of the
pumping characteristics.

A further effort to substantiate the inlet temperature effect was made by using a J47-GE-17 engine which has a power section similar to that of the J47-GE-25. Data were obtained with this engine at a Reynolds number index of 0.4 with inlet temperatures of 7° and -50° F, both with and without turbine-outlet straightening vanes.

The results of the data from this later investigation are presented in figures 8 and 9. Without straightening vanes, the corrected jet-thrust parameter (fig. 8(a)), the corrected exhaust-gas total temperature (fig. 8(b)), and the corrected ideal fuel-air ratio (fig. 8(c)) showed the same increase with increasing inlet temperature as these variables did for the J47-GE-25. However, with turbine-outlet straightening vanes installed (figs. 9(a), 9(b), and 9(c)), the trend was eliminated below a corrected engine speed of 7000 rpm and reduced at all higher engine speeds investigated.

The Reynolds number index method of investigation is still considered valid inasmuch as the effect of inlet temperature is believed to be peculiar to this engine and was of secondary importance. The effect of reducing inlet temperature from 7° to -50° F at a Reynolds number index of 0.4 was to decrease the corrected jet-thrust parameter about 2 percent, corrected exhaust-gas total temperatures about $2\frac{1}{2}$ percent, and corrected ideal fuel-air ratio about 5 percent. When the data are applied to flight conditions, these effects can be minimized by adjusting the data by use of the trend shown in figure 6.

Effect of Engine-Inlet Reynolds Number Index

With the reservations discussed in the previous paragraphs, the performance data obtained over a range of engine-inlet Reynolds number indices may be applied to a wide range of flight conditions. Figure 10 is presented in order to permit the determination of Reynolds number index as a function of altitude and flight Mach number. An example of the method of obtaining performance at a given flight condition is presented in appendix C.

Compressor performance. - Compressor performance characteristics are presented in figure 11 for the range of Reynolds number indices investigated. Compressor efficiency generalized for Reynolds number indices from 0.8 to 0.4 and decreased with further reduction in Reynolds number index, as shown in figure 11(a). The peak compressor efficiency occurred at a corrected engine speed of about 7000 rpm for all Reynolds number indices investigated and decreased from about 0.835 to about 0.815 as Reynolds number index was decreased from 0.4 to 0.2. Compressor efficiency decreased approximately 0.10 from the peak value as corrected engine speed was increased to 8500 rpm.

Corrected compressor air flow is shown as a function of corrected engine speed over the range of Reynolds number indices investigated in figure 11(b). At Reynolds number indices from 0.8 to 0.3, the corrected air flow generalized below a corrected engine speed of about 7500 rpm. At a corrected engine speed of 7950 rpm (sea-level rated), the corrected compressor air flow decreased from 104 to 99 pounds per second as Reynolds number index was decreased from 0.6 to 0.15. Compressor leakage at the engine midframe was measured by means of an orifice pipe and is presented in figure 11(c) as a function of compressor-outlet total pressure. This figure is necessary in determining the air flow through the combustor.

The variation of compressor pressure ratio with corrected engine speed is presented in figure 11(d), which shows that there was no effect of Reynolds number index on this relation. The failure of the compressor operating lines (compressor pressure ratio as a function of corrected air flow) to generalize with Reynolds number index variations (fig. 11 (e)) indicates that there was a shift in the compressor map as Reynolds number index was reduced.

Combustor performance. - Variation of the total-pressure-loss ratio across the combustor with corrected engine speed is shown in figure 12(a). Over the range of engine speeds investigated the total-pressure-loss ratio showed no apparent effect of Reynolds number index. Combustion efficiency (figs. 12(b) and 12(c)) was correlated with the parameter $\dfrac{\left(p_{3,b}\right)^2}{W_{a,3}}$ (fig. 12(b)), which is proportional to a combustion parameter derived in reference 5. According to this reference, correlation would be expected unless there were pronounced effects of fuel-air ratio or fuel spray pattern. At a value of the combustion parameter above 400,000, correlation was within ±0.015 and a constant combustion efficiency of about 0.99 was indicated. At lower values of the combustion parameter, combustion efficiency dropped rapidly and the data scatter was increased to ±0.02. From these data it is concluded that for the Reynolds number indices and the corrected engine speeds of this investigation, the effects of fuel-air ratio and fuel spray pattern were secondary.

A more convenient method of obtaining combustion efficiency for a given engine operating condition is presented in figure 12(c). An engine operating parameter $\delta \sqrt{\theta}(N/\sqrt{\theta})^3$ was obtained empirically, as in reference 6, from the engine operating characteristics. The correlation of combustion efficiency as a function of this engine operating parameter provides a more convenient method of obtaining combustion efficiency for given inlet conditions and a given corrected engine speed.

Turbine performance. - The trends in turbine performance (fig. 13) with variations in Reynolds number index were generally obscured by data scatter. The turbine total-pressure ratio (fig. 13(a)) was approximately 2.58 over the range of corrected engine speeds investigated. Turbine efficiency, illustrated in figure 13(b), increased from about 0.81 at 6400 rpm to about 0.825 at 7800 rpm and above. The corrected turbine gas flow (fig. 13(c)) increased from about 40 to 42 pounds per second as corrected engine speed was increased from 6250 to 8800 rpm. Close inspection of the data points on the latter two curves indicates the possible existence of a slight decrease in turbine efficiency and corrected turbine gas flow with decreasing Reynolds number index, although the magnitudes of the trends are not clearly discernible because of the data scatter.

Generalized engine performance. - The effect of Reynolds number index on generalized engine performance is shown in figure 14. The corrected exhaust-gas total temperature increased as Reynolds number index was decreased (figs. 14(a) and 14(b)) because of the shift in engine operating point caused primarily by the decrease in compressor efficiency. It was necessary to present these data on separate plots for the different inlet temperatures because of the temperature effect discussed previously. For the same reason, the data obtained at a Reynolds number index of 0.8, although included in table I, were omitted from the figures showing corrected exhaust-gas temperature and corrected ideal fuel-air ratio (figs. 14(a) and 14(c)). Corrected ideal fuel-air ratio (figs. 14(c) and 14(d)) increased as a result of the required additional power to overcome loss of compressor efficiency and corresponded to the increase in exhaust-gas temperature. This parameter isolates the fuel requirement from combustion efficiency and the decrease in air flow with decreased Reynolds number. The effect of Reynolds number index on the engine pumping characteristics is shown in figure 14(e). As Reynolds number index was reduced, pumping characteristic curves shifted in the direction of increased temperature ratio for a given pressure ratio. This result would be expected as a result of the decrease in compressor efficiency. The effect of Reynolds number index on the jet-thrust parameter is presented in figures 14(f) and 14(g). At a given engine speed there was an increase in temperature ratio, a slight increase in engine pressure ratio, and a decrease in engine corrected air flow as Reynolds number index was reduced. At Reynolds number indices from 0.8 to 0.4 there was no apparent effect on the jet-thrust parameter. However, as Reynolds number index was decreased from 0.4 to 0.15 (fig. 14(g)), there was an increase in the jet-thrust parameter due to the increase in temperature ratio and pressure ratio, which offset the decrease in corrected air flow.

It can be shown from the performance data that the combined effect of reducing the Reynolds number index from 0.6 to 0.15 and the inlet temperature from 7° to -50° F resulted in a 10 percent increase in corrected fuel flow and a 2 percent increase in jet-thrust parameter at a corrected engine speed of 7950 rpm.

Net thrust and specific fuel consumption. - The conventional per-
formance parameters such as net thrust and net-thrust specific fuel con-
sumption may be obtained for any flight condition from the data presented.
These calculations have been made for the sea-level static condition and
for altitudes of 16,700, 31,400, and 51,500 feet at a flight Mach number
of 0.8 and are presented in figure 15. An example of the technique used
in obtaining these values is presented in appendix C.

The net thrust (fig. 15(a)) at the sea-level static condition
exceeded the manufacturer's guarantee by about 100 pounds at rated engine
speed. As the altitude was increased, the net thrust decreased. At an
altitude of 51,500 feet and a Mach number of 0.8, the net thrust was
970 pounds for rated speed. The net-thrust specific fuel consumption
for the sea-level condition was lower than the manufacturer's guarantee
at rated engine speed, but was approximately the same at an engine speed
of 7000 rpm which corresponds to the minimum specific fuel consumption
of 0.99 pound of fuel per hour per pound of thrust at this condition.
For a flight Mach number of 0.8 and the range of altitude, the engine
speed which corresponds to minimum specific fuel consumption decreased
from approximately 7400 rpm at an altitude of 16,700 feet to 7100 rpm at
an altitude of 51,500 feet. The minimum value of the specific fuel con-
sumption decreased over this range of altitude from approximately
1.33 pounds of fuel per hour per pound of thrust at 16,700 feet to
1.23 pounds of fuel per hour per pound of thrust at 51,500 feet. This
decrease in specific fuel consumption occurred even though the corrected
specific fuel consumption increased because of the decreasing inlet
temperature with increasing altitude. The minimum specific fuel consump-
tion probably occurred at about 35,000 feet.

Effect of Design Modifications

The effect of the design modifications proposed by the engine manu-
facturer as a block change is presented in figures 16 through 19 for
Reynolds number indices of 0.8, 0.4, and 0.2. Data for all configurations
were obtained at the same inlet temperatures. The ratio of compressor
leakage air flow to inlet air flow is presented as a function of corrected
compressor discharge pressure in figure 16. Figure 16 indicates that the
improved twelfth-stage seal of configuration B reduced this leakage by
25 to 50 percent of its original value at the higher compressor discharge
pressures. Figure 17 presents a comparison of the pumping characteristics
for configuration A (standard engine) and configuration B. For a given
temperature ratio, configuration B has a lower pressure ratio than con-
figuration A. Examination of component performance at a constant cor-
rected engine speed shows no change for the compressor and turbine pres-
sure ratios and a very small increase in combustor total-pressure-loss
ratio (less than 0.0025). However, there was a greater indicated pres-
sure loss in the tail pipe for configuration B. The increase in pressure
loss is attributed to the increased velocity in the tail pipe due to the
higher air flow (caused by less compressor leakage) through the turbine
and the change in area ratio caused by the larger nozzle. The change in

area ratio results in approaching critical Mach numbers at the tail-pipe instrumentation. The jet-thrust parameter (fig. 18) showed no effect from the added air flow resulting from the improved seal because of the counter effect of the greater tail-pipe pressure loss caused by the increased mass flow and velocity.

Combustion efficiency is presented in figure 19. There was no significant difference in the combustion efficiencies of configurations A and B. The addition of shrouded fuel nozzles did not change the peak efficiencies but indicated a slightly higher efficiency at lower values of the engine operating parameter. The modifications proposed by the manufacturer as a block change to the twelfth-stage compressor seal, the engine combustor, and the turbine shroud ring did not provide any significant improvement in engine performance.

CONCLUDING REMARKS

An investigation was conducted in an altitude test chamber to evaluate the performance of an axial-flow turbojet engine over a range of engine-inlet Reynolds number indices. The range of Reynolds number indices investigated provided data which were applicable over a range of flight conditions, for example, altitudes from 15,000 to 55,000 feet at a flight Mach number of 0.7.

This investigation indicated that secondary effects of nozzle flow coefficient and inlet temperature must be known before the effect of variations in engine-inlet Reynolds number index can be analyzed. The nozzle flow coefficient increased with increasing nozzle pressure ratio up to a value of about 2.3, which corresponds to a ram pressure ratio of about 125 percent of the ram pressure ratio required to produce choked flow in the nozzle. Consequently, below this value of ram pressure ratio there was a significant effect of ram pressure ratio on generalized performance. There was a secondary effect of inlet temperature at a constant Reynolds number index. As inlet temperature was increased at a given Reynolds number index, the corrected jet-thrust parameter, corrected exhaust-gas temperature, and corrected ideal fuel-air ratio each increased slightly. This effect was reduced when turbine-outlet straightening vanes were installed.

In general, the effect of reducing the Reynolds number index was to lower the compressor efficiency and air flow resulting in a shift in the compressor map and a rematching of the compressor and turbine. There was only a slight effect of Reynolds number index variation on the turbine performance. The combined effect of reducing the Reynolds number index from 0.6 to 0.15 and the inlet temperature from 7° to -50° F resulted in about a 10 percent increase in corrected fuel flow and about a 2 percent increase in corrected jet-thrust parameter at a corrected engine speed of 7950 rpm.

The engine modifications proposed by the manufacturer resulted in no significant improvement in engine performance. The modified twelfth-stage compressor seal reduced the leakage at the engine midframe by about 20 to 50 percent of its original value. However, the resultant increase in air flow and velocity in the tail pipe caused higher pressure loss and no improvement in thrust. The incorporation of shrouded fuel nozzles resulted in slightly higher combustion efficiency at low values of the engine operating parameter, but the effect was not discernible at high values.

Lewis Flight Propulsion Laboratory
    National Advisory Committee for Aeronautics
        Cleveland, Ohio

APPENDIX A

SYMBOLS

The following symbols are used in this report:

A area, sq ft

C_d exhaust-nozzle flow coefficient, ratio of effective flow area to physical flow area

C_j jet-thrust coefficient, $F_{j,s}/F_{j,r}$

C_T thermal expansion coefficient, ratio of hot exhaust-nozzle area to cold exhaust-nozzle area

F_d thrust system scale reading, lb

F_j jet thrust, lb

F_n net thrust, lb

f fuel-air ratio

g acceleration of gravity, ft/sec^2

h enthalpy, Btu/lb

h_f lower heating value of fuel, Btu/lb

M Mach number

N engine speed, rpm

P total pressure, lb/sq ft

p static pressure, lb/sq ft

R gas constant, ft-lb/(lb)($^{\circ}$R)

T total temperature, $^{\circ}$R

t static temperature, $^{\circ}$R

V velocity, ft/sec

W_a air flow, lb/sec

W_f fuel flow, lb/hr

W_g gas flow, lb/sec

γ ratio of specific heats

δ ratio of engine-inlet total pressure P_1 to NACA standard sea-
           level pressure, 2116 lb/sq ft

θ ratio of engine-inlet total temperature T_1 to NACA standard
           sea-level temperature, 519° R

θ_4 ratio of product of T_4 and γ_4 to product of T and γ for
           NACA standard sea-level conditions, $\gamma_4 T_4 / (519)(1.4)$

φ ratio of coefficient of viscosity corresponding to T_1 to
           coefficient of viscosity corresponding to NACA standard sea-
           level temperature, 519° R. This ratio is a function of
           only temperature and is equal to $735\, \theta^{1.5}/(T + 216)$.

η efficiency

$\dfrac{\delta}{\varphi \sqrt{\theta}}$ Reynolds number index

Subscripts:

a   air

b   combustor

c   compressor

cl   compressor twelfth-stage leakage air flow

i   indicated

m   fuel manifold

n   vena contracta at exhaust-nozzle outlet

r   rake

s   scale

t   turbine

tc   turbine cooling

Station numbers:

0   ambient or free-stream conditions

0a   bellmouth inlet

1   engine inlet

2   compressor inlet

3   compressor outlet or combustor inlet

3b   combustor

4   combustor outlet or turbine inlet

5   turbine outlet

9   exhaust-nozzle inlet

10   exhaust-nozzle outlet

APPENDIX B

METHODS OF CALCULATION

Temperature. - Total temperature was determined by use of a calibrated thermocouple with an impact-recovery factor of 0.85 from the indicated temperature and the following equation:

$$T = \frac{T_i \left(\frac{P}{p}\right)^{\frac{\gamma-1}{\gamma}}}{1 + 0.85 \left[\left(\frac{P}{p}\right)^{\frac{\gamma-1}{\gamma}} - 1\right]}$$

Engine air flow. - Early in the investigation, it was found that an excess of air was leaking from the engine behind the inlet measuring station 1. This air was leaking from sheet-metal joints between stations 1 and 2, from open bolt holes at the compressor inlet, and from twelfth-stage deicing-air lines. It was assumed in the calculation that all unmeasured leakage occurred between stations 1 and 2. The gas flow was determined at the exhaust-nozzle outlet from total pressure and temperature at the nozzle inlet (station 9) by the following equation with the assumption that no energy loss occurred between the nozzle inlet and outlet:

$$W_{g,n} = c_T c_d A_{10} p_n \sqrt{\frac{2\gamma_9}{\gamma_9-1} \frac{g}{RT_9} \left[\left(\frac{P_9}{p_n}\right)^{\frac{\gamma_9-1}{\gamma_9}} - 1\right] \left(\frac{P_9}{p_n}\right)^{\frac{\gamma_9-1}{\gamma_9}}}$$

where in the subsonic case,

$$p_n = p_0$$

and in the choked case,

$$p_n = \frac{P_9}{\left(\frac{1 + \gamma_9}{2}\right)^{\frac{\gamma_9}{\gamma_9-1}}}$$

The value of the flow coefficient C_d was determined from reference 4 using the area ratio and cone angle of the particular nozzle employed in this investigation. The magnitude of the flow coefficient is presented in figure 4(a).

The compressor-inlet air flow was then determined from the nozzle gas flow by

$$W_{a,2} = W_{g,n} - \frac{W_f}{3600} + W_{a,cl}$$

where the compressor leakage air flow $W_{a,cl}$ was measured at two instrumented bleed ports and found to be a function of compressor-outlet pressure P_3 (fig. 11(c)).

The engine-inlet air flow $W_{a,1}$ based on pressure and temperature measurements in a bellmouth mounted on the front of the engine was determined by the same general equation as for the tail-pipe gas flow. The percentage of leakage for the section between stations 1 and 2 is

$$\frac{W_{a,1} - W_{a,2}}{W_{a,2}}$$

and after an attempt was made to plug the leaks, it was approximately 3.3 percent of the compressor-inlet air flow $W_{a,2}$ for the range of conditions covered.

Combustor air flow $W_{a,3}$ used in calculating fuel-air ratio was

$$W_{a,3} = W_{g,n} - W_{a,tc} - \frac{W_f}{3600} = W_{a,2} - W_{a,cl} - W_{a,tc}$$

where $W_{a,tc}$ was the turbine cooling air flow which was found to be half of 1 percent of $W_{a,2}$. Therefore

$$W_{a,3} = 0.995\ W_{a,2} - W_{a,cl}$$

Combustion efficiency. - Combustion efficiency was defined as the fraction of the lower heat of combustion of the liquid fuel effective in increasing the enthalpy across the combustor and was calculated from T_1, T_9, and f based on $W_{a,3}$ by the following formula:

$$\eta_b = \frac{h_a \Big]_{T_1}^{T_9} + f\left(\dfrac{Am + B}{m + 1}\right)\Big]_{T_m}^{T_9}}{f\, h_f}$$

where

$$\frac{Am + B}{m + 1}$$

accounts for the difference between the enthalpy of carbon dioxide and water vapor in the burned mixture and the enthalpy of oxygen removed from the air by their formation (ref. 7), and T_m is the temperature of the fuel in the manifold (540° R).

When the ideal fuel-air ratio was calculated, the combustion efficiency was assumed the same as the ratio of fuel ideally required to the fuel actually required, which is given by

$$\frac{f_{ideal}}{f} = \frac{\eta_b h_f + \dfrac{Am + b}{m + 1}\Big]_{T_m}^{T_9}}{h_f + \dfrac{Am + b}{m + 1}\Big]_{T_m}^{T_9}}$$

The difference in the ratio $\dfrac{f_{ideal}}{f}$ and η_b for the range of combustion efficiencies of this investigation was a maximum of 0.003.

Jet-thrust parameter. - The jet thrust as determined from the thrust system measurements was calculated from the equation

$$F_{j,s} = F_d + (A_{seal} - A_9)(P_1 - p_{seal}) + A_9(P_1 - p_0) + 0.80\left(\frac{1}{2}\frac{W_{a,1}}{g}V_{0a}\right)$$

where F_d is equal to the thrust system scale reading adjusted for the pressure difference on the link connecting the thrust bed in the test chamber and the measuring cell outside the test chamber, and the last term $0.8\left(\dfrac{1}{2}\dfrac{W_{a,1}}{g}\right)V_{0a}$ is the momentum force existing at the bellmouth inlet because of failure of the bellmouth to provide the acceleration of $W_{a,1}$ to V_1. This force was determined experimentally by instrumentation located on the surface of the bellmouth along with the instrumentation at station 1.

The jet-thrust parameter $\dfrac{F_j + A_{10}p_0}{\delta}$ is used to generalize the thrust data for variations in inlet conditions and ram ratio. The value of A_{10} used in calculating this parameter was 2.073 square feet. This was the cold area of the nozzle used in this investigation and facilitates correcting the parameter to a flight condition.

Jet-thrust coefficient. - The jet-thrust velocity coefficient is defined as the ratio of scale jet thrust to rake jet thrust

$$C_j = \frac{F_{j,s}}{F_{j,r}}$$

where

$$F_{j,r} = \frac{W_{g,n}}{g}V_n + A_n(p_n - p_0)$$

The charts in reference 7 were used in the solution of the preceding equation. When all the data obtained in this investigation were employed, the jet-thrust coefficient was found to be independent of exhaust-nozzle pressure ratio and was a constant value of 0.995. The scatter in the coefficient values was approximately ±1 percent for the range of conditions investigated.

APPENDIX C

CORRECTING TEST VALUES TO FLIGHT CONDITIONS

An example of the method of correcting test values to flight conditions has been given in reference 3. For a given flight condition, the value of Reynolds number index can be obtained from figure 10. Values for δ and θ can be readily calculated from engine-inlet total pressure and temperature. If these generalizing parameter values are known, air flow, ideal fuel-air ratio, combustion efficiency, and exhaust-gas temperature can be obtained from the various performance curves. In order to determine the net thrust, the jet-thrust parameter must be first corrected to the desired flight condition to obtain the jet thrust. Then, in order to obtain net thrust, the leakage between stations 1 and 2 must be added to the air flow for station 2, so that

$$F_n = F_j - \left(\frac{W_{a,2} + W_{a,1-2}}{g}\right)V_0$$

The values of net thrust and net-thrust specific fuel consumption presented in figure 15 were obtained in this manner. The following example is a sample calculation of one of the points.

For this calculation an altitude of 51,500 feet and a flight Mach number of 0.8 were selected. These correspond to a Reynolds number index of 0.2 (fig. 10). For the given flight condition, the inlet temperature, pressure, and correction parameters are:

$$T_1 = 443^\circ \text{ R}$$

$$P_1 = 345.1 \text{ lb/sq ft}$$

$$p_0 = 226.4 \text{ lb/sq ft}$$

$$\delta_1 = 0.1631$$

$$\theta_1 = 0.8536$$

$$t_0 = 393^\circ \text{ R}$$

From figure 14(g) a value of 11,693 pounds for the jet-thrust parameter is obtained for a corrected engine speed $N/\sqrt{\theta} = 8652$. The difference between the desired T_1 and the T_1 at which the data were obtained

was about 30°. For a difference of 60° (fig. 8(c)), a change of about 200 pounds is found in the parameter. Therefore an allowance of 100 pounds was made for the inlet temperature, making the jet-thrust parameter 11,793 pounds. This value is then reduced to jet thrust.

$$F_j = 11{,}793 \times \delta - p_0 A_{10} = (11{,}793 \times 0.1631) - (226.4 \times 2.073) = 1454 \text{ pounds}$$

For determination of the inlet momentum $m_1 V_0$, the mass flow is that entering the bellmouth. This is determined either from the measured values or approximately by

$$m_1 = \left(\frac{W_a \sqrt{\theta}}{\delta}\right)_2 \frac{\delta}{\sqrt{\theta}\, g \left(\frac{W_{a,2}}{W_{a,1}}\right)} = (105.6)\, \frac{0.1631}{0.9239 \times 32.2 \times 0.967} = 0.599 \text{ slug}$$

The free-stream velocity V_0 can be determined from the flight Mach number

$$V_0 = M_0 \sqrt{\gamma g R t} = 0.8 \sqrt{1.4 \times 32.2 \times 53.37 \times 393} = 778 \text{ ft/sec}$$

Then the net thrust is

$$F_n = F_j - m_1 V_0 = 1454 - 0.599 \times 778 = 988 \text{ pounds}$$

The net-thrust specific fuel consumption was computed from

$$\text{sfc} = \frac{W_f}{F_n} = \frac{3600\, f\, W_{a,3}}{F_n}$$

where

F_n has been calculated equal to 988 pounds

$$f = (\eta_b f/\theta)_{\text{ideal}}\, \theta/\eta_b = 0.0225 \times 0.8536/0.967 = 0.0199\, \frac{\text{lb fuel}}{\text{lb air}}$$

$\left(\dfrac{\eta_b f}{\theta}\right)_{\text{ideal}}$ is obtained from figure 14(d)

η_b is obtained from figure 12(c)

$$\delta \sqrt{\theta} \ (N/\sqrt{\theta})^3 = 9.760 \times 10^{10}$$

$$W_{a,3} = 0.995 \ W_{a,2} - W_{a,cl} = 0.995 \ \frac{105.6 \times 0.1631}{0.9239} - 0.32 = 18.23 \ \text{lb/sec}$$

where $0.995 \ W_{a,2}$ accounts for the air bled from the compressor discharge for turbine cooling, and where the compressor leakage at the engine midframe W_{cl} was determined from figure 11(c) for which compressor discharge total pressure was calculated by

$$P_3 = P_1 \left(\frac{P_3}{P_1} \right) = (345.1)(6.010) = 2074$$

where P_3/P_1 was obtained from figure 11(e).

Then the sfc $= \dfrac{3600 \times 0.0199 \times 18.23}{988} = 1.32 \ \dfrac{\text{lb fuel/hr}}{\text{lb thrust}}$

The engine speed was obtained from the corrected speed using the equation

$$N = N/\sqrt{\theta} \times \sqrt{\theta} = 8652 \times 0.9239 = 7994 \ \text{rpm}$$

REFERENCES

1. Fleming, William A.: Effects of Altitude on Turbojet Engine Perform-
   ance. NACA RM E51J15, 1951.

2. Renas, Paul E., and Jansen, Emmert T.: Altitude Performance Character-
   istics of the J47-25 Turbojet Engine - Data Presentation.
   NACA RM E52G22. (Supersedes NACA TN 1757.)

3. Walker, Curtis L., Huntley, S. C., and Braithwaite, W. M.: Component
   and Over-all Performance Evaluation of an Axial-Flow Turbojet Engine
   over a Range of Engine-Inlet Reynolds Numbers. NACA RM E52B08, 1952.

4. Grey, Ralph E., Jr., and Wilsted, H. Dean: Performance of Conical
   Jet Nozzles in Terms of Flow and Velocity Coefficients. NACA Rep.
   933, 1949. (Supersedes NACA TN 1757.)

5. Childs, J. Howard: Preliminary Correlation of Efficiency of Aircraft
   Gas-Turbine Combustors for Different Operating Conditions. NACA
   RM E50F15, 1950.

6. Wilsted, H. D., and Grey, R. E.: Altitude Performance Investigation
   of Centrifugal-Flow-Compressor Turbojet Engine. NACA RM E51B07,
   1951.

2717

7. Turner, L. Richard, and Bogart, Donald: Constant-Pressure Combustion Charts Including Effects of Diluent Addition. NACA Rep. 937, 1949. (Supersedes NACA TN's 1086 and 1655.)

8. Turner, L. Richard, Addie, Albert N., and Zimmerman, Richard H.: Charts for the Analysis of One-Dimensional Steady Compressible Flow. NACA TN 1419, 1948.
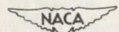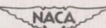
TABLE I. - PERFORMANCE

Run	Reynolds number index, $\delta/(\varphi\sqrt{\theta})$	Engine speed, N, rpm	Jet thrust, F_j, lb	Engine-inlet air flow, $W_{a,1}$, lb/sec	Compressor-inlet air flow, $W_{a,2}$, lb/sec	Combustor-inlet air flow, $W_{a,3}$, lb/sec	Exhaust-nozzle gas flow, $W_{g,9}$, lb/sec	Fuel flow, W_f, lb/hr	Engine-inlet total pressure, P_1, lb/sq ft	Engine-inlet total temperature, T_1, °R	Compressor-outlet total pressure, P_3, lb/sq ft	Compressor-outlet total temperature, T_3, °R	Combustor total static pressure, $P_{3,b}$, lb/sq ft	Turbine-inlet total pressure, P_4, lb/sq ft	Calculated turbine-inlet total temperature, T_4, °R	Turbine-outlet total pressure, P_5, lb/sq ft	Exhaust-nozzle inlet total pressure, P_g, lb/sq ft	Exhaust-gas total temperature, T_g, °R	Manufacturer's indicated exhaust-gas temperature, 4-probe, $T_{g,m,4}$, °R	5-probe, $T_{g,m,5}$, °R
1	0.805	7951	6265	88.0	84.9	82.6	84.5	4953	1779	538	9155	939	8856	8690	2045	3385	3261	1701	1648	1652
2	.796	7947	6297	88.6	84.9	82.7	84.5	4922	1786	539	9150	935	8856	8685	2042	3384	3257	1700	1642	1649
3	.809	7727	5891	86.9	83.6	81.4	83.1	4406	1788	537	8763	918	8501	8542	1945	3249	3123	1612	1565	1562
4	.805	7725	5903	87.2	83.2	81.1	82.7	4415	1784	538	8734	918	8475	8312	1950	3235	3108	1615	1561	1563
5	.807	7568	5552	85.4	82.1	80.0	81.5	4086	1786	537	8449	905	8207	8054	1882	3126	3008	1549	1510	1504
6	.804	7568	5588	85.7	81.7	79.6	81.1	4100	1780	537	8425	902	8183	8025	1885	3118	2998	1559	1510	1509
7	.809	7409	5302	83.8	80.4	78.3	79.8	3765	1789	537	8153	892	7917	7771	1812	3013	2897	1498	1454	1448
8	.801	7409	5312	83.4	79.7	77.7	79.1	3747	1773	537	8091	888	7857	7708	1812	2981	2871	1501	1453	1453
9	.806	7197	4902	81.3	77.5	75.6	76.9	3338	1773	535	7693	869	7462	7322	1730	2851	2720	1425	1382	1381
10	.809	7197	4852	82.1	77.2	76.0	77.3	3323	1790	537	7732	874	7499	7563	1725	2845	2735	1419	1380	1373
11	.807	6817	4037	76.8	72.6	70.5	72.0	2548	1772	534	6849	835	6615	6497	1545	2503	2401	1272	1235	1236
12	.807	6817	4029	76.8	72.6	70.9	72.0	2538	1785	537	6894	841	6658	6543	1542	2523	2415	1266	1230	1228
13	.806	6360	3083	69.2	65.1	63.7	64.5	1693	1780	532	5799	793	5565	5467	1330	2100	2010	1085	1050	1056
14	.807	6372	3093	69.7	66.1	64.7	65.5	1716	1788	558	5884	801	5646	5551	1330	2134	2047	1085	1051	1058
15	0.607	7949	4792	61.5	59.5	58.0	59.4	3656	1151	471	6419	874	6224	6107	2050	2369	2288	1708	1659	1656
16	.597	7951	4716	60.2	58.2	56.7	58.1	3595	1114	472	6302	875	6109	5994	2060	2320	2240	1712	1663	1659
17	.602	7722	4491	60.3	58.1	57.0	58.2	3217	1125	472	6122	852	5922	5812	1925	2245	2167	1594	1546	1544
18	.609	7578	4367	60.3	58.2	56.8	58.0	3005	1123	467	5981	831	5782	5675	1850	2190	2111	1525	1483	1481
19	.608	7411	4146	59.5	57.2	55.8	56.9	2765	1118	466	5764	816	5572	5470	1780	2107	2031	1466	1424	1422
20	.605	7193	3920	59.4	56.5	55.2	56.2	2380	1124	470	5492	802	5327	5229	1693	2015	1955	1393	1357	1353
21	.610	6813	3485	55.8	53.5	52.5	53.2	2009	1123	467	5008	768	4883	4773	1530	1831	1759	1258	1251	1227
22	.613	6362	2815	51.9	49.2	48.3	48.9	1455	1121	464	4352	730	4204	4128	1152	1582	1514	1097	1069	1069
23	.610	5930	2138	47.0	44.2	43.4	43.8	982	1127	468	3663	697	3503	3442	1152	1311	1256	931	901	907
24	0.506	7943	3858	50.6	48.8	47.6	48.7	3032	927	465	5301	869	5139	5045	2062	1954	1882	1716	1665	1665
25	.503	7943	3838	50.6	48.6	47.4	48.5	3015	930	468	5268	872	5106	5011	2055	1948	1873	1711	1659	1661
26	.505	7953	3880	51.0	49.1	47.9	49.0	3032	940	471	5320	875	5157	5062	2055	1960	1891	1711	1659	1660
27	.509	7722	3663	50.7	48.9	47.7	48.7	2722	939	469	5138	848	4972	4880	1933	1887	1818	1600	1550	1551
28	.502	7718	3637	50.0	48.2	47.1	48.1	2513	931	469	5073	851	4908	4818	1937	1862	1794	1602	1555	1555
29	.508	7566	3559	50.3	48.5	47.1	48.1	2513	942	467	4985	835	4818	4730	1860	1829	1759	1537	1491	1490
30	.508	7409	3404	49.7	47.7	46.6	47.5	2317	938	468	4750	818	4589	4504	1785	1776	1699	1469	1424	1422
31	.508	7193	3188	48.6	46.8	45.7	46.5	2098	940	468	4609	801	4465	4387	1700	1689	1624	1399	1362	1356
32	.509	6817	2798	46.7	44.5	43.6	44.3	1708	939	467	4201	770	4081	4006	1543	1537	1475	1271	1240	1236
33	.509	6362	2250	42.9	40.8	40.0	40.5	1248	944	469	3629	735	3505	3442	1350	1517	1262	1106	1079	1080
34	.510	5929	1721	38.0	37.0	36.3	36.7	858	940	467	3085	696	2958	2907	1160	1106	1060	940	911	917
35	0.406	7956	2762	40.2	38.8	37.8	38.7	2480	746	466	4285	868	4166	4089	2092	1580	1523	1748	1698	1691
36	.399	7947	2724	39.9	38.5	38.0	38.9	2480	741	470	4258	868	4132	4056	2080	1580	1521	1734	1679	1678
37	.404	7570	2466	39.6	38.1	37.2	38.0	2049	747	468	3973	854	3839	3769	1885	1468	1410	1555	1508	1505
38	.397	7405	2267	38.4	37.1	36.2	36.9	1872	737	470	3834	824	3705	3638	1812	1403	1347	1415	1371	1372
39	.405	7199	2204	38.5	36.9	36.1	36.7	1708	739	464	3699	803	3581	3516	1715	1356	1302	1413	1371	1372
40	.401	6813	1877	34.9	34.1	33.6	34.1	1365	744	469	3549	778	3433	3253	1565	1233	1182	1294	1256	1258
41	.404	6360	1488	33.8	32.2	31.6	32.1	1062	743	466	2919	741	2824	2775	1375	1072	1030	1135	1102	1107
42	0.413	7962	2828	39.7	39.1	38.1	39.1	2555	710	438	4251	845	4127	4052	2090	1585	1527	1735	1678	1682
43	.426	7741	2716	40.5	38.9	38.0	38.9	2268	728	441	4157	830	4010	3957	1960	1524	1469	1622	1570	1575
44	.416	7565	2576	39.5	38.5	37.6	38.4	2082	720	443	3998	812	3870	3801	1868	1469	1415	1541	1496	1498
45	.425	7407	2497	39.5	38.3	37.5	38.3	1944	720	438	3925	792	3795	3728	1793	1435	1380	1475	1431	1431
46	.431	7112	2298	38.1	36.8	36.3	37.5	1700	725	443	3728	763	3603	3559	1660	1337	1302	1369	1331	1329
47	.419	6817	2011	37.2	35.8	34.9	35.4	1418	719	443	3371	746	3275	3216	1540	1240	1189	1268	1231	1231
48	0.431	6362	1650	35.4	33.7	33.1	33.6	1116	721	434	3013	703	2920	2869	1360	1106	1062	1116	1084	1086
49	.434	5930	1295	32.5	31.0	30.5	30.9	838	718	430	2619	663	2527	2483	1197	958	922	979	950	957
50	.395	7909	2719	36.2	35.0	34.1	34.9	2284	624	415	3826	825	3713	3646	2070	1408	1353	1719	1657	1665
51	.396	7714	2587	36.2	34.8	34.0	34.8	2057	624	415	3709	801	3600	3536	1950	1358	1305	1614	1561	1565
52	.398	7582	2518	36.0	34.9	34.1	34.9	1928	627	415	3629	786	3520	3457	1873	1333	1281	1548	1500	1502
53	.400	7407	2419	36.0	34.6	33.9	34.6	1777	628	414	3501	768	3389	3328	1787	1289	1238	1470	1425	1428
54	.395	7203	2250	35.4	34.0	33.4	34.0	1608	624	416	3352	749	3238	3181	1685	1231	1183	1385	1346	1346
55	.399	6817	2024	34.5	33.2	32.5	33.1	1346	626	414	3112	714	3011	2958	1520	1138	1093	1248	1214	1217
56	.401	6360	1704	32.8	31.0	30.5	31.0	1045	628	413	2753	679	2673	2626	1347	1004	965	1105	1074	1077
57	.403	5927	1336	29.6	28.8	28.2	28.5	777	630	412	2396	644	2314	2274	1185	866	833	962	931	938
58	0.302	7725	1995	27.1	26.6	26.0	26.6	1647	469	411	2818	800	2756	2685	1985	1054	1009	1652	1597	1602
59	.303	7574	1982	27.1	26.4	25.9	26.5	1524	473	412	2755	784	2673	2624	1892	1024	981	1570	1519	1523
60	.297	7570	1741	26.8	25.9	25.2	25.8	1463	466	413	2699	786	2619	2571	1880	995	954	1557	1508	1514
61	.300	7415	1852	26.7	25.9	25.4	25.9	1388	469	412	2651	786	2568	2521	1800	974	934	1486	1437	1447
62	.298	7407	1691	26.7	25.8	25.1	25.6	1376	466	413	2622	770	2540	2494	1800	965	926	1484	1438	1444
63	.303	7193	1758	26.5	25.7	25.2	25.7	1244	473	412	2561	746	2475	2431	1692	936	899	1398	1358	1360
64	.297	7195	1560	26.2	25.3	24.8	25.3	1246	468	415	2523	752	2438	2395	1700	926	888	1400	1359	1362
65	.311	6822	1600	26.2	25.3	25.3	25.7	1042	486	412	2446	715	2365	2324	1535	890	855	1268	1227	1233
66	.296	6817	1393	25.6	24.4	24.0	24.4	1038	468	416	2335	719	2259	2218	1540	854	819	1271	1233	1239
67	.302	6360	1303	24.3	23.5	23.1	23.4	768	473	413	2092	679	2031	1995	1362	764	735	1122	1088	1094
68	0.248	7570	1566	22.2	21.6	21.2	21.7	1255	389	413	2276	787	2208	2167	1897	837	805	1571	1513	1524
69	.247	7409	1441	21.9	21.3	20.9	21.3	1161	388	414	2189	770	2120	2081	1810	805	772	1497	1446	1455
70	.250	7207	1420	21.9	21.1	20.7	21.1	1062	391	413	2118	750	2047	2010	1717	777	745	1418	1369	1375
71	.248	6815	1268	21.2	20.5	20.1	20.5	883	389	414	1958	718	1894	1860	1550	714	686	1279	1240	1244
72	.248	6358	1071	19.8	19.3	18.9	19.2	687	389	414	1724	682	1674	1644	1380	632	608	1138	1105	1111
73	.249	5921	851	18.4	17.7	17.4	17.6	516	392	414	1483	647	1434	1409	1210	543	523	992	964	967
74	0.198	7725	1285	17.7	17.4	17.0	17.4	1153	311	414	1899	807	1843	1807	2030	702	671	1694	1636	1639
75	.199	7574	1250	17.6	17.2	16.8	17.2	1059	311	413	1829	791	1776	1743	1930	675	646	1602	1551	1558
76	.200	7407	1188	17.6	17.1	16.8	17.1	973	313	412	1780	772	1725	1692	1843	655	627	1531	1471	1478
77	.202	7205	1128	17.6	17.0	16.6	17.0	883	316	412	1713	753	1656	1626	1750	637	604	1442	1395	1405
78	.201	6801	991	16.9	16.4	16.1	16.4	730	313	412	1582	718	1529	1501	1572	577	555	1300	1265	1274
79	.200	6362	814	16.0	15.3	15.1	15.3	575	313	413	1403	684	1361	1337	1405	513	491	1162	1124	1132
80	.202	5927	626	14.7	14.2	14.0	14.2	438	315	412	1211	650	1173	1152	1232	443	427	1007	981	986
81	0.150	7707	911	12.9	12.8	12.6	12.9	883	235	413	1412	810	1371	1344	2065	528	504	1729	1668	1670
82	.151	7578	840	13.1	12.9	12.6	12.9	822	237	414	1385	800	1345	1319	1970	516	492	1639	1582	1590
83	.154	7409	824	13.1	12.9	12.6	12.9	762	241	414	1358	780	1318	1292	1885	504	481	1563	1512	1521
84	.156	7193	776	13.2	12.9	12.7	12.9	696	246	415	1335	761	1291	1267	1785	490	468	1477	1427	1446

AND OPERATIONAL DATA

NACA

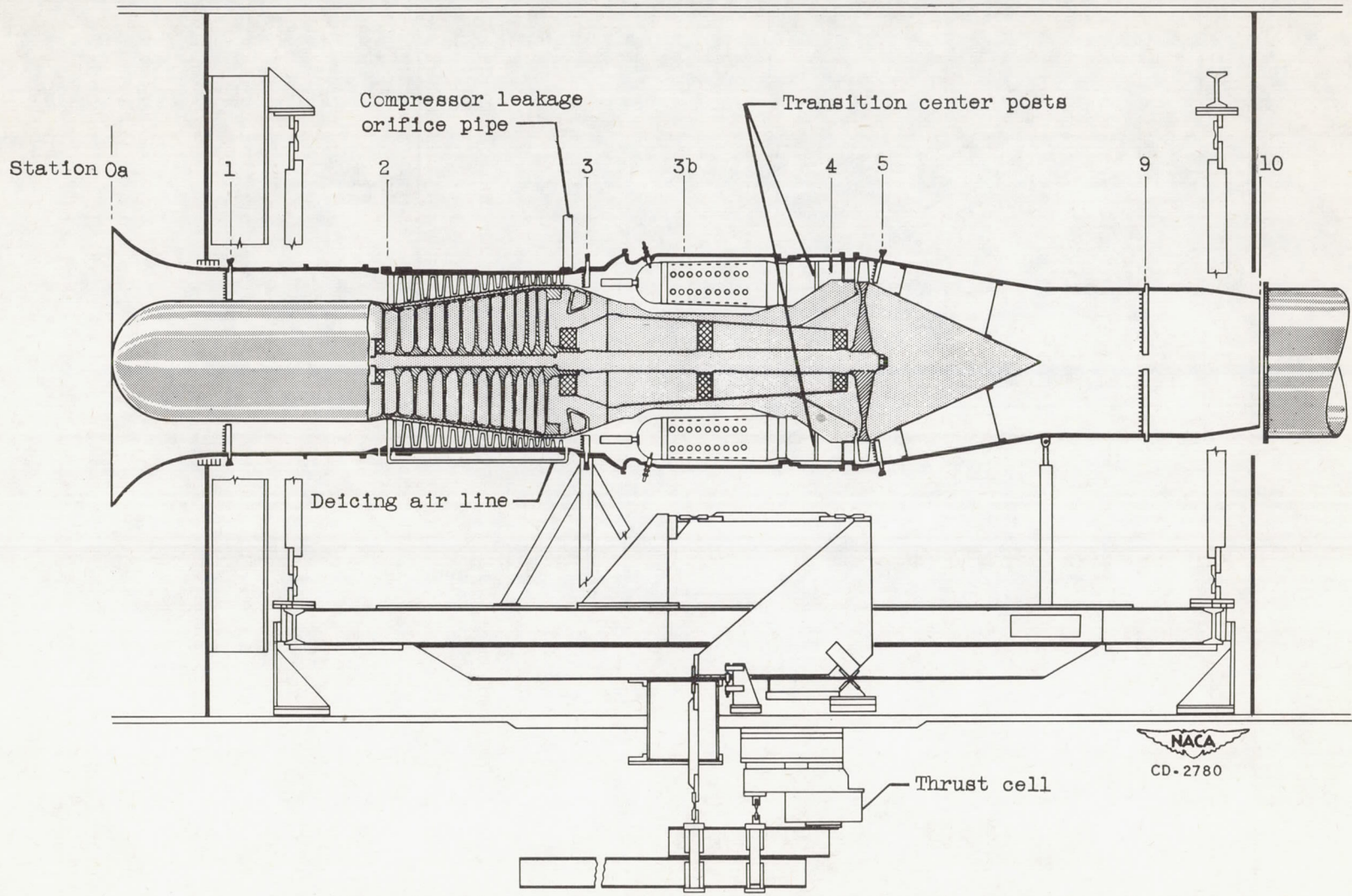| Corrected engine speed, $\frac{N}{\sqrt{\theta}}$, rpm	Ram pressure ratio, $\frac{P_1}{P_0}$	Compressor total-pressure ratio, $\frac{P_3}{P_1}$	Corrected compressor air flow, $\frac{W_{a,2}\sqrt{\theta}}{\delta}$, lb/sec	Compressor efficiency, η_c	Combustor total-pressure-loss ratio, $\frac{P_3-P_4}{P_3}$	Combustion efficiency, η_b	Engine operating parameter, $\delta\sqrt{\theta}\left(\frac{N}{\sqrt{\theta}}\right)^3$	Combustion parameter, $\frac{(P_{3,b})^2}{W_{a,3}}$	Turbine total-pressure ratio, $\frac{P_4}{P_5}$	Corrected turbine gas flow, $\frac{W_{g,4}\sqrt{\theta_4}}{\delta_4}\left(\frac{\gamma_4}{1.4}\right)$, lb/sec	Turbine efficiency, η_t	Tailpipe total-pressure-loss ratio, $\frac{P_5-P_9}{P_5}$	Engine total-pressure ratio, $\frac{P_9}{P_1}$	Engine total-temperature ratio, $\frac{T_9}{T_1}$	Corrected fuel flow, $\frac{W_f}{\delta\sqrt{\theta}}$, lb/hr	Corrected ideal fuel-air ratio, $\frac{\eta_b f}{\theta}$	Corrected exhaust-gas total temperature, $\frac{T_9}{\theta}$, °R	Corrected jet-thrust parameter, $\frac{F_j+A_{10}P_0}{\delta}$, lb	Run
7809	1.72	5.15	102.8	0.802	.0508	.985	4.08×10⁵	94.9×10⁴	2.57	41.9	0.825	.037	1.833	3.162	5784	0.0159	1641	9,999	1
7721	1.75	5.12	103.6	.810	.0508	.988	4.00	94.8	2.57	42.0	.825	.038	1.824	3.156	5666	.0157	1638	9,971	2
7596	1.70	4.90	100.5	.811	.0481	1.004	3.77	88.8	2.57	41.8	.830	.039	1.747	3.002	5124	.0146	1558	9,552	3
7587	1.74	4.90	100.5	.815	.0483	.994	3.75	88.6	2.57	41.9	.835	.039	1.742	3.001	5142	.0145	1558	9,522	4
7440	1.70	4.73	98.9	.817	.0468	.987	3.54	84.3	2.58	41.9	.850	.038	1.684	2.885	4760	.0136	1497	9,160	5
7439	1.74	4.73	98.9	.825	.0475	.997	3.52	84.2	2.57	41.8	.835	.039	1.684	2.903	4792	.0137	1506	9,174	6
7284	1.71	4.56	96.7	.822	.0469	.985	3.32	80.0	2.58	41.5	.825	.039	1.619	2.790	4379	.0129	1448	8,860	7
7283	1.74	4.56	96.8	.833	.0473	.998	3.29	79.5	2.59	41.5	.815	.037	1.619	2.795	4394	.0128	1450	8,865	8
7088	1.74	4.34	93.8	.837	.0482	.998	3.03	73.7	2.59	41.4	.830	.039	1.534	2.665	3922	.0118	1382	8,374	9
7075	1.71	4.32	93.7	.828	.0477	1.004	3.05	74.0	2.59	41.4	.835	.039	1.528	2.642	3861	.0117	1371	8,309	10
6723	1.73	3.87	87.5	.837	.0514	.994	2.58	62.1	2.60	40.9	.810	.041	1.355	2.384	3000	.0097	1237	7,356	11
6702	1.70	3.86	87.5	.833	.0509	.982	2.59	62.5	2.59	40.8	.820	.043	1.353	2.358	2957	.0095	1224	7,355	12
6284	1.74	3.30	79.2	.828	.0573	.990	2.09	48.6	2.60	40.4	.820	.043	1.142	2.041	2011	.0072	1059	6,233	13
6259	1.74	3.29	79.6	.830	.0566	.980	2.11	49.3	2.60	40.4	.820	.041	1.145	2.017	1994	.0070	1047	6,235	14
8346	2.13	5.68	106.1	0.752	.0486	.996	2.96×10⁵	66.7×10⁴	2.58	42.0	0.825	.034	2.023	3.626	7182	0.0191	1882	11,022	15
8341	2.14	5.66	105.4	.751	.0489	.994	2.91	65.8	2.58	41.9	.825	.035	2.011	3.627	7157	.0191	1883	11,003	16
8100	2.14	5.44	104.8	.774	.0506	.995	2.69	61.5	2.59	41.8	.835	.035	1.926	3.373	6348	.0171	1751	10,499	17
7987	2.14	5.33	104.0	.787	.0512	.997	2.57	58.8	2.59	41.8	.835	.036	1.880	3.266	5967	.0162	1694	10,275	18
7819	2.15	5.16	102.6	.797	.0510	.999	2.39	55.6	2.60	41.7	.845	.036	1.817	3.146	5522	.0155	1633	9,891	19
7560	2.14	4.89	101.2	.813	.0479	.985	2.18	51.4	2.59	41.9	.830	.030	1.739	2.964	4908	.0139	1539	9,435	20
7188	2.16	4.46	95.5	.829	.0469	1.002	1.87	45.2	2.61	41.2	.815	.039	1.566	2.694	3993	.0118	1399	8,598	21
6725	2.16	3.88	87.9	.830	.0515	1.010	1.52	36.6	2.61	40.8	.810	.043	1.351	2.382	2904	.0094	1226	7,346	22
6244	2.17	3.25	78.8	.821	.0603	.961	1.23	28.3	2.63	40.5	.835	.042	1.114	1.988	1942	.0067	1032	6,041	23
8388	1.95	5.72	105.4	0.744	.0483	.991	2.45×10⁵	55.5×10⁴	2.58	41.8	0.820	.037	2.029	3.690	7306	0.0196	1915	11,055	24
8364	1.94	5.66	105.1	.744	.0488	.990	2.44	55.0	2.57	41.9	.820	.039	2.014	3.656	7223	.0193	1897	11,000	25
8351	1.95	5.66	105.3	.748	.0485	.993	2.47	55.0	2.58	41.9	.820	.035	2.011	3.633	7163	.0192	1866	10,978	26
8139	1.94	5.47	104.6	.767	.0502	.994	2.27	51.8	2.59	41.8	.830	.037	1.937	3.416	6467	.0177	1778	10,524	27
8119	1.95	5.45	104.2	.766	.0503	.995	2.24	51.2	2.59	41.8	.835	.037	1.927	3.416	6411	.0174	1773	10,516	28
7959	1.96	5.29	103.0	.782	.0512	1.001	2.14	49.3	2.59	41.7	.830	.038	1.867	3.277	5935	.0163	1701	10,229	29
7806	1.98	5.06	102.1	.789	.0518	1.000	2.00	45.2	2.54	42.3	.855	.043	1.809	3.139	5497	.0152	1629	9,883	30
7574	1.95	4.91	100.0	.810	.0482	.999	1.83	43.7	2.60	41.5	.830	.039	1.729	2.989	4975	.0140	1551	9,429	31
7185	1.96	4.47	95.2	.824	.0464	1.001	1.56	38.2	2.61	41.1	.810	.042	1.570	2.722	4056	.0120	1412	8,548	32
6693	1.98	3.84	86.8	.828	.0515	.982	1.27	30.7	2.61	40.7	.810	.042	1.337	2.358	2942	.0093	1224	7,286	33
6249	1.95	3.28	79.0	.825	.0577	.954	1.03	24.1	2.63	40.3	.820	.042	1.127	2.015	2036	.0069	1045	6,123	34
8394	1.35	5.75	104.4	0.741	.0458	.996	1.98×10⁵	45.9×10⁴	2.57	41.4	0.805	.036	2.043	3.751	7425	0.0202	1947	11,087	35
8352	1.35	5.75	105.8	.748	.0475	.980	1.94	45.0	2.57	41.7	.825	.037	2.053	3.685	7444	.0197	1912	11,031	36
7971	1.35	5.32	102.5	.771	.0514	.984	1.70	39.6	2.57	41.6	.845	.040	1.888	3.523	6115	.0168	1724	10,241	37
7783	1.32	5.20	101.2	.800	.0511	.984	1.56	37.9	2.59	41.1	.830	.040	1.827	3.181	5647	.0156	1650	9,826	38
7617	1.35	5.00	99.8	.808	.0495	.984	1.46	35.6	2.59	41.0	.825	.040	1.761	3.045	5172	.0145	1581	9,558	39
7167	1.34	4.50	94.3	.827	.0463	.975	1.23	31.0	2.59	40.7	.800	.041	1.586	2.759	3172	.0123	1432	8,610	40
6710	1.34	3.93	87.1	.836	.0493	.946	1.01	25.2	2.59	40.4	.795	.039	1.387	2.436	3193	.0099	1261	7,517	41
8671	1.39	5.99	107.0	0.712	.0468	.984	2.01×10⁵	44.7×10⁴	2.56	42.1	0.845	.037	2.151	3.961	8294	0.0217	2056	11,588	42
8399	1.42	5.86	104.3	.730	.0484	.984	1.88	42.3	2.58	41.6	.835	.036	2.018	3.678	7153	.0193	1909	10,978	43
8193	1.41	5.56	104.4	.760	.0493	.989	1.73	39.8	2.59	41.5	.835	.037	1.967	3.479	6631	.0177	1806	10,685	44
8066	1.42	5.45	103.4	.772	.0502	.992	1.64	38.4	2.60	41.3	.840	.038	1.916	3.368	6219	.0168	1778	10,456	45
7759	1.43	5.15	100.5	.797	.0507	.988	1.47	35.3	2.61	40.9	.815	.041	1.797	3.140	5518	.0150	1629	9,786	46
7383	1.43	4.69	96.6	.812	.0460	.989	1.26	30.9	2.59	40.9	.810	.041	1.653	2.862	4516	.0130	1486	8,995	47
6960	1.42	4.18	90.4	0.815	.0478	.972	1.05×10⁵	25.8×10⁴	2.59	40.6	0.809	.040	1.472	2.571	3582	0.0108	1335	7,931	48
6517	1.42	3.65	83.2	.827	.0519	.94	.85	20.9	2.59	40.4	.805	.037	1.285	2.277	2716	.0087	1182	6,916	49
8834	1.68	6.13	106.1	.691	.0471	.986	1.62	40.4	2.59	41.6	.831	.039	2.168	4.132	8649	.0208	2019	11,363	50
8624	1.70	5.95	105.6	.715	.0467	.995	1.69	38.1	2.60	41.4	.828	.039	2.092	3.889	7800	.0208	1937	11,099	51
8477	1.69	5.79	105.4	.730	.0474	1.000	1.61	36.3	2.59	41.5	.831	.039	2.054	3.730	7277	.0195	1843	10,743	52
8298	1.69	5.58	104.1	.743	.0494	.995	1.51	33.9	2.58	41.7	.843	.040	1.972	3.551	6709	.0181	1843	10,223	53
8046	1.69	5.37	103.4	.772	.0510	.988	1.37	31.4	2.58	41.6	.837	.039	1.896	3.329	6092	.0164	1728	10,223	54
7635	1.69	4.97	100.0	.803	.0495	.980	1.18	27.9	2.60	41.2	.821	.040	1.745	3.014	5092	.0140	1565	9,431	55
7130	1.69	4.38	93.3	.817	.0461	.947	.96	23.4	2.62	40.7	.793	.039	1.536	2.676	3917	.0115	1389	8,334	56
6650	1.66	3.81	85.6	.827	.0509	.947	.78	19.0	2.63	40.5	.820	.037	1.324	2.335	2930	.0091	1212	7,135	57
8683	1.68	6.01	106.7	0.708	.0472	.981	1.29×10⁵	28.8×10⁴	2.55	42.0	0.827	.043	2.151	4.019	8351	0.0218	2086	11,611	58
8498	1.71	5.83	105.3	.726	.0476	.981	1.22	27.5	2.56	41.8	.826	.042	2.075	3.811	7654	.0201	1978	11,436	59
8486	1.38	5.80	104.6	.723	.0474	.984	1.20	27.2	2.58	41.4	.826	.042	2.049	3.770	7454	.0198	1957	11,096	60
8320	1.69	5.66	104.3	.747	.0490	.968	1.14	26.0	2.59	41.5	.828	.041	1.993	3.607	7033	.0185	1872	10,569	61
8303	1.38	5.63	103.9	.739	.0488	.965	1.12	25.7	2.58	41.4	.836	.041	1.987	3.593	7008	.0184	1865	10,873	62
8071	1.71	5.41	102.5	.766	.0508	.964	1.05	24.3	2.60	41.2	.814	.040	1.899	3.393	6294	.0169	1761	10,275	63
8044	1.36	5.39	102.2	.762	.0507	.963	1.03	24.0	2.59	41.2	.831	.041	1.896	3.373	6294	.0167	1751	10,275	64
7654	1.74	5.03	99.8	.799	.0494	.975	.92	22.2	2.61	40.9	.796	.040	1.759	3.078	5247	.0145	1598	9,491	65
7612	1.33	4.99	98.9	.801	.0501	.957	.87	21.3	2.60	40.8	.804	.041	1.751	3.055	5243	.0143	1586	9,591	66
7130	1.73	4.42	93.6	.823	.0464	.959	.72	17.9	2.61	40.8	.791	.038	1.553	2.717	4082	.0118	1410	8,364	67
8486	1.64	5.85	105.0	0.726	.0479	.969	1.00×10⁵	23.0×10⁴	2.59	41.4	0.828	.042	2.062	3.804	7653	0.0201	1975	11,198	68
8298	1.63	5.63	103.8	.744	.0493	.964	.94	21.5	2.58	41.5	.822	.042	1.987	3.616	7083	.0186	1877	10,816	69
8079	1.64	5.43	102.1	.762	.0510	.963	.87	20.2	2.59	41.3	.821	.041	1.906	3.435	6448	.0172	1782	10,368	70
7635	1.64	5.03	99.5	.800	.0501	.955	.73	17.8	2.60	41.0	.805	.039	1.762	3.089	5374	.0148	160	9,586	71
7121	1.63	4.43	93.6	.820	.0464	.952	.59	14.8	2.60	40.9	.792	.039	1.562	2.749	4186	.0121	1427	8,516	72
6632	1.62	3.79	85.3	.824	.0499	.926	.48	11.8	2.60	40.8	.797	.037	1.335	2.396	312	.0095	1244	7,310	73
8652	1.48	6.10	105.6	0.713	.0485	.948	0.85×10⁵	20.0×10⁴	2.57	41.4	0.811	.044	2.156	4.092	8798	0.0225	212	11,693	74
8490	1.51	5.87	104.4	.720	.0470	.942	.80	18.7	2.58	41.4	.822	.044	2.073	3.879	8067	.0207	201	11,352	75
8311	1.50	5.69	103.1	.738	.0494	.957	.76	17.8	2.58	41.3	.810	.045	2.006	3.716	7388	.0194	1929	10,968	76
8084	1.50	5.43	101.6	.752	.0508	.958	.70	16.5	2.58	41.5	.835	.042	1.914	3.500	6641	.0177	1817	10,688	77
7631	1.48	5.05	98.9	.793	.0513	.949	.59	14.5	2.60	41.0	.797	.038	1.772	3.155	5532	.0151	1638	9,669	78
7132	1.46	4.48	92.4	.817	.0471	.940	.48	12.3	2.61	40.4	.782	.042	1.569	2.814	4357	.0125	1461	8,616	79
6650	1.45	3.84	85.1	.813	.0487	.899	.39	9.8	2.60	40.5	.809	.036	1.354	2.444	3299	.0099	1269	7,228	80
8640	1.22	6.02	103.5	0.698	.0482	.948	0.64×10⁵	15.0×10⁴	2.54	41.6	0.812	.047	2.148	4.186	8931	0.0252	2173	11,812	81
8487	1.21	5.85	103.1	.705	.0477	.942	.61	14.4	2.56	41.4	.824	.046	2.080	3.959	8233	.021	2055	11,151	82
8298	1.20	5.63	101.2	.723	.0486	.945	.58	13.8	2.57	41.3	.828	.045	1.993	3.775	7484	.0199	1960	10,890	83
8042	1.21	5.43	99.4	.746	.0509	.951	.54	13.2	2.58	40.9	.821	.045	1.905	3.559	6696	.0182	1848	10,308	84

Figure 1. - Schematic diagram of engine in altitude chamber showing station locations.

30°

● Static-pressure tube (wall or rake)
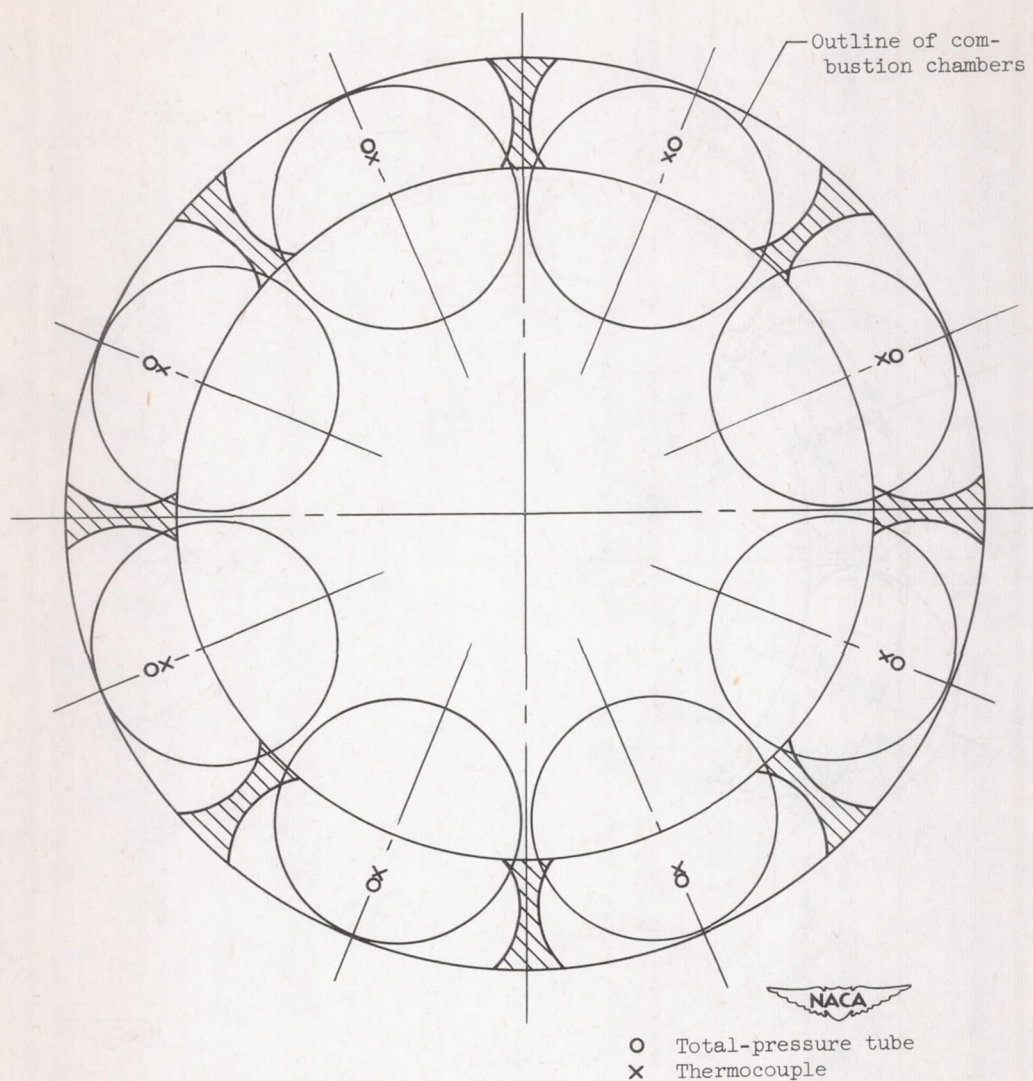○ Total-pressure tube
✕ Thermocouple
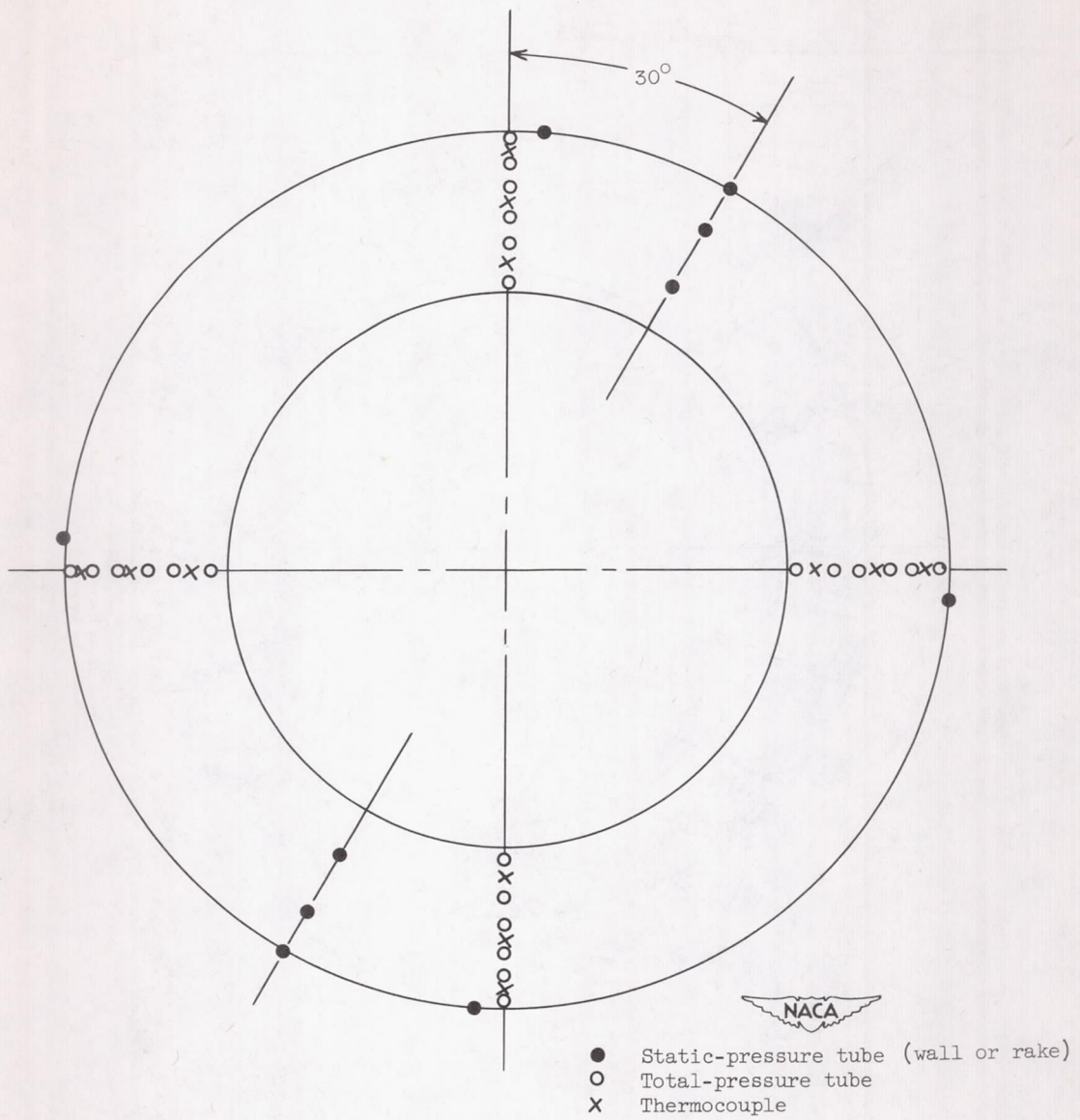
(a) Instrumentation at engine inlet, station 1, 21 inches upstream of leading edge of compressor-inlet guide vanes.

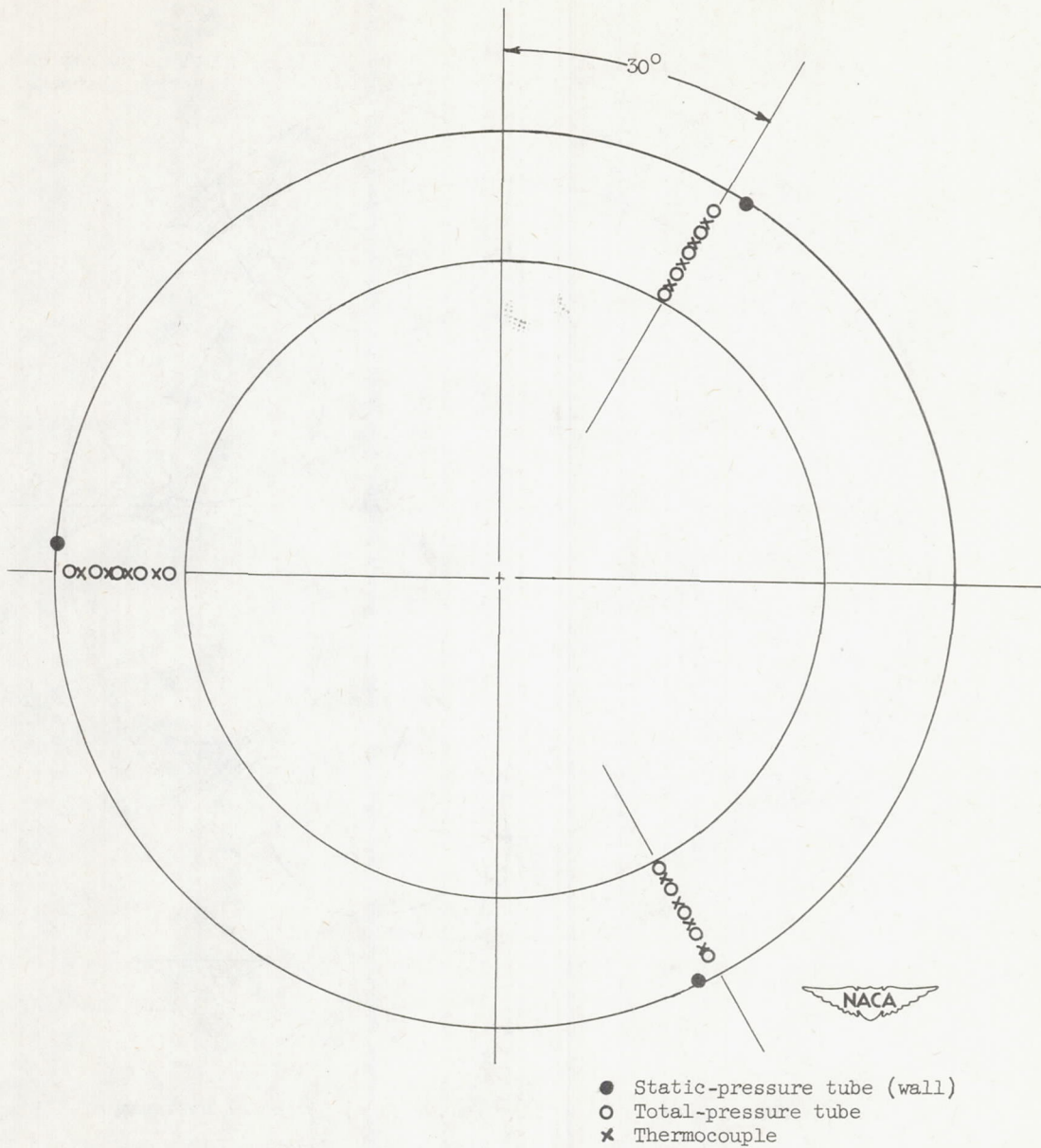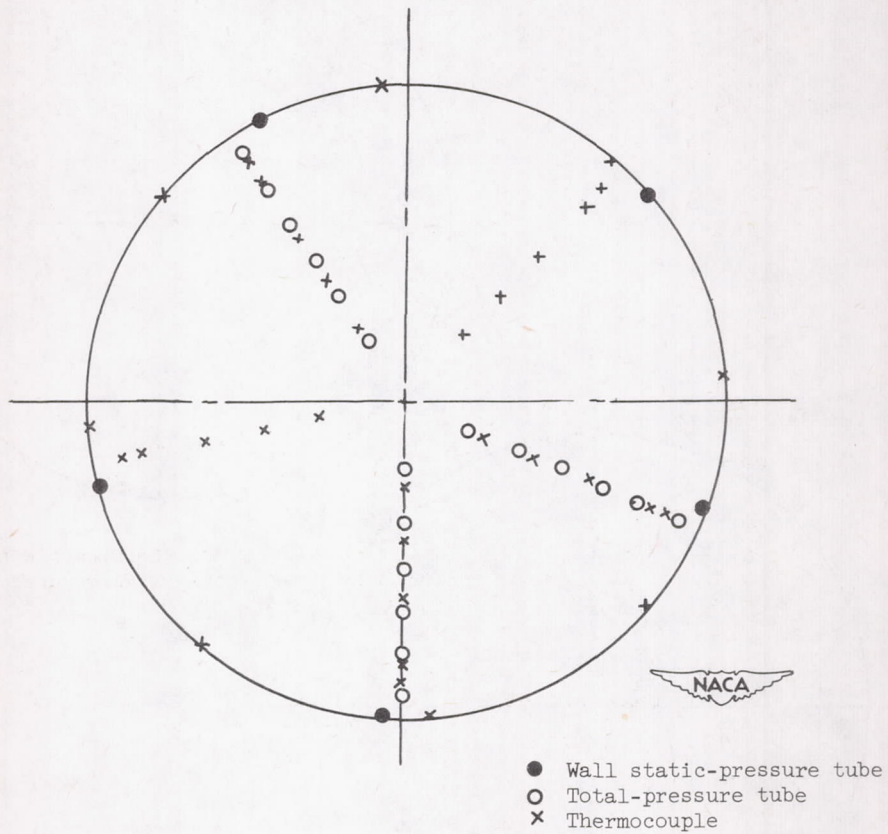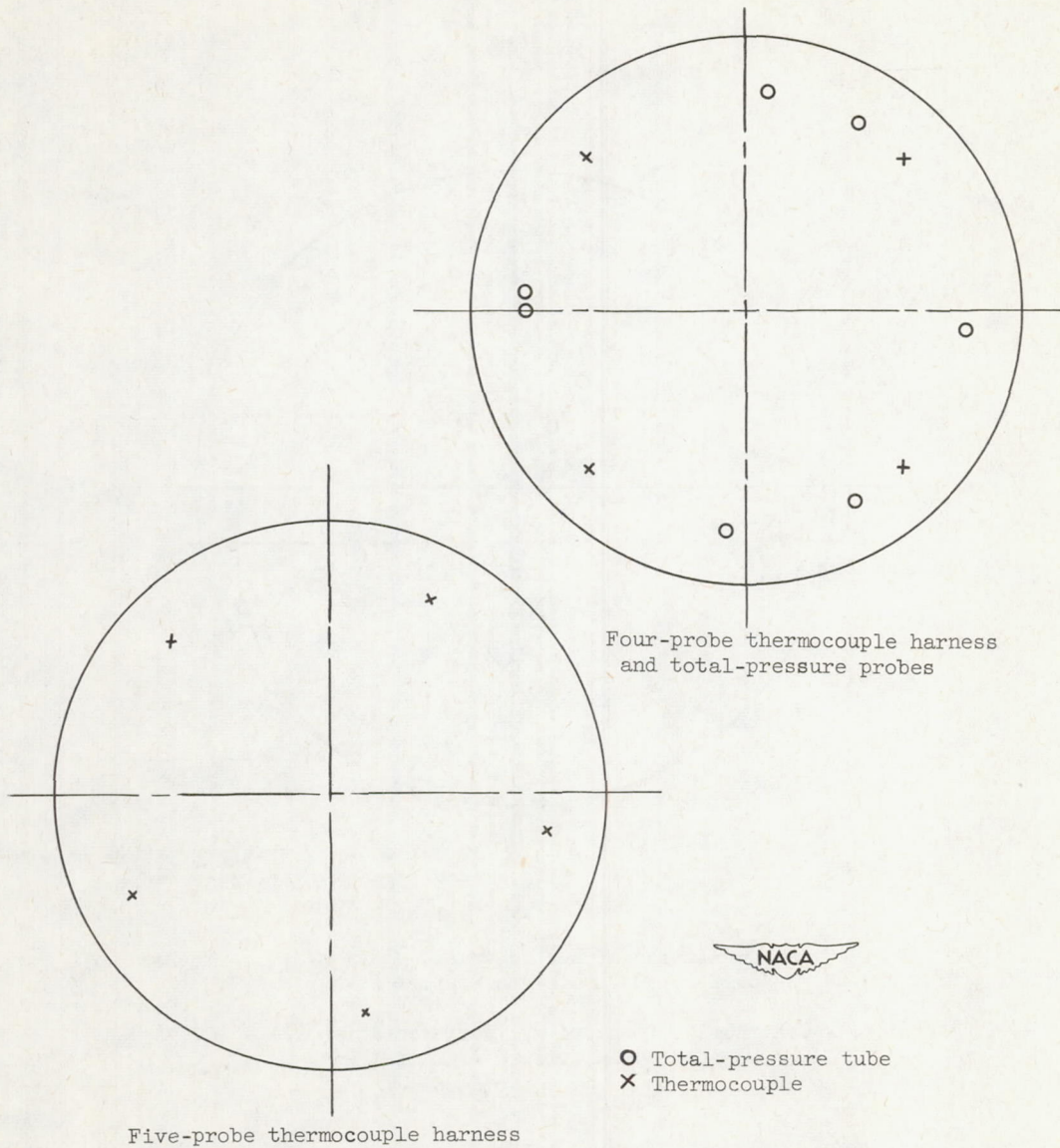Figure 2. - Location of instrumentation at various measuring stations as viewed from upstream.

Outline of com-
bustion chambers

●   Static-pressure tube (wall)
○   Total-pressure tube
✕   Thermocouple
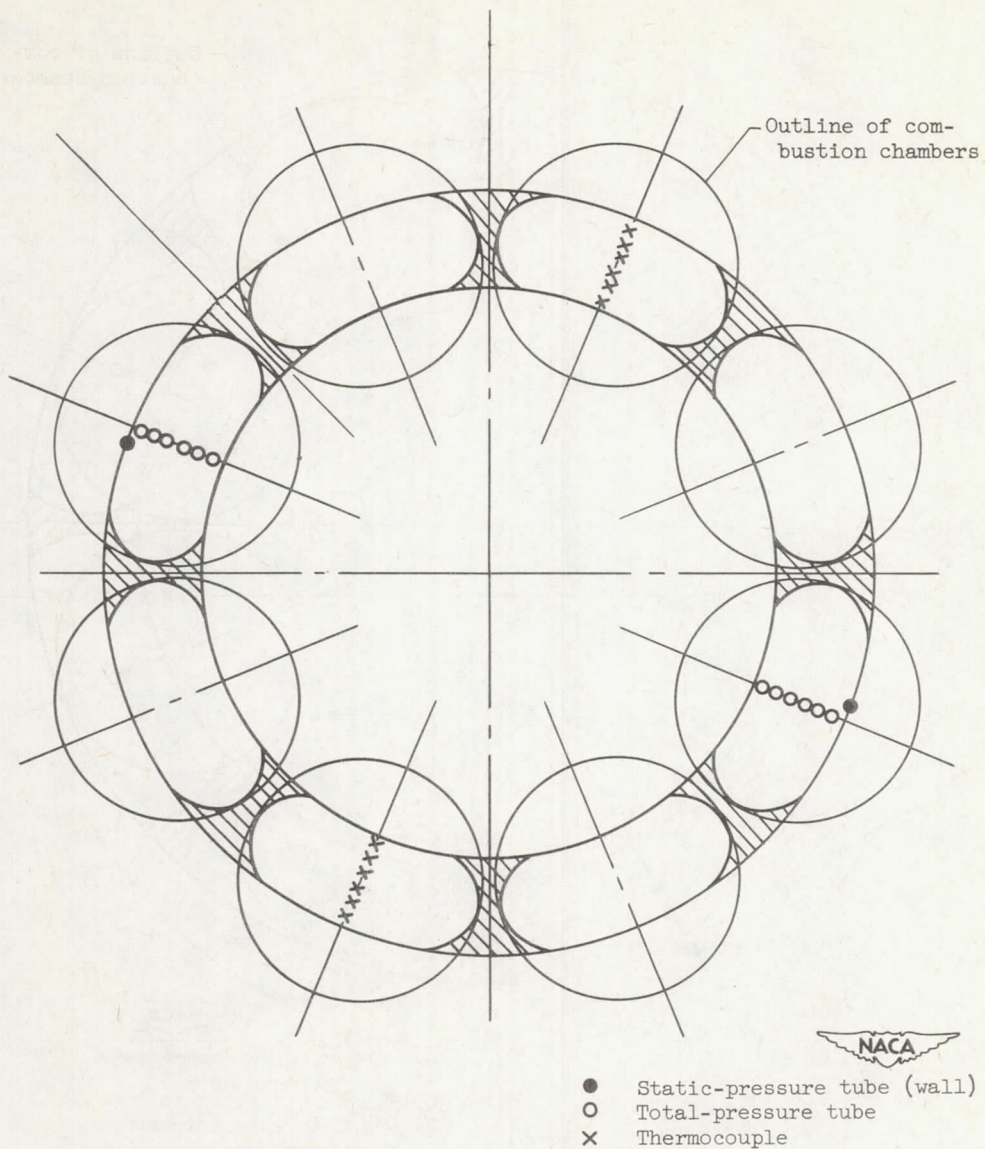
(b) Instrumentation at compressor outlet, station 3, 2 inches downstream of
trailing edge of compressor-outlet guide vanes.

Figure 2. - Continued. Location of instrumentation at various measuring
stations as viewed from upstream.

(c) Instrumentation at turbine inlet, station 4, $1\frac{3}{4}$ inches upstream of leading edge of turbine-inlet guide vanes.

Figure 2. - Continued. Location of instrumentation at various measuring stations as viewed from upstream.

● Static-pressure tube (wall)
○ Total-pressure tube
✗ Thermocouple

(d) Instrumentation at turbine outlet, station 5, $4\frac{7}{8}$ inches downstream of trailing edge of turbine blades.

Figure 2. - Continued. Location of instrumentation at various measuring stations as viewed from upstream.

● Wall static-pressure tube
○ Total-pressure tube
✗ Thermocouple

(e) NACA instrumentation at nozzle inlet, station 9, $15\frac{1}{8}$ inches downstream of tail-cone-outlet flange.

Figure 2. - Continued.   Location of instrumentation at various measuring stations as viewed from upstream.

Four-probe thermocouple harness
and total-pressure probes

O Total-pressure tube
X Thermocouple

Five-probe thermocouple harness

(f) Manufacturer's instrumentation at nozzle inlet, station 9,
$15\frac{1}{8}$ inches downstream of tail-cone-outlet flange.

Figure 2. - Continued. Location of instrumentation at various measuring
stations as viewed from upstream.

2717

45°

● Static-pressure tube
   (wall and rake)
✗ Thermocouple
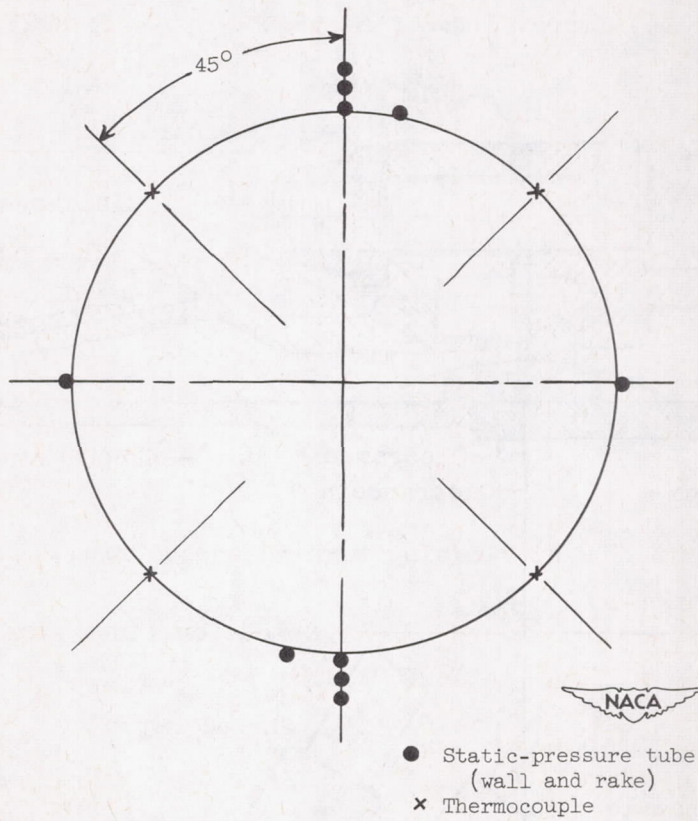
(g) Instrumentation at nozzle lip, station 10.

Figure 2. - Concluded. Location of instrumentation at various
   measuring stations as viewed from upstream.
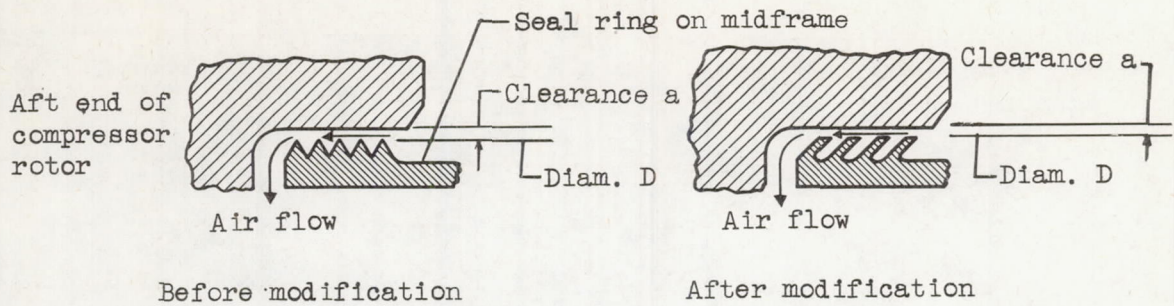
Seal ring on midframe

Clearance a

Aft end of
compressor
rotor

Diam. D

Clearance a

Diam. D

Air flow

Air flow

Before modification

After modification

(a) Improved twelfth-stage compressor seal.

Shim

Clearance b

Tail cone

Turbine
casing

Clearance c

Clearance a

Shroud ring

Nozzle diaphragm

(b) Floating turbine shroud ring.

Combustor liner dome

Shroud cap

Duplex fuel nozzle
used on standard
engine

Standard nozzle threaded
to receive shroud cap

Air inlet holes
in shroud cap
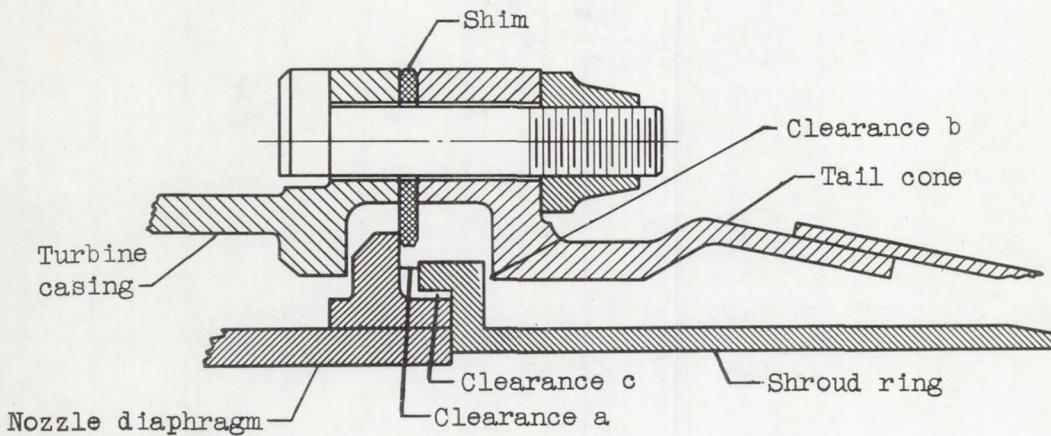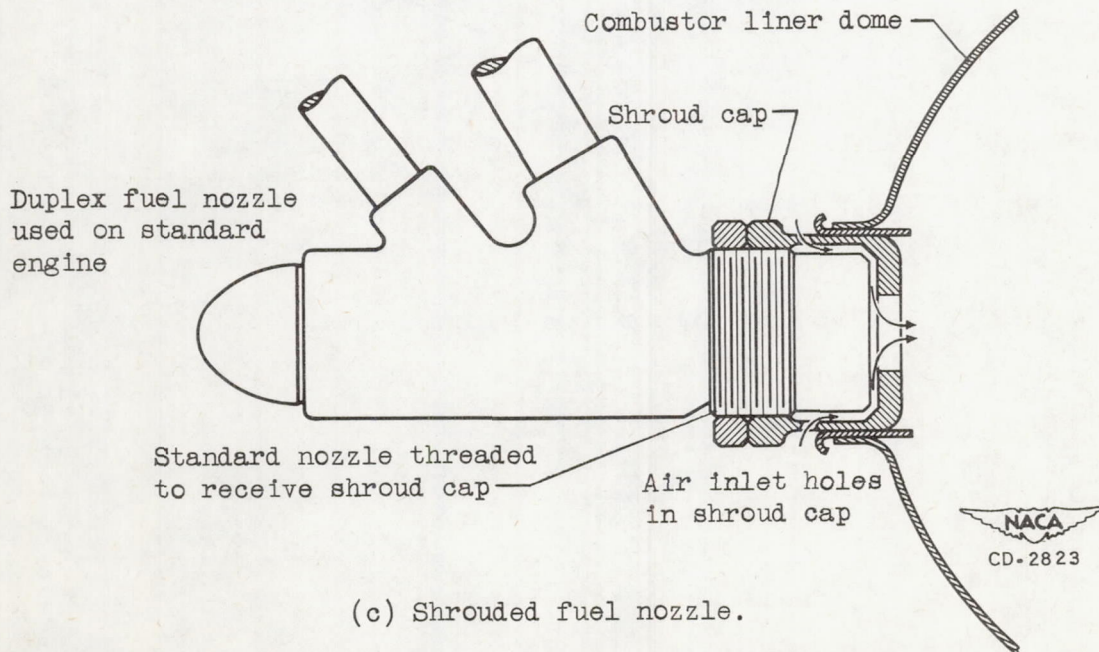
NACA

CD-2823

(c) Shrouded fuel nozzle.

Figure 3. - Engine modifications incorporated in configurations B and C.
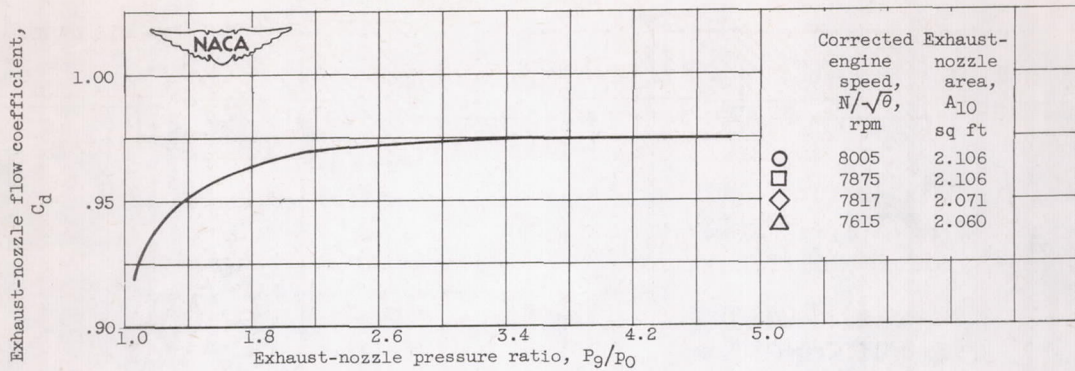
(a) Exhaust-nozzle flow coefficient as function of nozzle
pressure ratio (ref. 4).
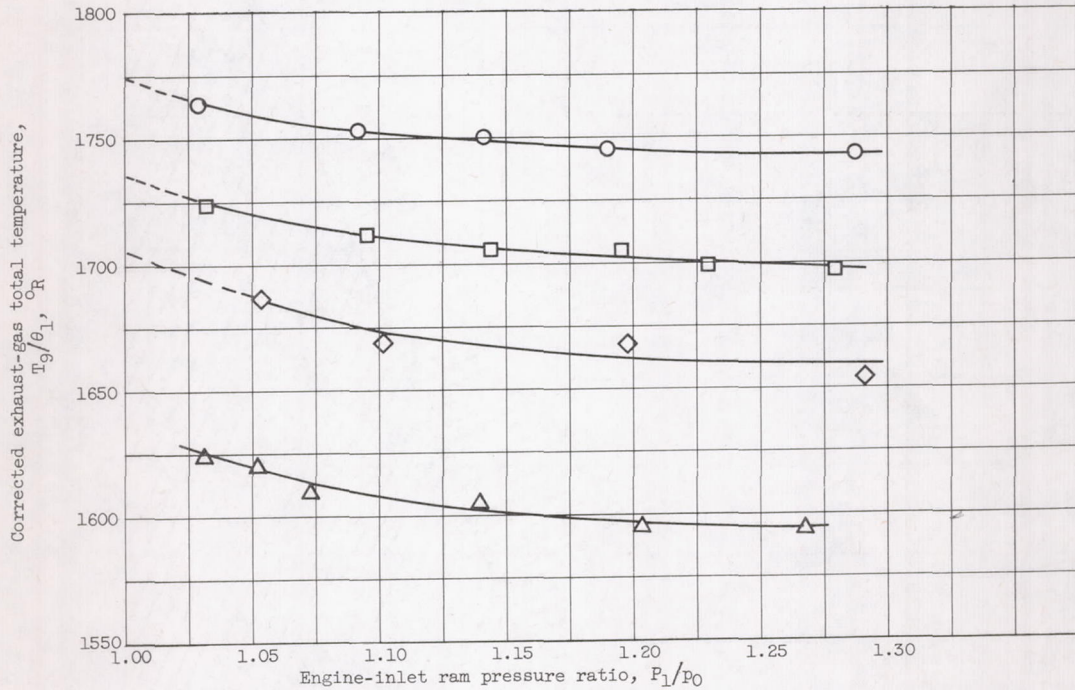
(b) Corrected exhaust-gas total temperature.
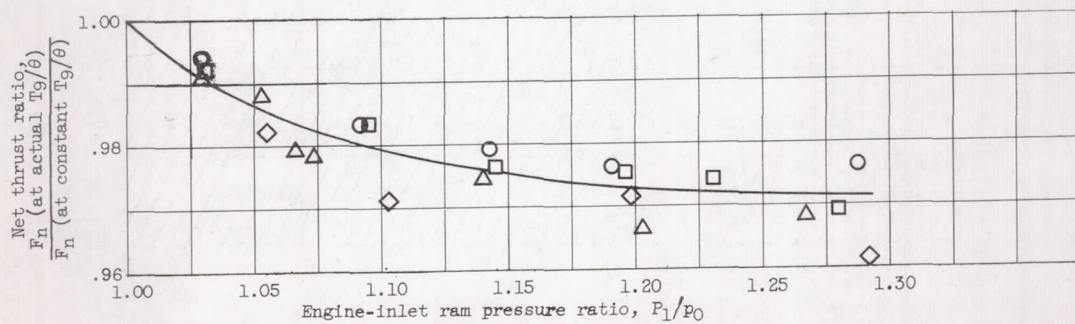
(c) Net thrust loss.

Figure 4. - Effect of exhaust-nozzle flow coefficient on engine performance.
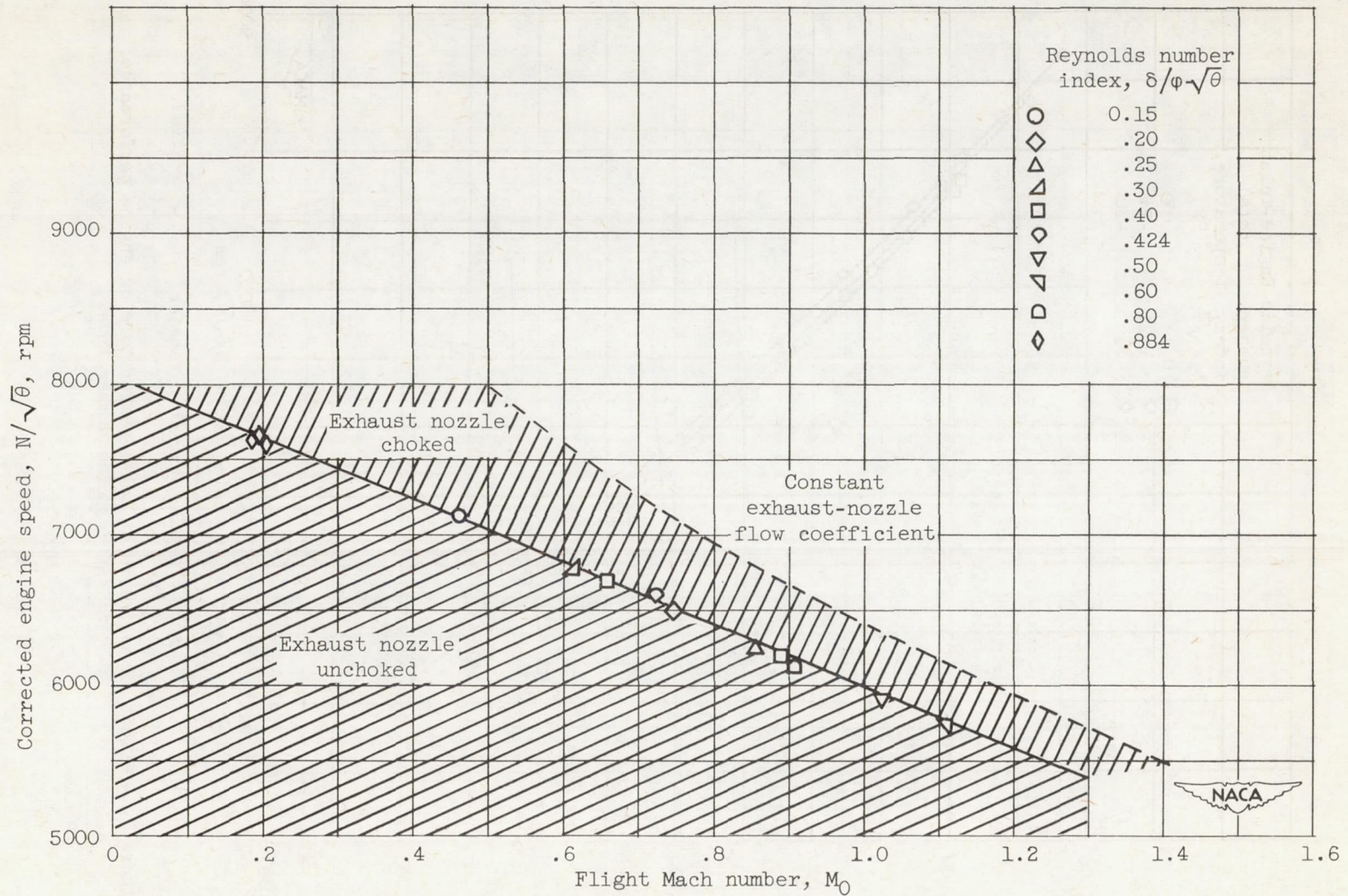
Figure 5. - Flight conditions for which varying flow coefficient corrections must be applied to performance data.

Reynolds number index, $\delta/\varphi\sqrt{\theta}$	Engine-inlet total temperature, $^{\circ}F$
□ 0.4	7
◇ .424	-24
◊ .4	-50
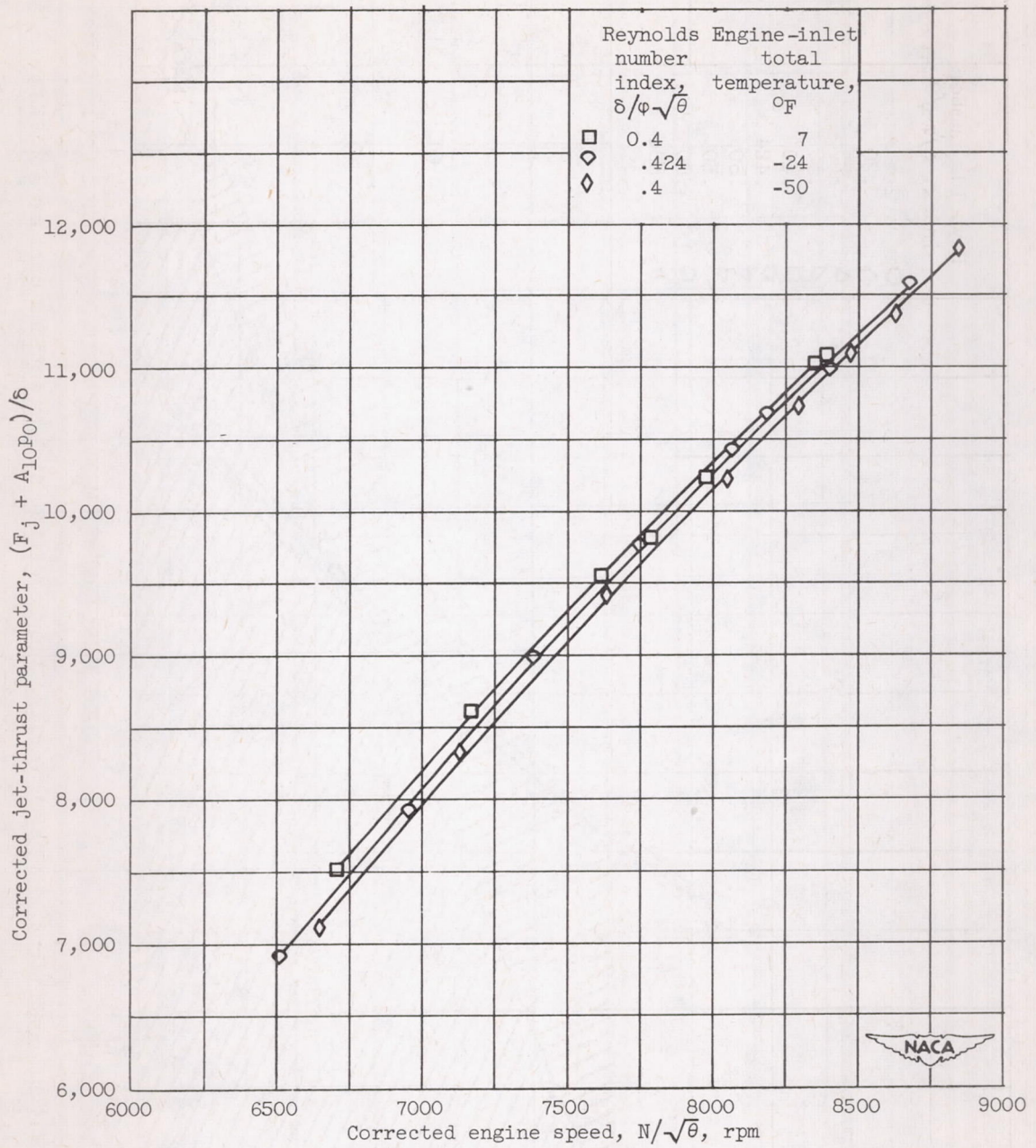
(a) Jet-thrust parameter.

Figure 6. - Effect of engine-inlet total temperature on engine performance at constant Reynolds number index.

Reynolds | Engine-inlet
number | total
index, | temperature,
$\delta/\varphi\sqrt{\theta}$ | ^{o}F

□   0.4   7
◇   .424   -24
◇   .4   -50

2200

2000

1800

1600

1400

1200

1000

Corrected exhaust-gas total temperature, T_9/θ_1, ^{o}R

6000   6500   7000   7500   8000   8500   9000

Corrected engine speed, $N/\sqrt{\theta}$, rpm

NACA
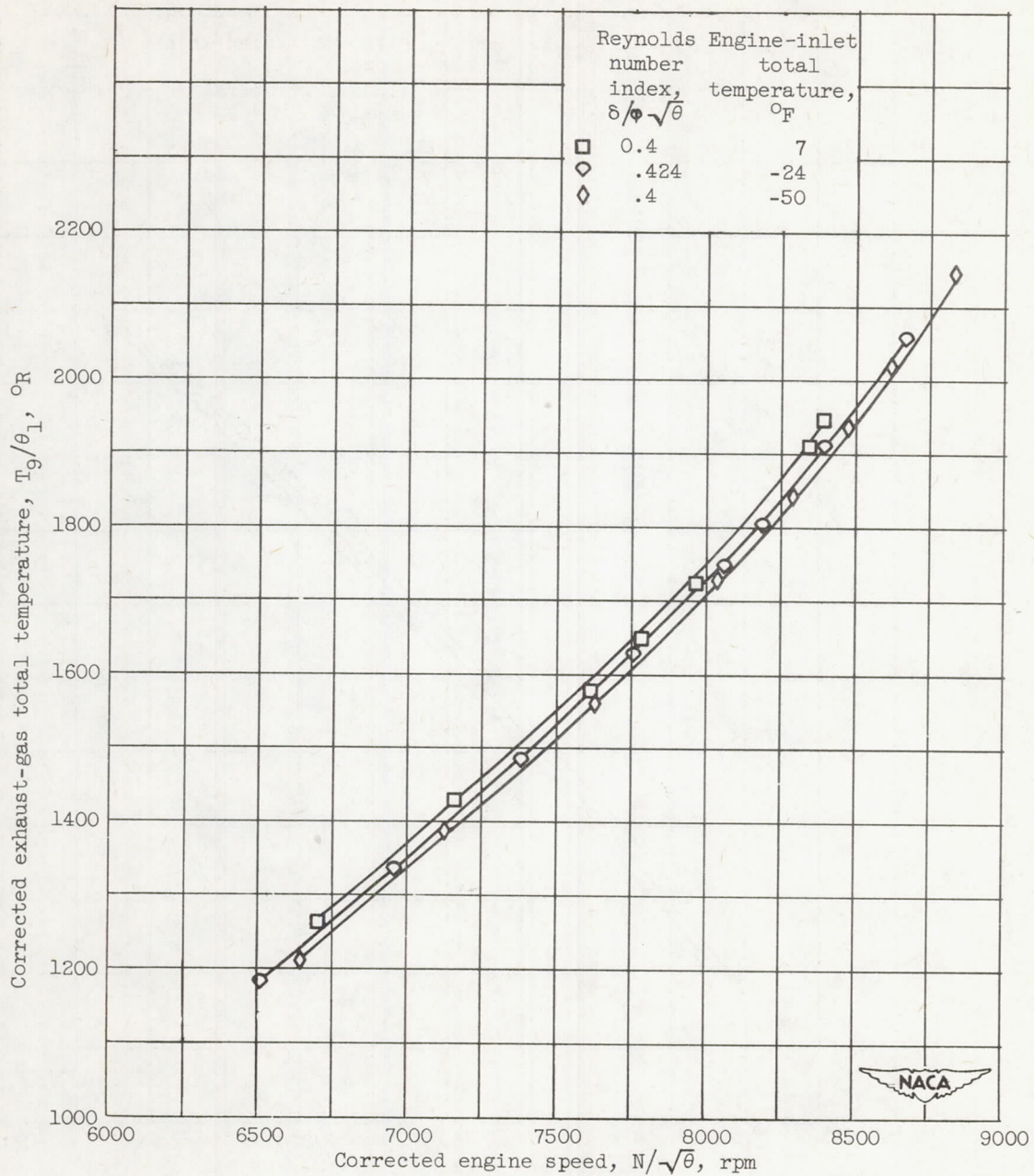
(b) Corrected exhaust-gas total temperature.

Figure 6. - Continued. Effect of engine-inlet total temperature on engine
performance at constant Reynolds number index.

2717

The legend in the chart reads:

Reynolds number index, $\delta/\varphi\sqrt{\theta}$	Engine-inlet total temperature, $^{\circ}F$
□ 0.4	7
◇ .424	-24
◇ .4	-50

Vertical axis: Corrected ideal fuel-air ratio, $\eta_b f/\theta$

Horizontal axis: Corrected engine speed, $N/\sqrt{\theta}$, rpm
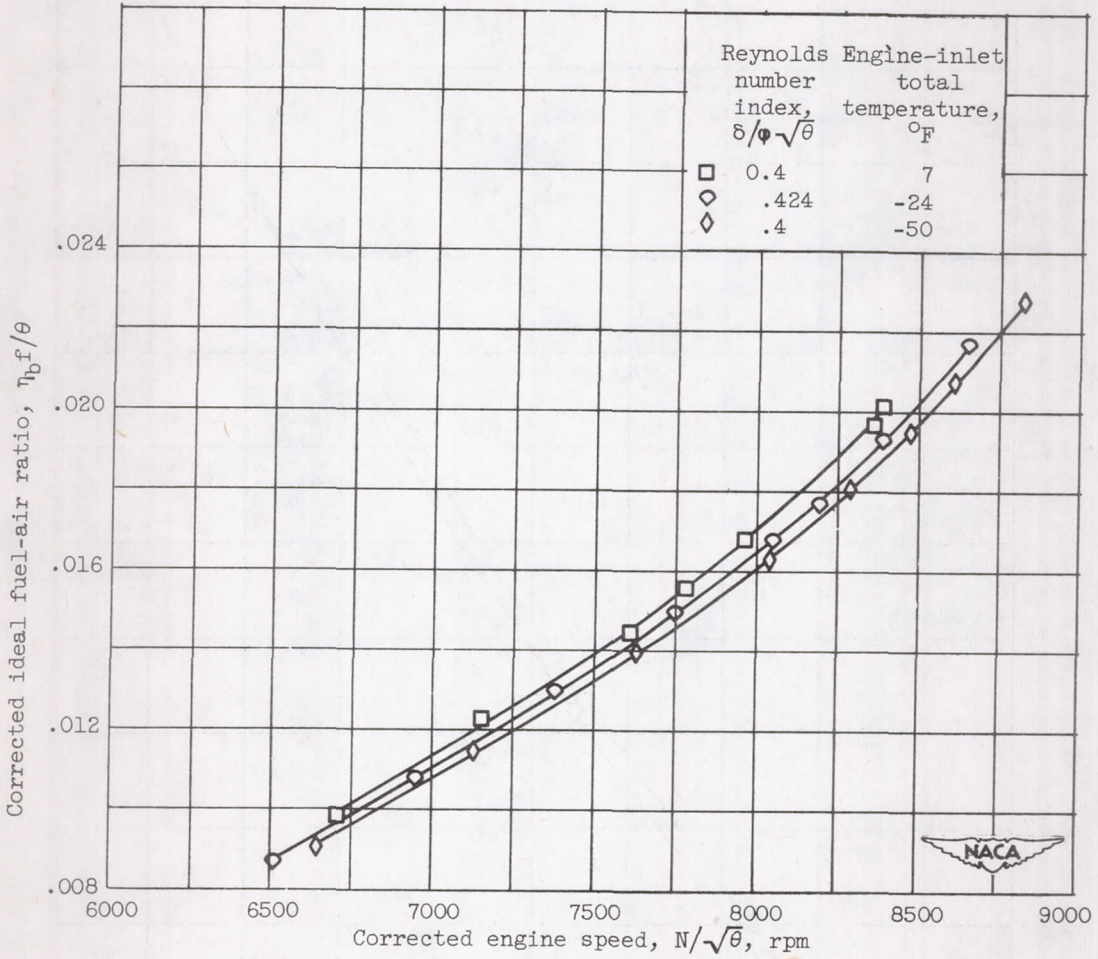
(c) Corrected ideal fuel-air ratio.

Figure 6. - Concluded. Effect of engine-inlet total temperature on engine performance at constant Reynolds number index.
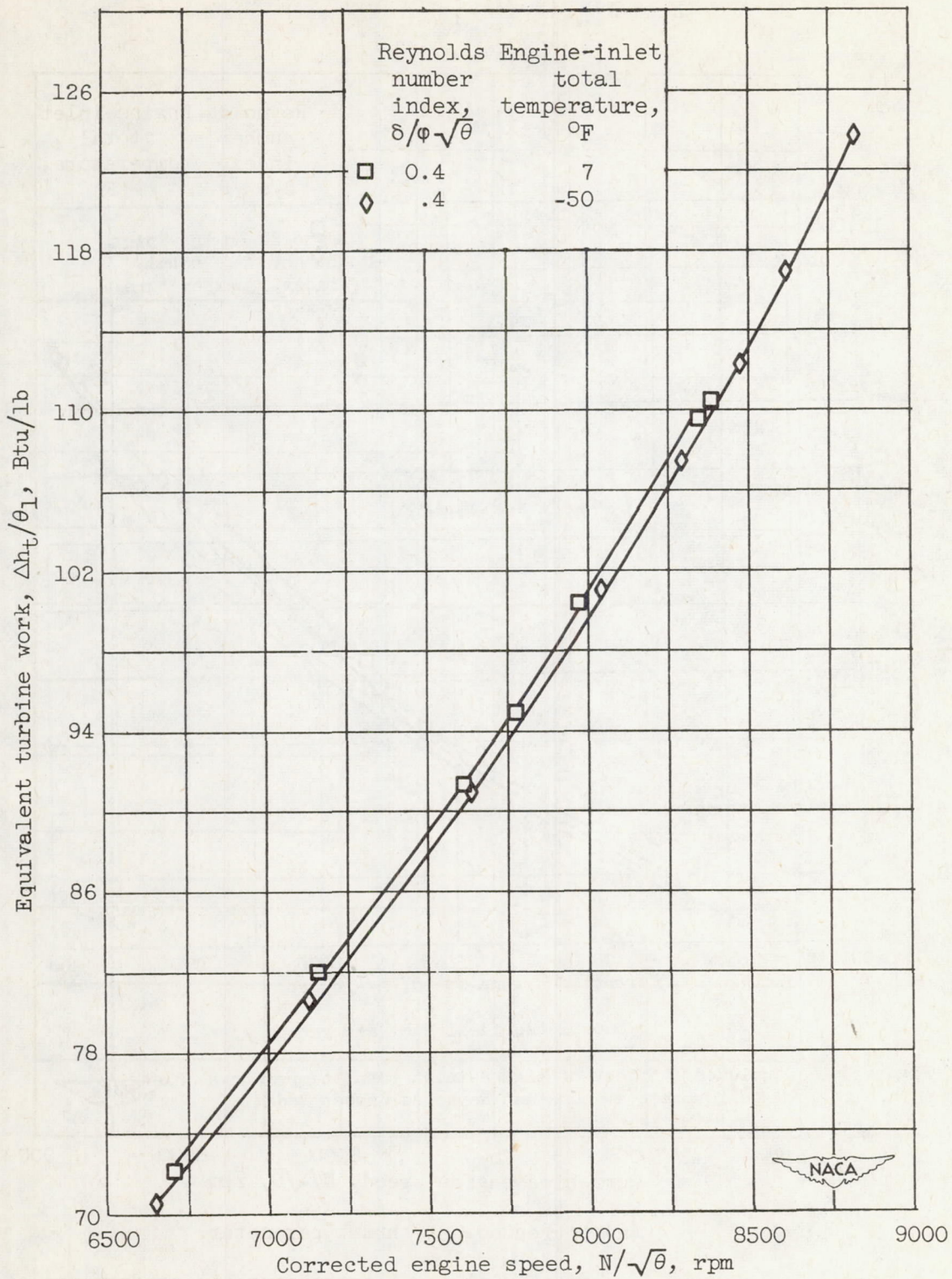
Figure 7. - Effect of engine-inlet total temperature on
equivalent turbine work.
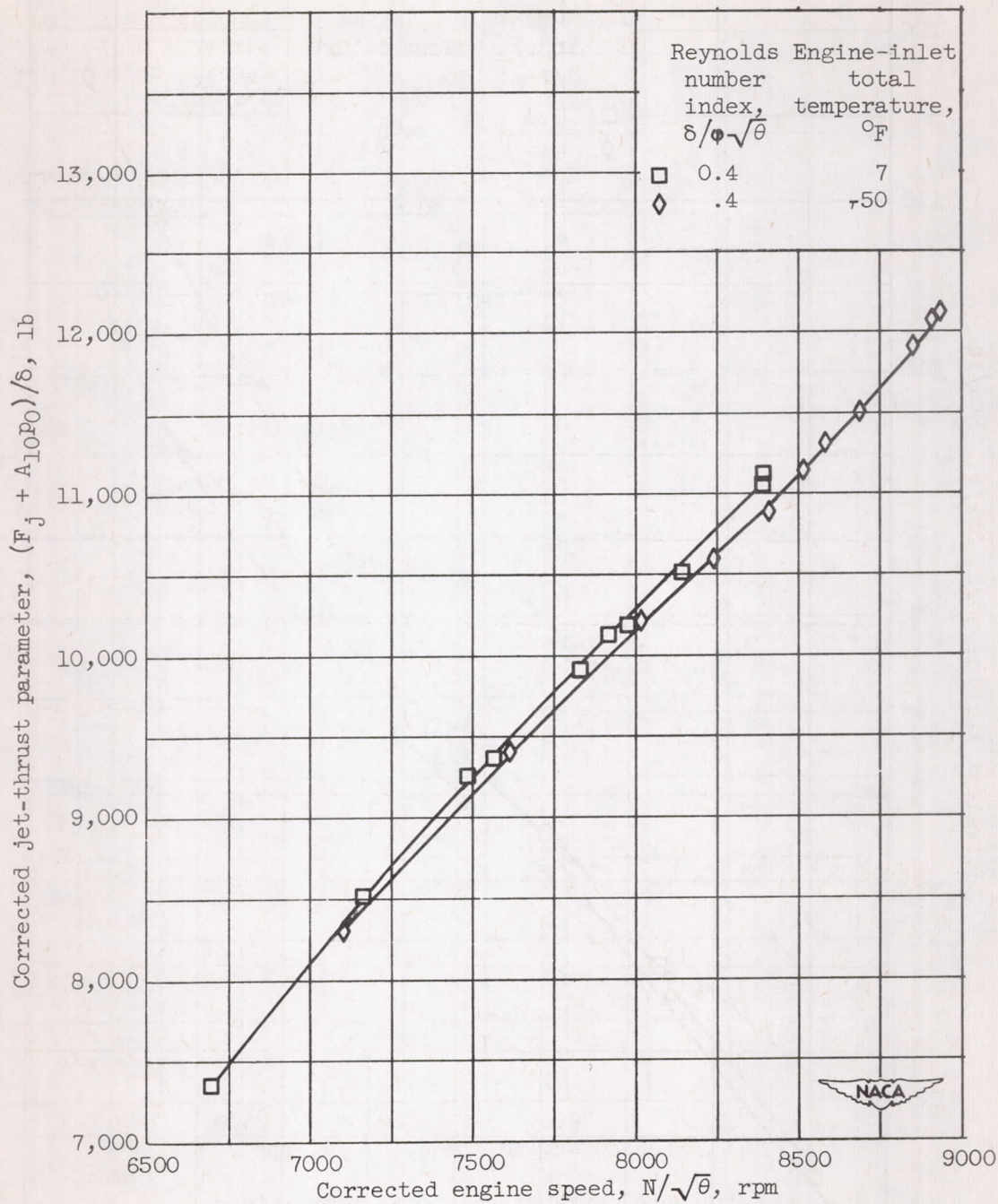
(a) Corrected jet-thrust parameter.

Figure 8. - Effect of engine-inlet total temperature on performance of J47-GE-17 engine with no turbine-outlet straightening vanes installed.
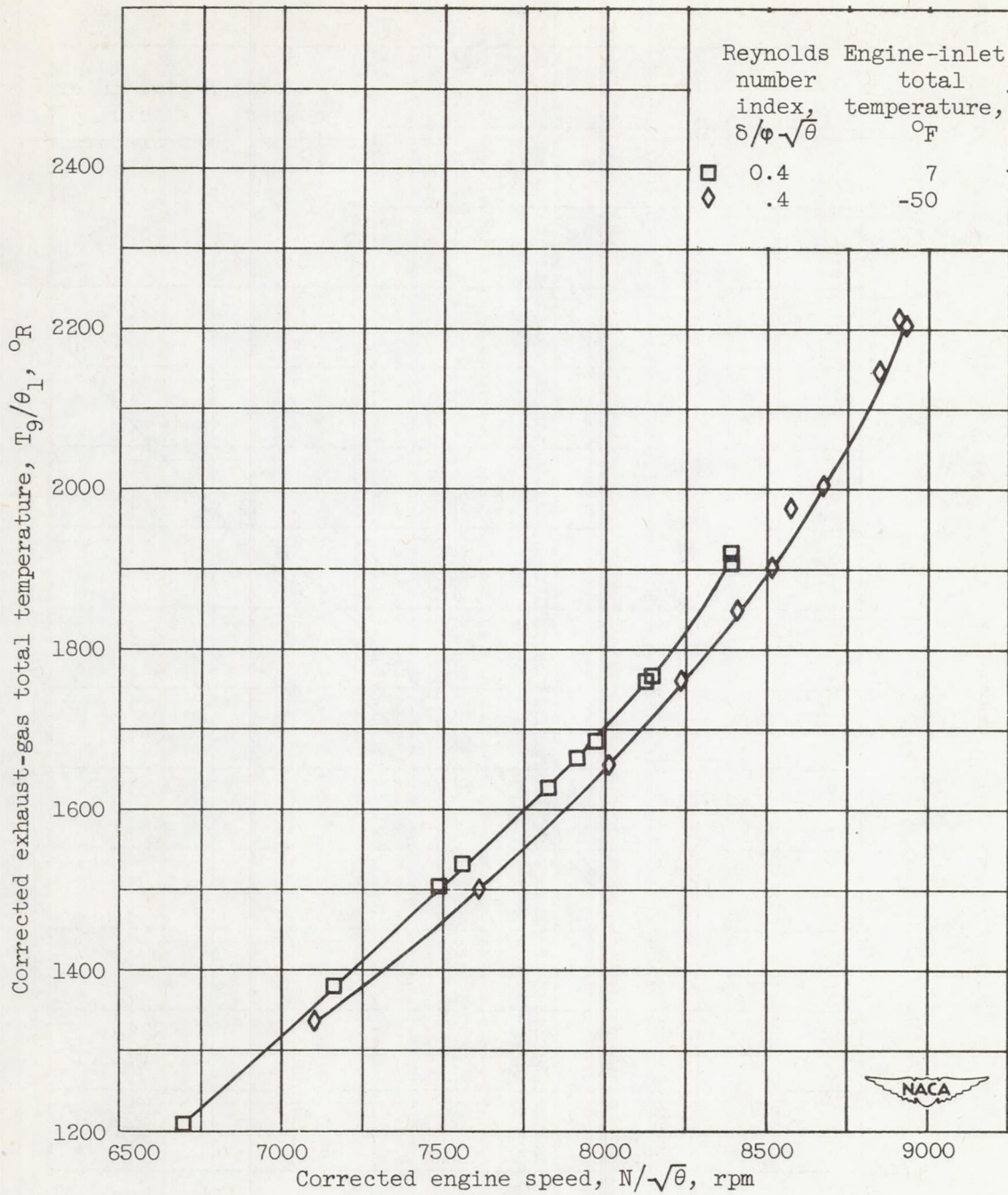
(b) Corrected exhaust-gas total temperature.

Figure 8. - Continued. Effect of engine-inlet total temperature on
   performance of J47-GE-17 engine with no turbine-outlet straightening
   vanes installed.
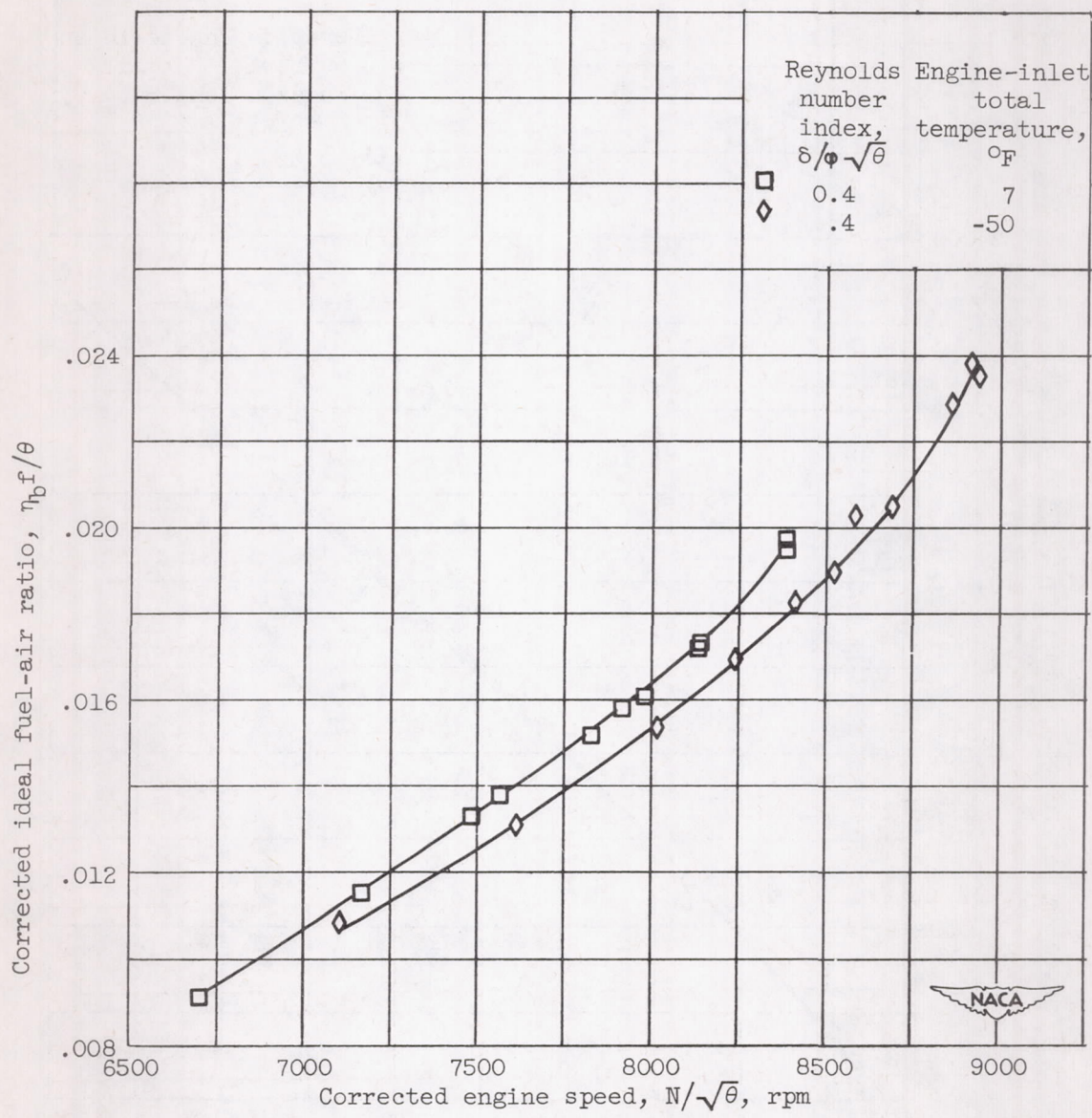
(c) Corrected ideal fuel-air ratio.

Figure 8. - Concluded. Effect of engine-inlet total temperature on
performance of J47-GE-17 engine with no turbine-outlet straightening
vanes installed.
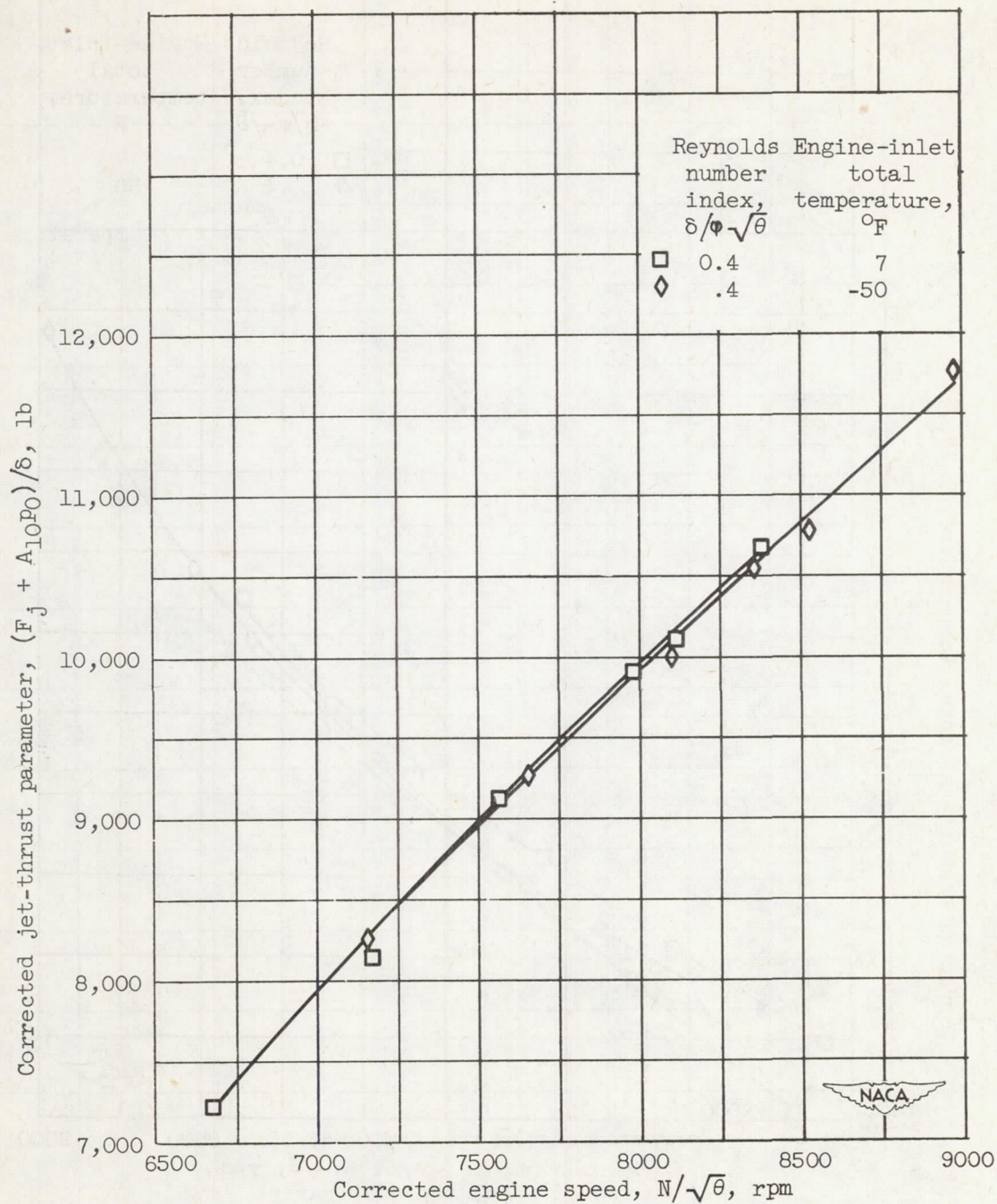
(a) Corrected jet-thrust parameter.

Figure 9. - Effect of engine-inlet total temperature on performance of J47-GE-17 engine with turbine-outlet straightening vanes installed.
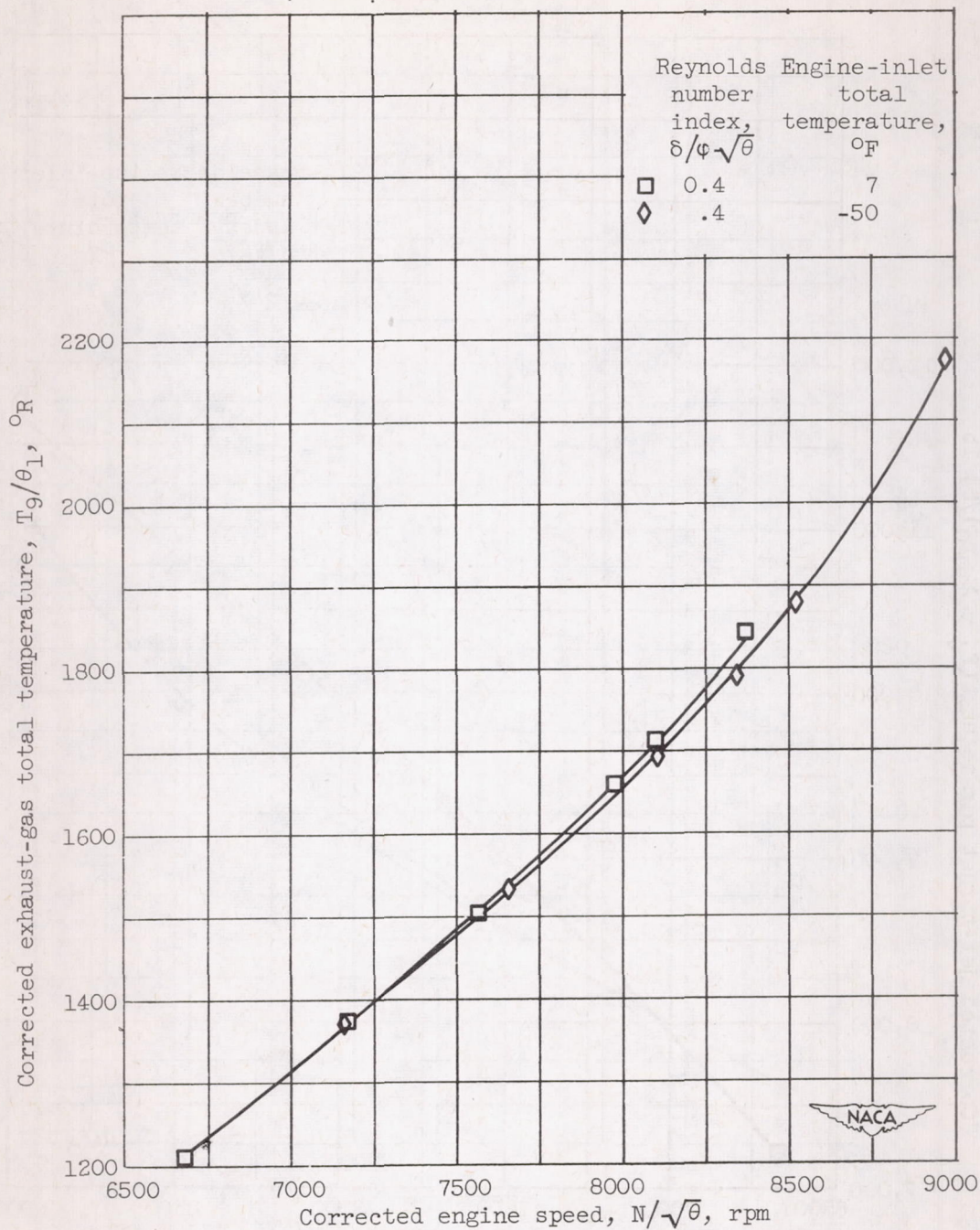
(b) Corrected exhaust-gas total temperature.

Figure 9. - Continued. Effect of engine-inlet total temperature on performance of J47-GE-17 engine with turbine-outlet straightening vanes installed.
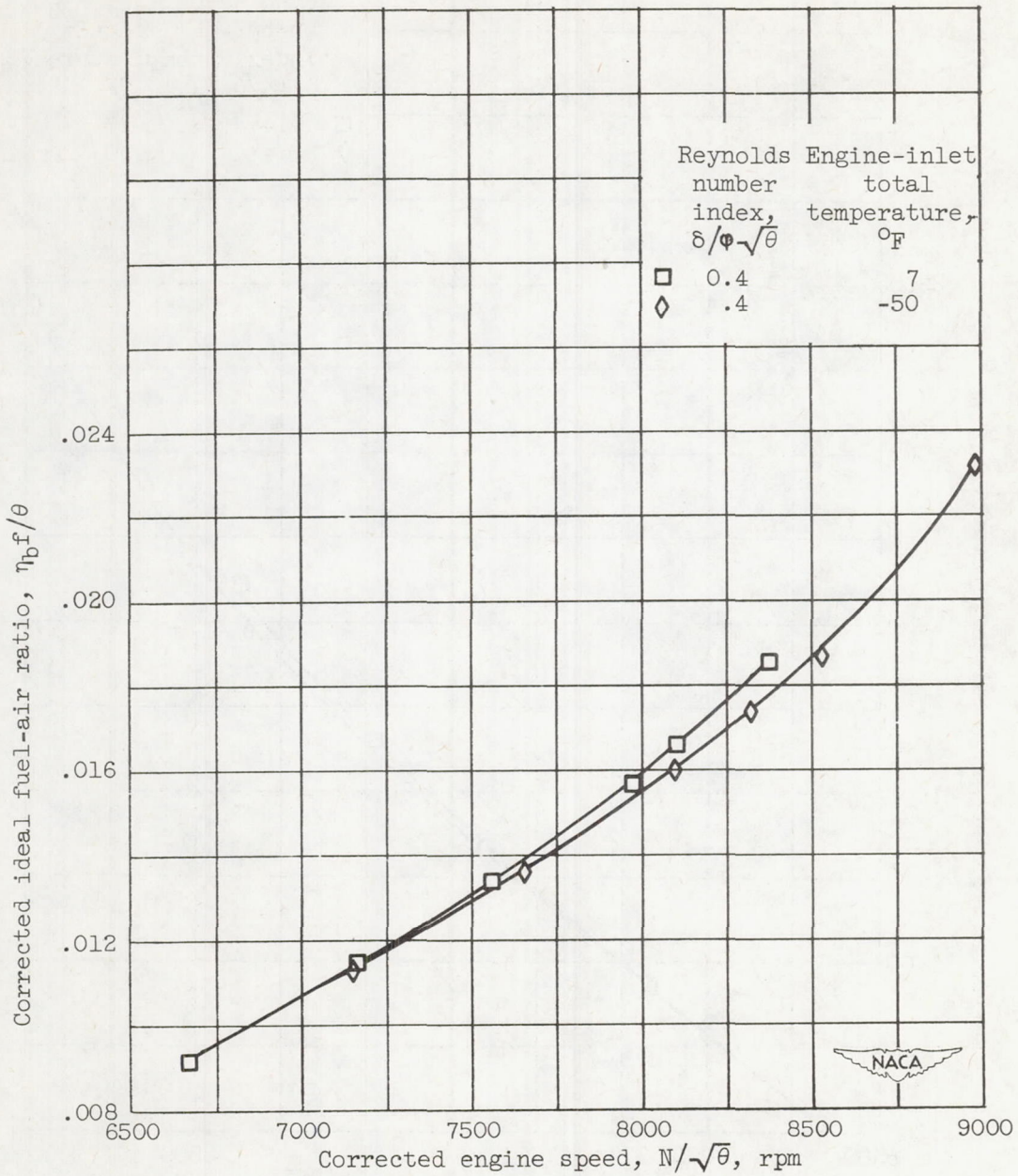
(c) Corrected ideal fuel-air ratio.

Figure 9. - Concluded. Effect of engine-inlet total temperature on
performance of J47-GE-17 engine with turbine-outlet straightening
vanes installed.
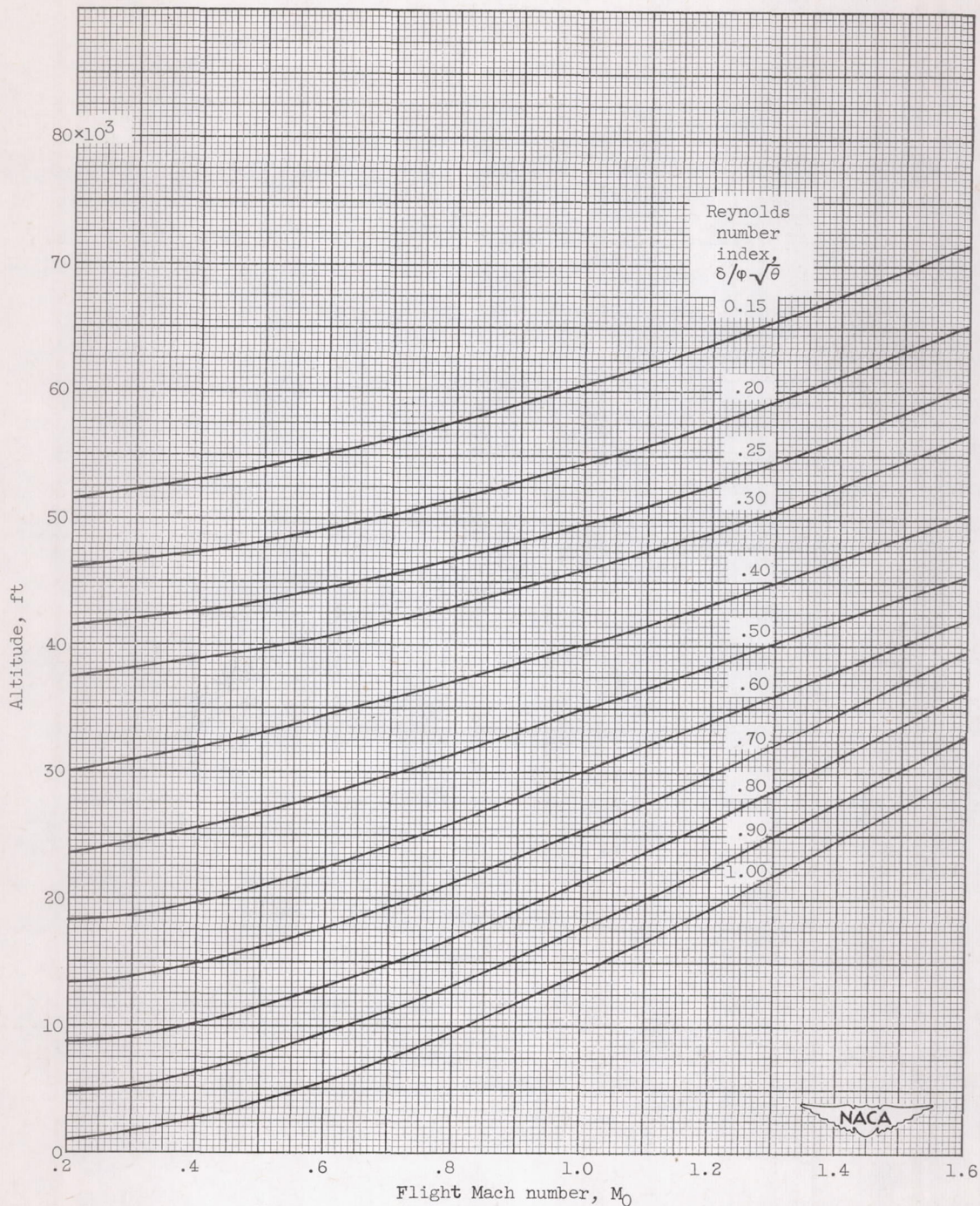
Figure 10. - Reynolds number index as a function of altitude and Mach number assuming 100 percent ram pressure recovery.
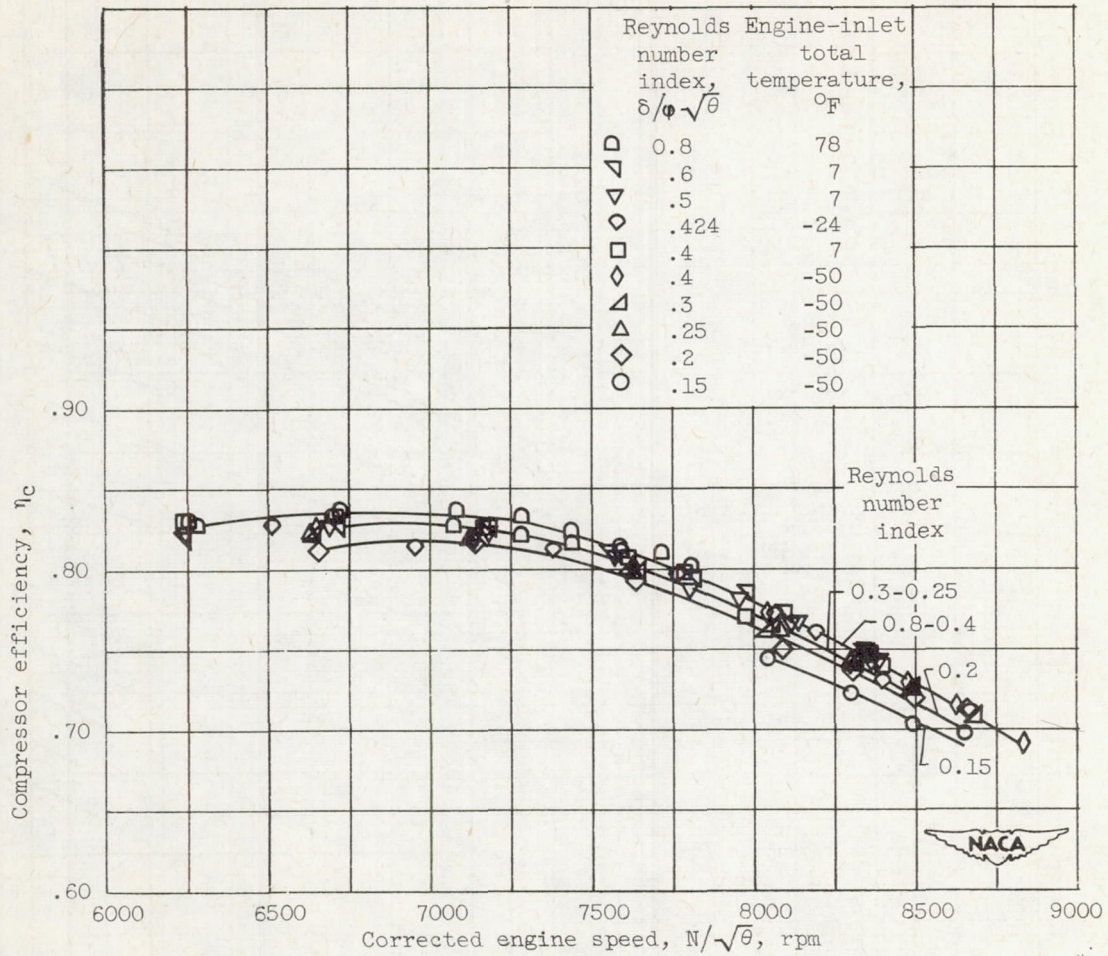
(a) Compressor efficiency.

Figure 11. - Effect of Reynolds number index on compressor performance.
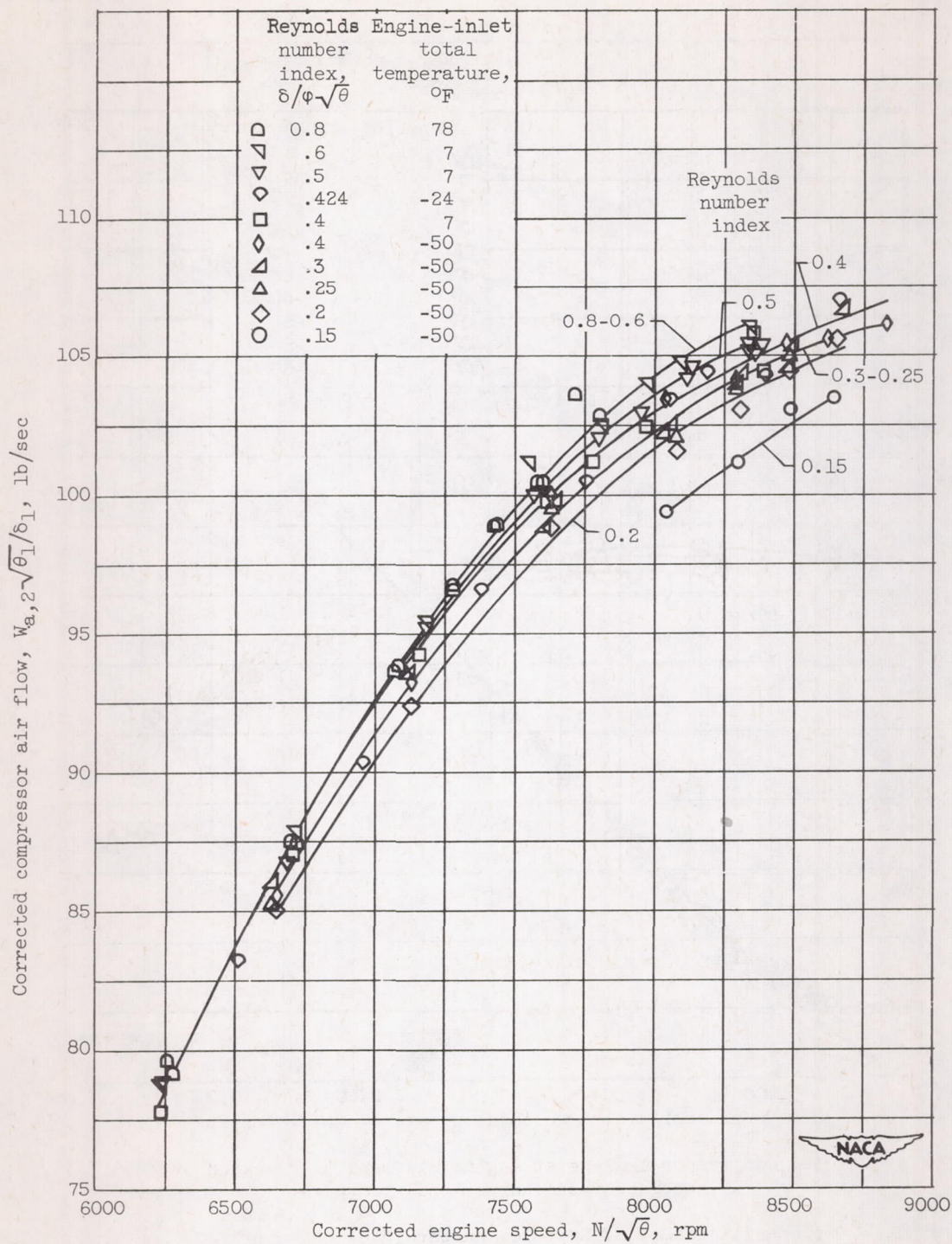
2717

(b) Corrected compressor air flow.

Figure 11. - Continued. Effect of Reynolds number index on compressor performance.

	Reynolds number index, $\delta/\varphi\sqrt{\theta}$	Engine-inlet total temperature, °F
◻	0.8	78
◁	.6	7
▽	.5	7
◇	.424	-24
◻	.4	7
◇	.4	-50
◁	.3	-50
△	.25	-50
◇	.2	-50
○	.15	-50
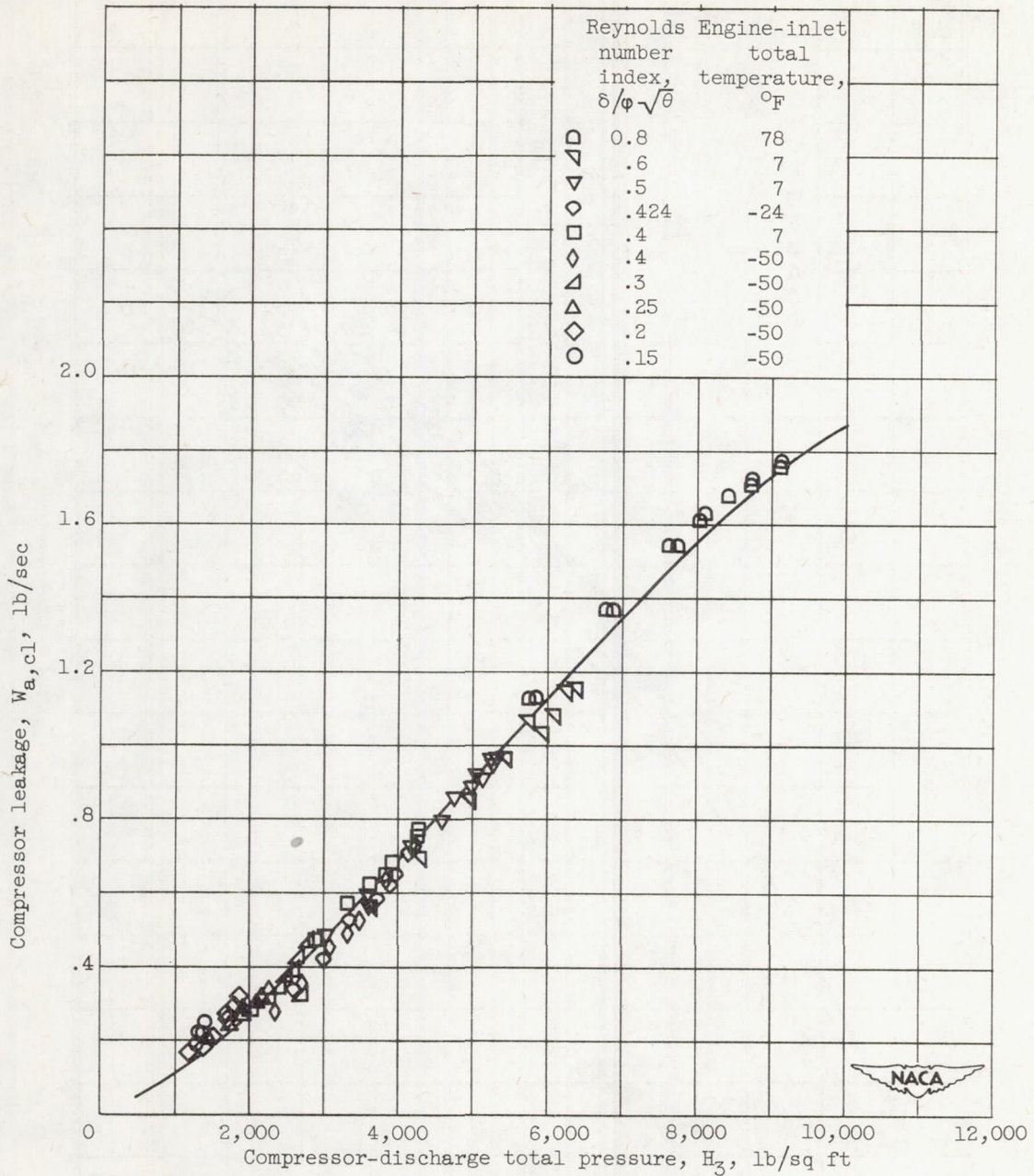
(c) Compressor leakage at engine midframe as function of compressor-discharge total pressure.

Figure 11. - Continued. Effect of Reynolds number index on compressor performance.

Reynolds number index, $\delta/\varphi\sqrt{\theta}$	Engine-inlet total temperature, °F
0.8	78
.6	7
.5	7
.424	-24
.4	7
.4	-50
.3	-50
.25	-50
.2	-50
.15	-50
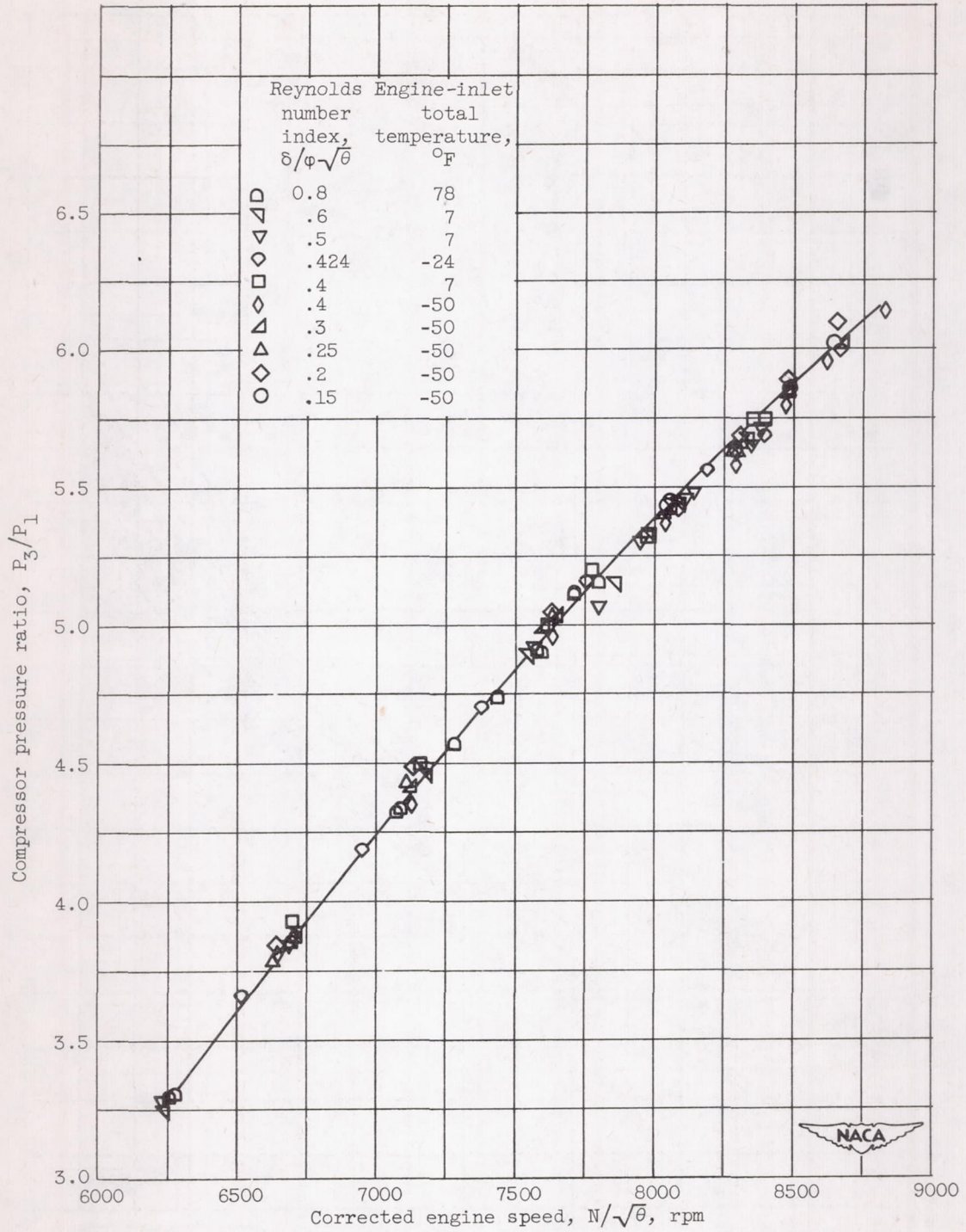
(d) Compressor pressure ratio as function of corrected engine speed.

Figure 11. - Continued. Effect of Reynolds number index on compressor performance.

	Reynolds number index, $\delta/\varphi\sqrt{\theta}$	Engine-inlet total temperature, °F
◁ ◻	0.8	78
▽	.6	7
▽	.5	7
◇	.424	-24
◻	.4	7
◇	.4	-50
◁	.3	-50
△	.25	-50
◇	.2	-50
○	.15	-50

Compressor pressure ratio, P_3/P_1

Corrected compressor air flow, $W_{a,2}\sqrt{\theta_1}/\delta_1$, lb/sec
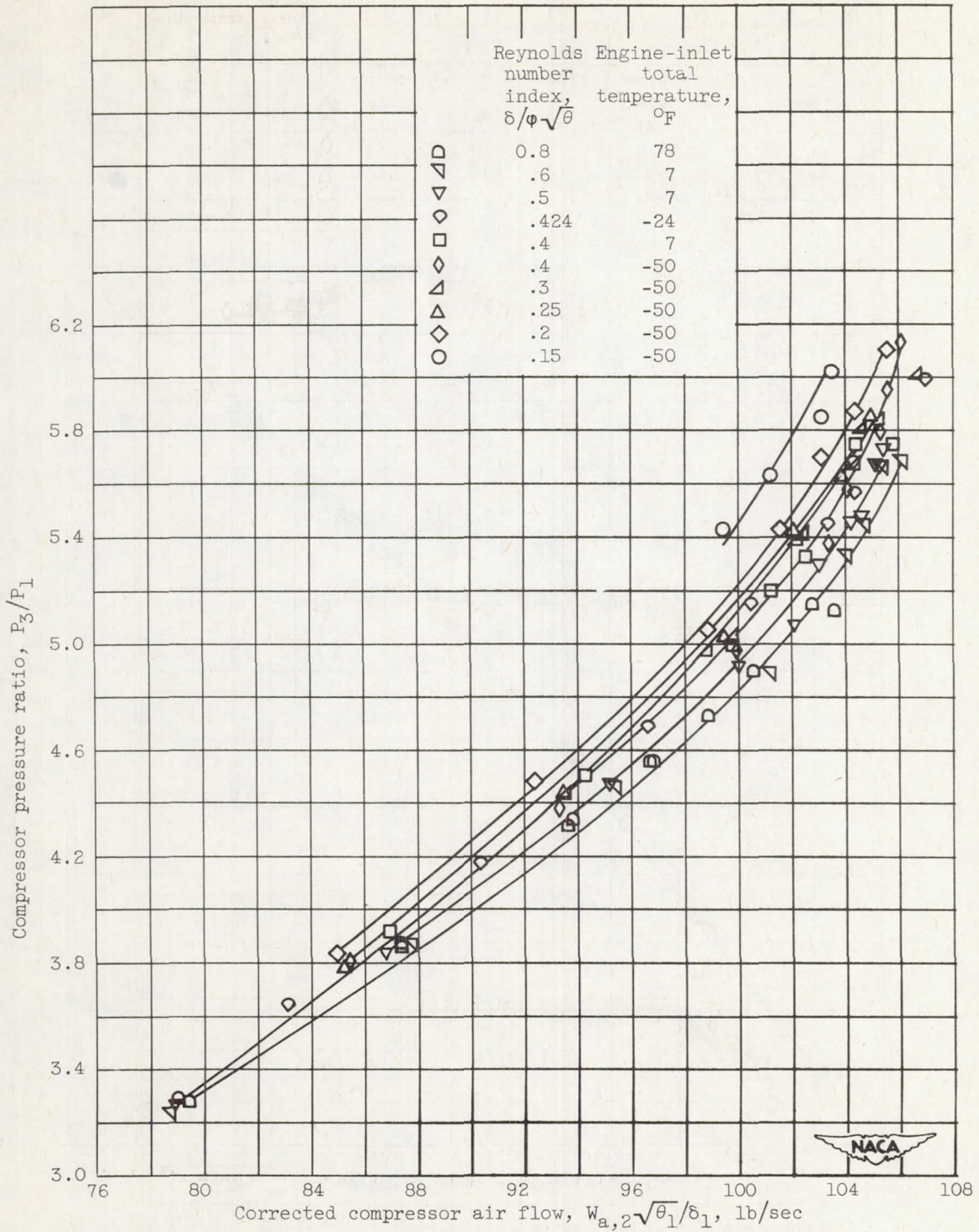
(e) Compressor pressure ratio as function of corrected compressor air flow.

Figure 11. - Concluded.   Effect of Reynolds number index on compressor performance.

Reynolds number index, $\delta/\varphi\sqrt{\theta}$	Engine-inlet total temperature, °F
0.8	78
.6	7
.5	7
.424	-24
.4	7
.4	-50
.3	-50
.25	-50
.2	-50
.15	-50
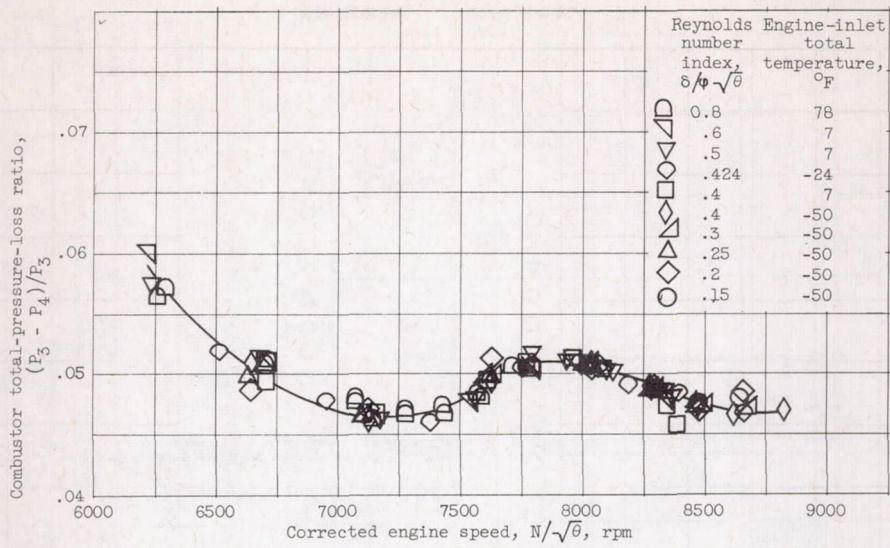
(a) Combustor pressure loss ratio.
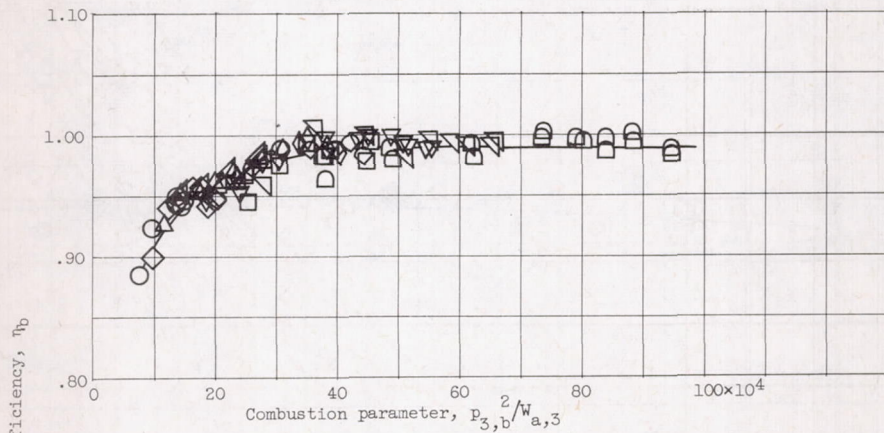
(b) Combustion efficiency.
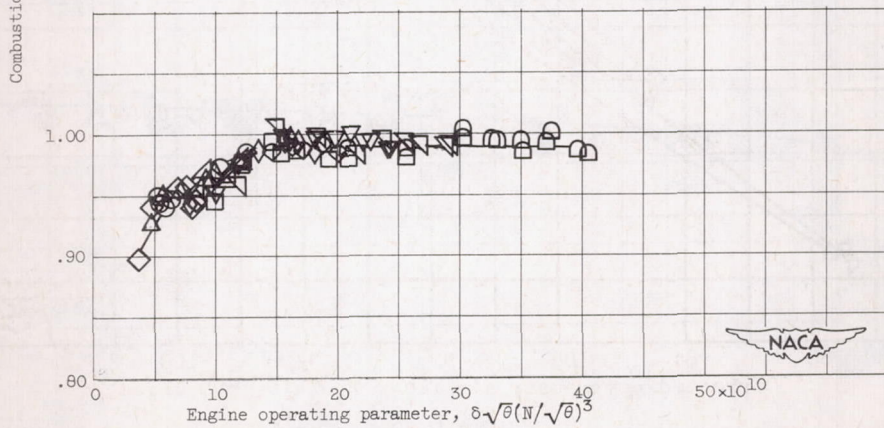
(c) Combustion efficiency as function of inlet conditions.

Figure 12. - Effect of Reynolds number index on combustor performance.
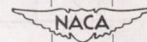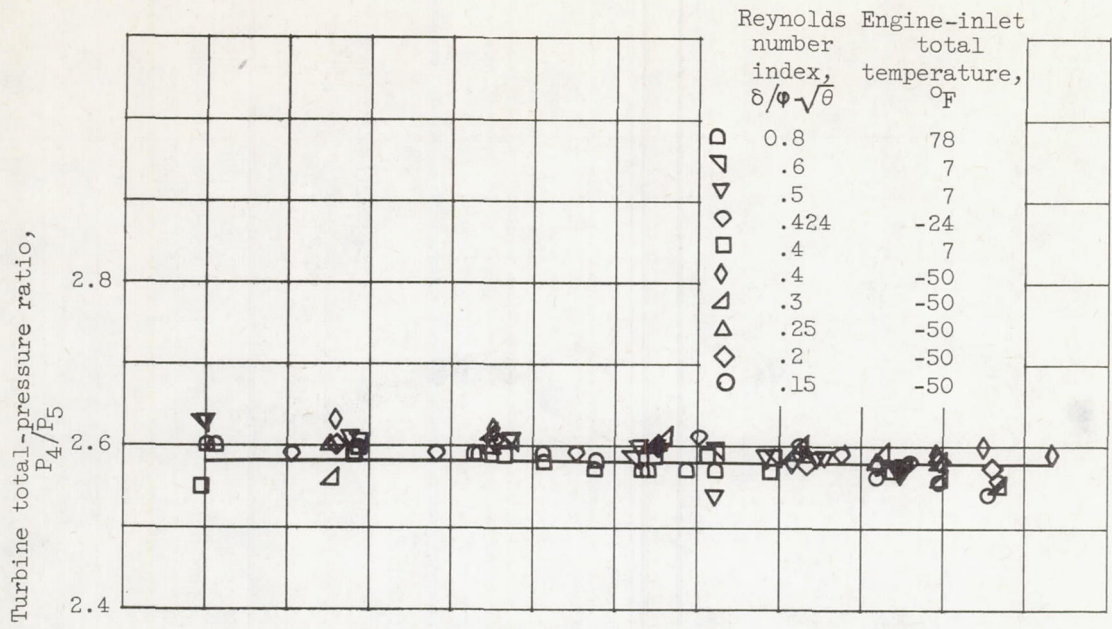
(a) Turbine pressure ratio.
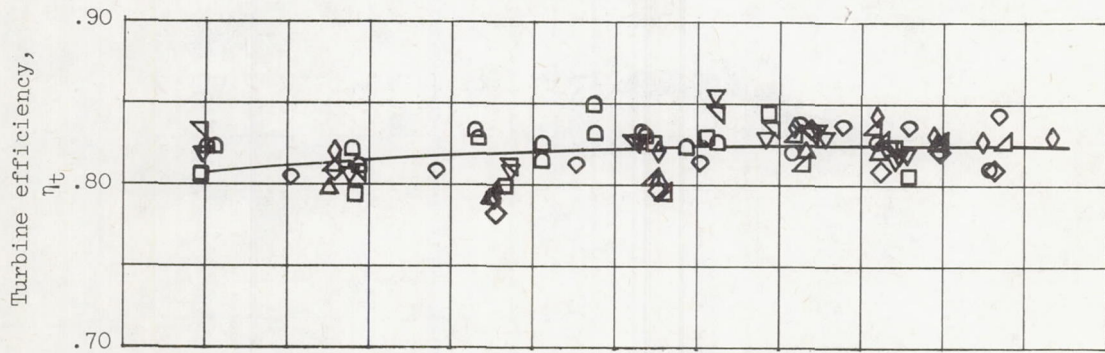
(b) Turbine efficiency.
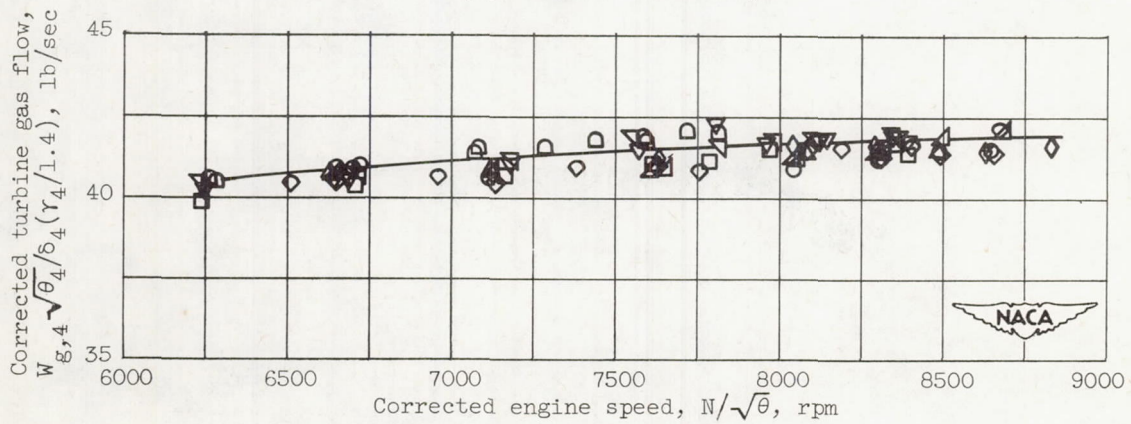
(c) Corrected turbine gas flow.

Figure 13. - Effect of Reynolds number index on turbine performance.

2717
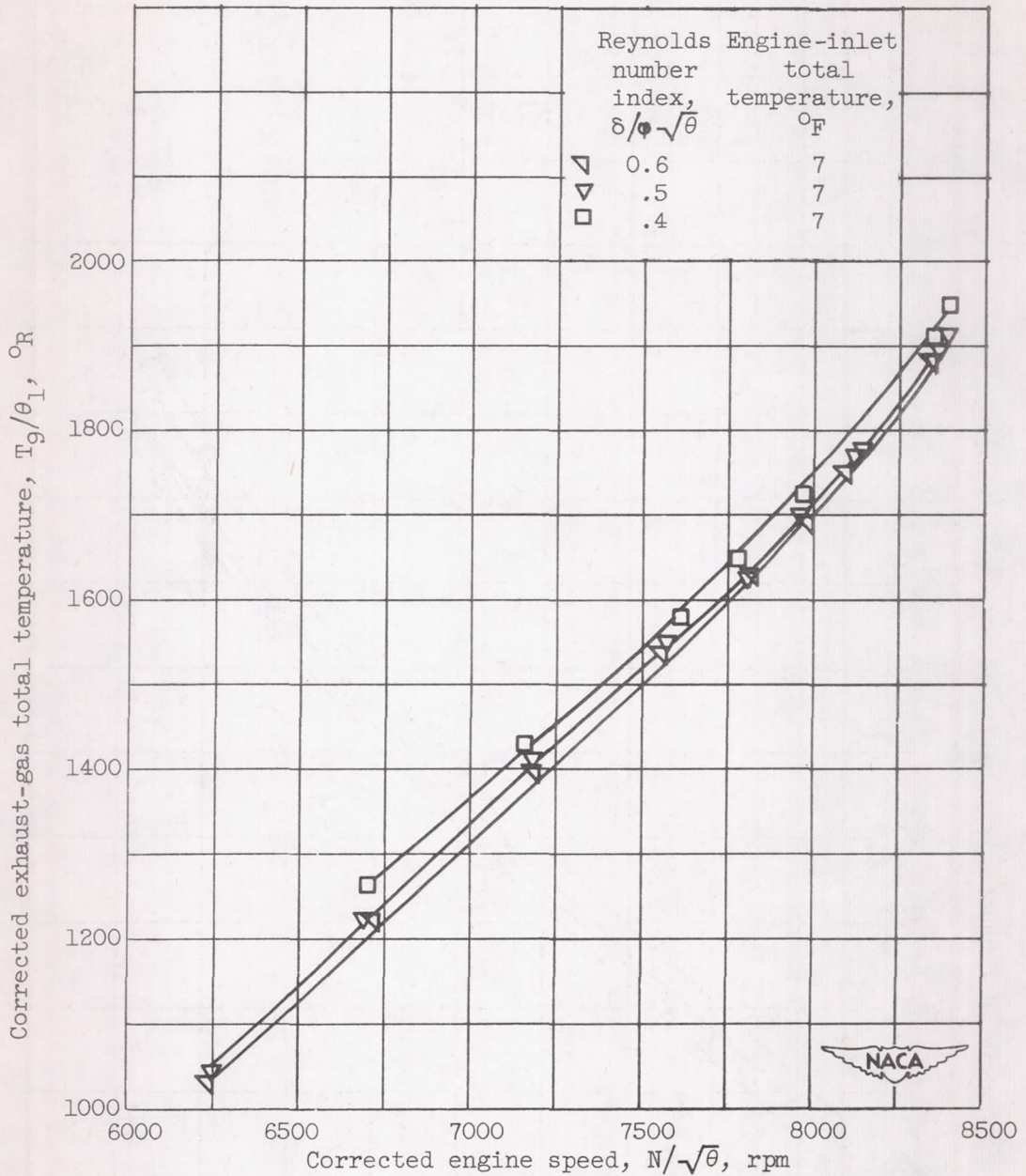
(a) Corrected exhaust-gas total temperature at inlet
temperature of 7° F.

Figure 14. - Effect of Reynolds number index on over-all
engine performance.
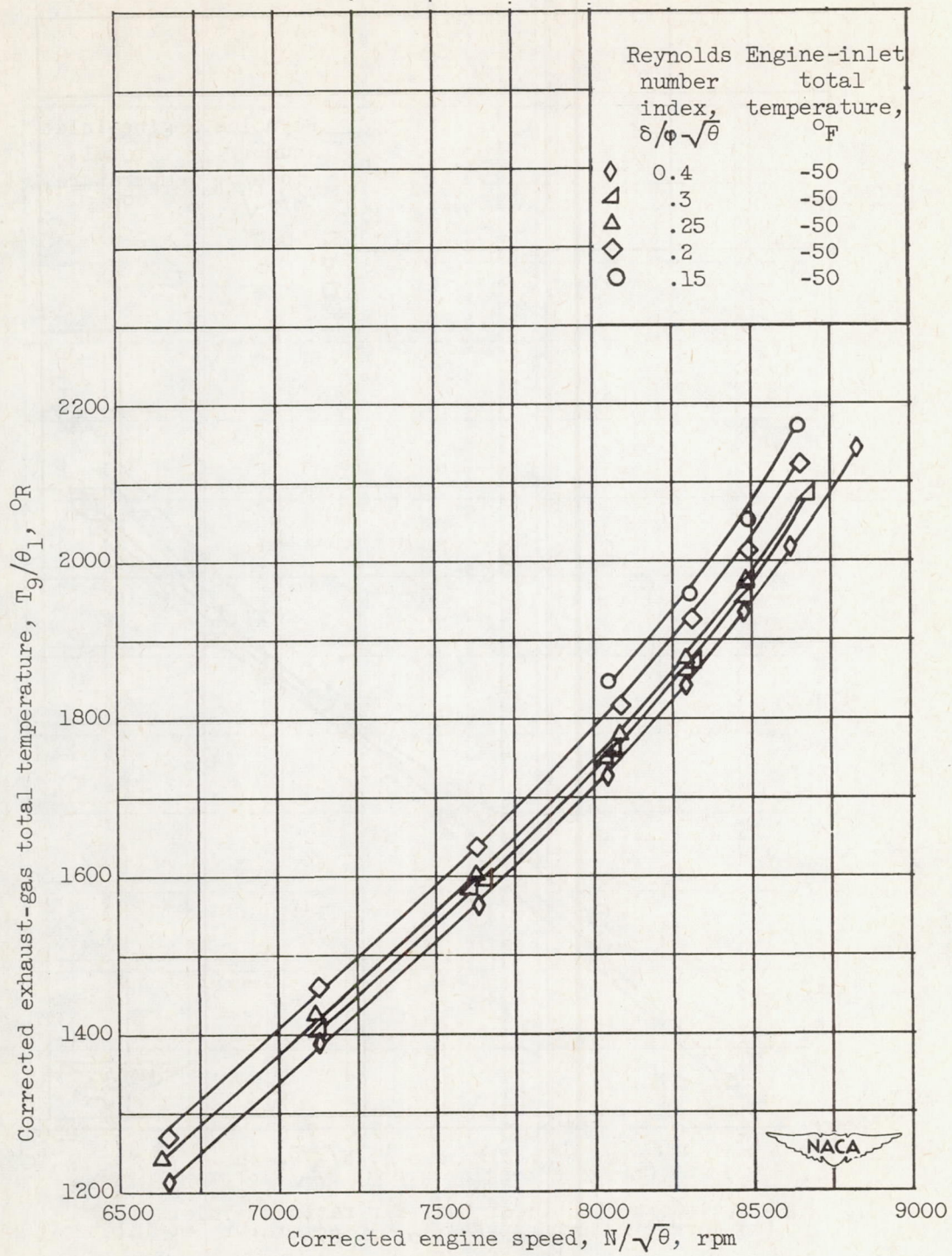
(b) Corrected exhaust-gas total temperature at inlet
temperature of -50° F.

Figure 14. - Continued. Effect of Reynolds number index on
over-all engine performance.
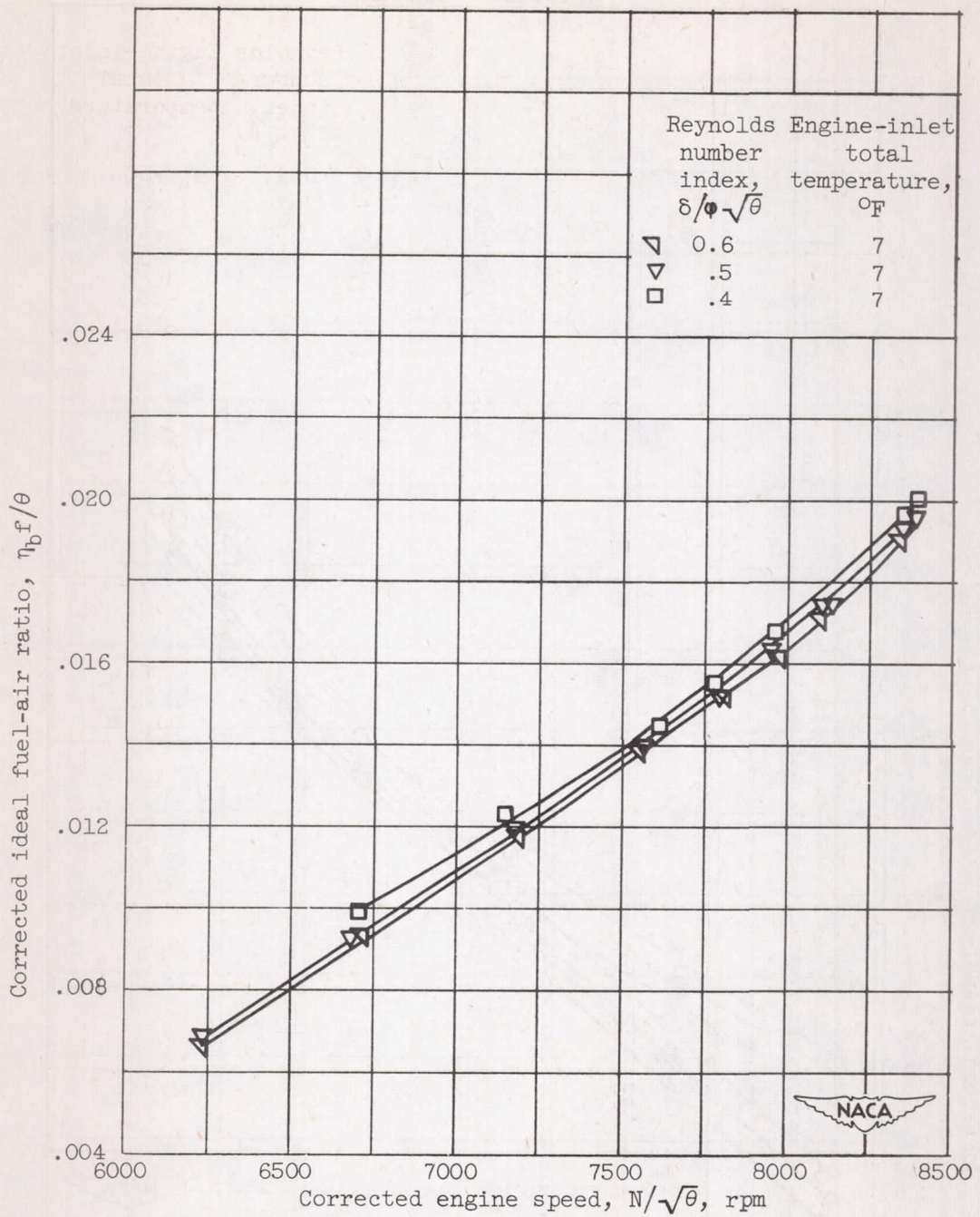
2717

(c) Corrected ideal fuel-air ratio at inlet
temperature of 7° F.

Figure 14. - Continued. Effect of Reynolds number index on
over-all engine performance.
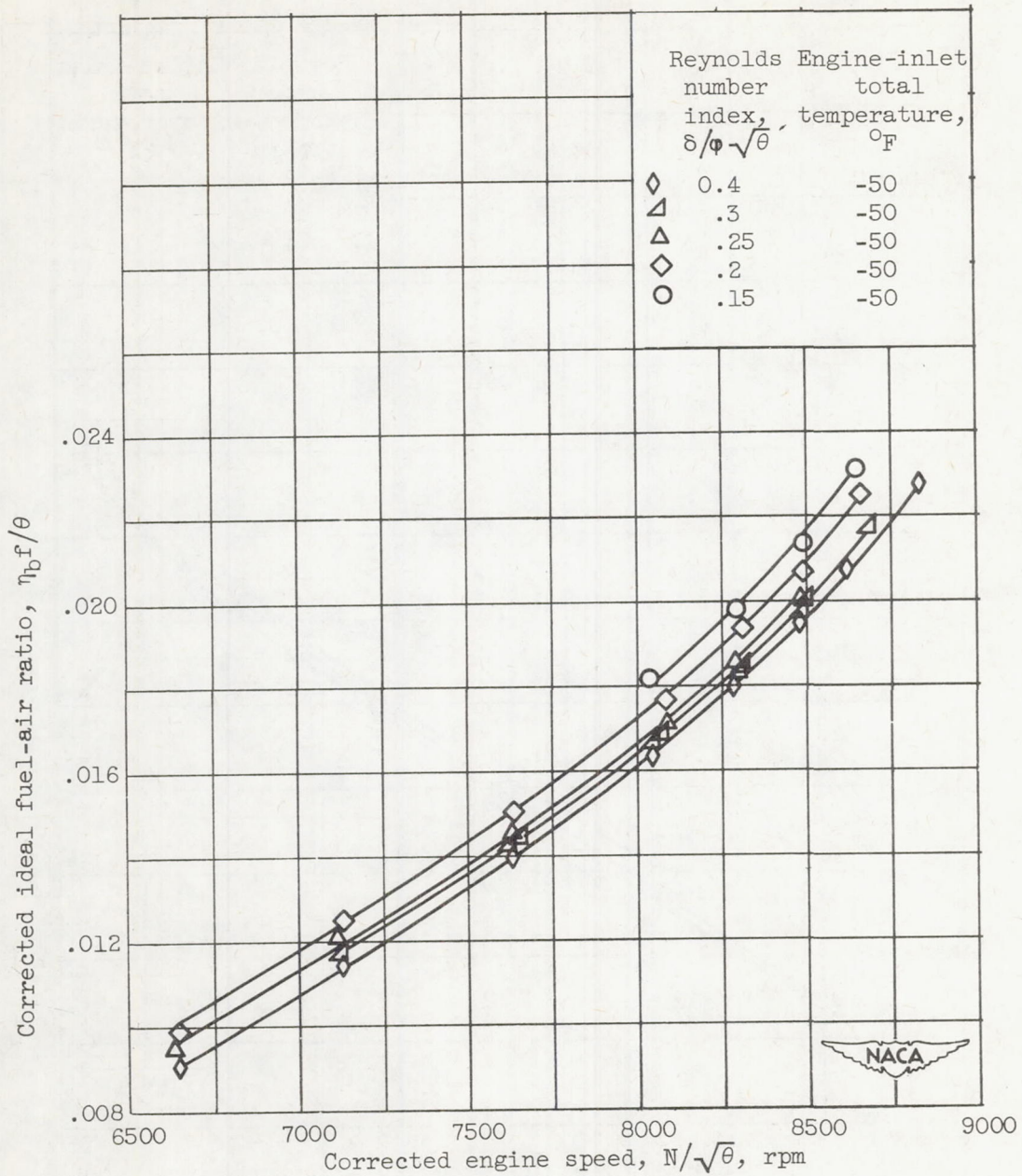
(d) Corrected ideal fuel-air ratio at inlet
temperature of -50° F.

Figure 14. - Continued. Effect of Reynolds number index on
over-all engine performance.
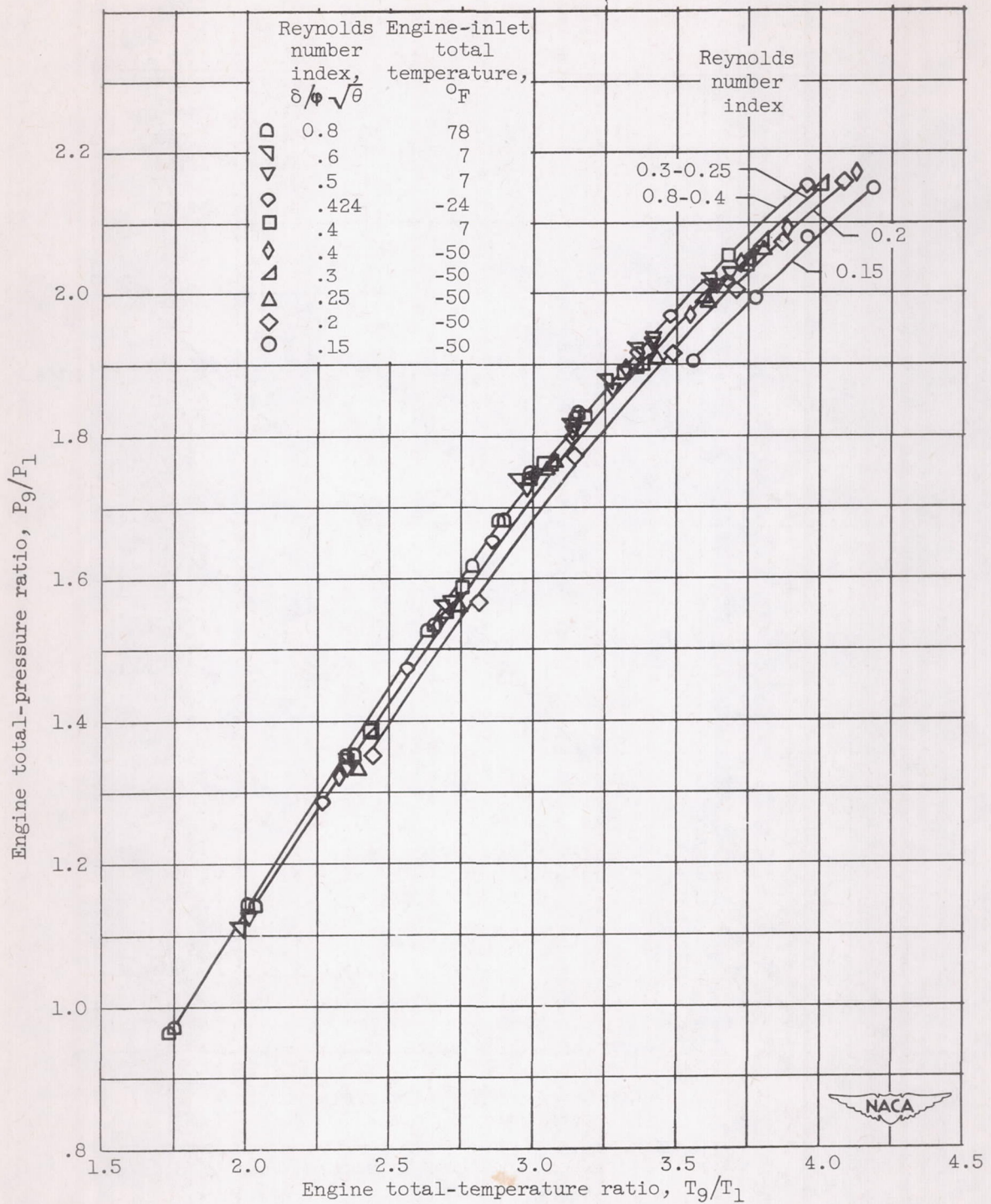
(e) Engine pumping characteristics.

Figure 14. - Continued. Effect of Reynolds number index on over-all
engine performance.
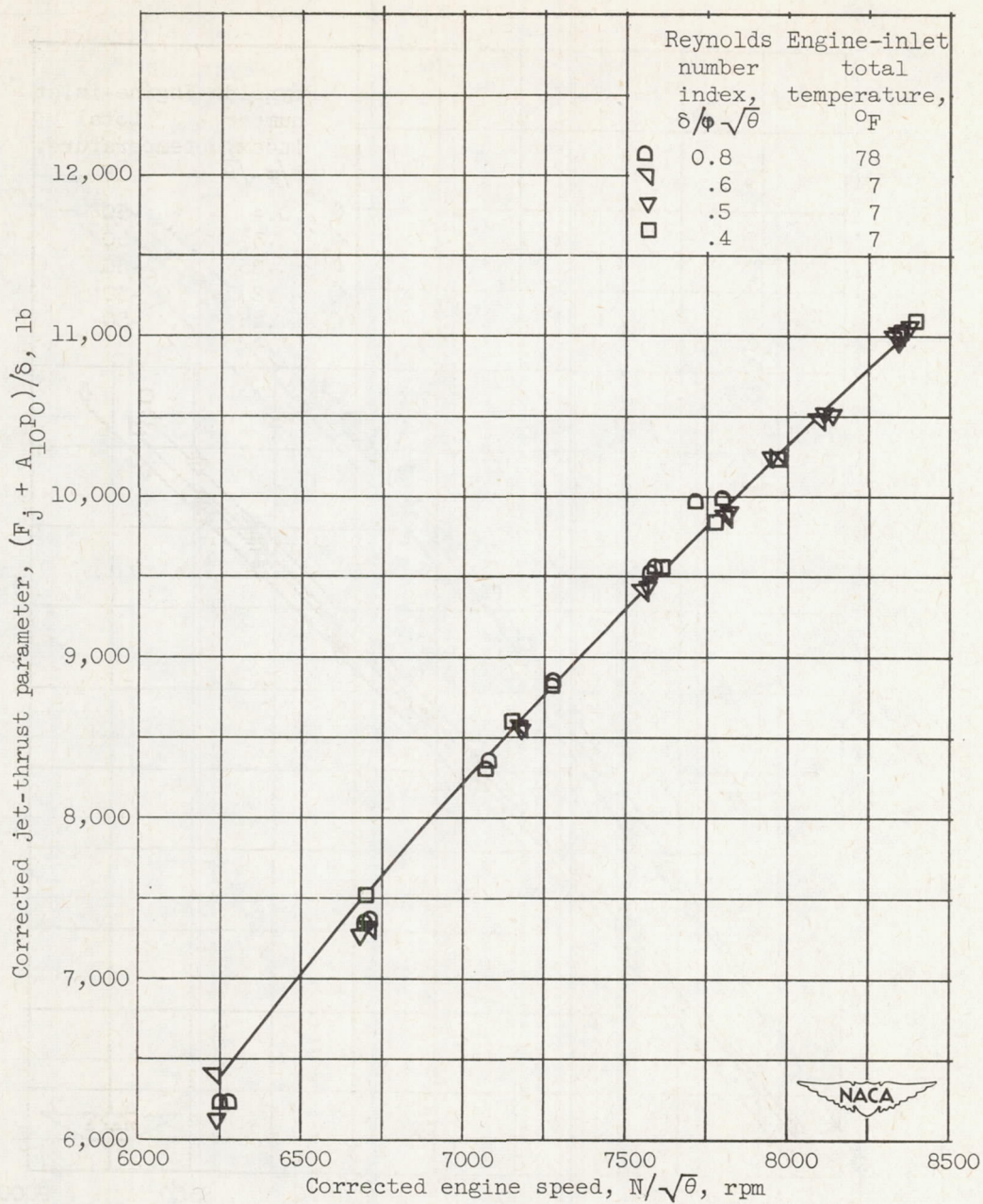
(f) Corrected jet-thrust parameter at inlet
temperatures of 7° and 78° F.

Figure 14. - Continued.   Effect of Reynolds number index on over-all
engine performance.
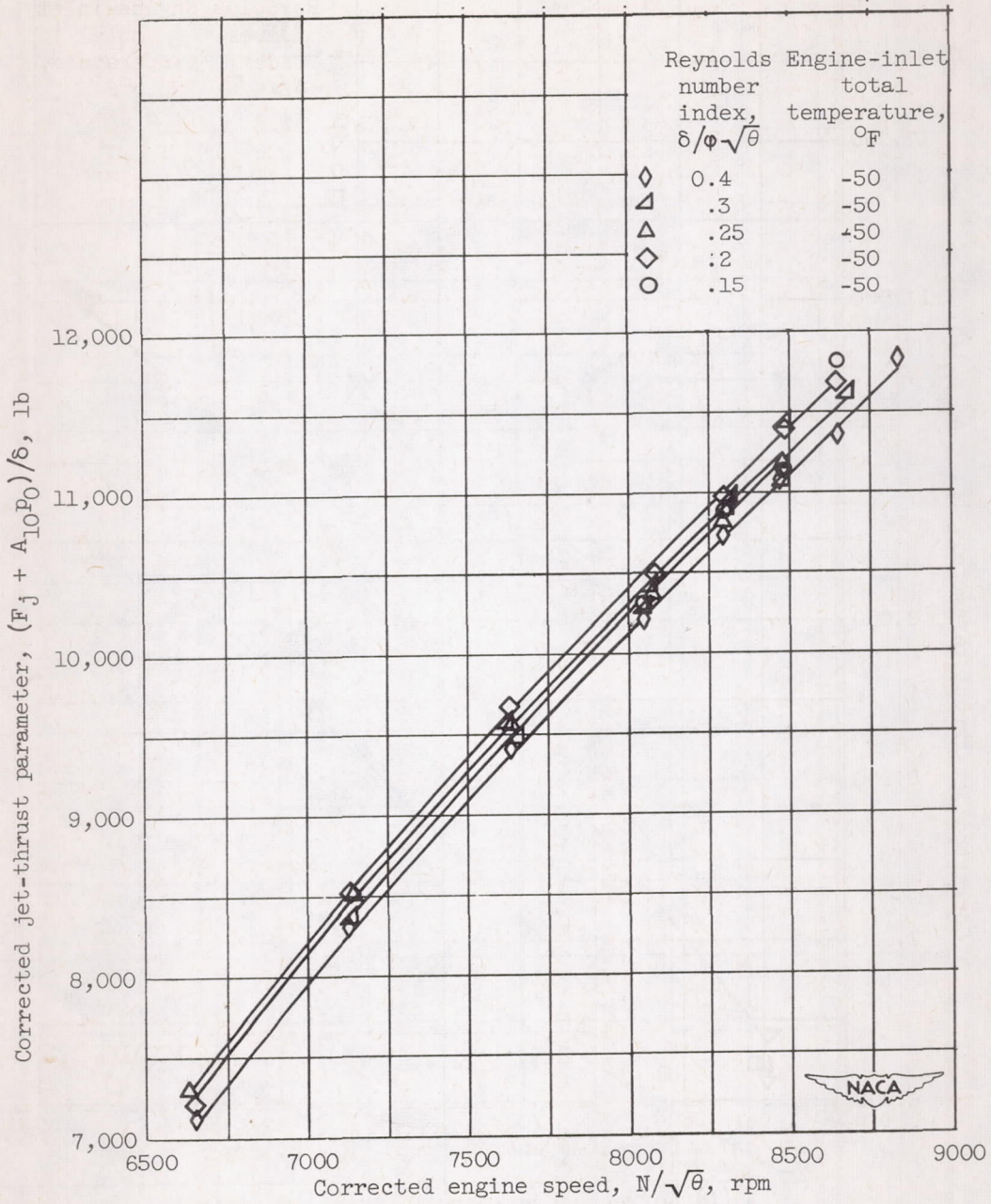
(g) Corrected jet-thrust parameter at inlet
temperature of -50° F.

Figure 14. - Concluded. Effect of Reynolds number index on over-all
engine performance.
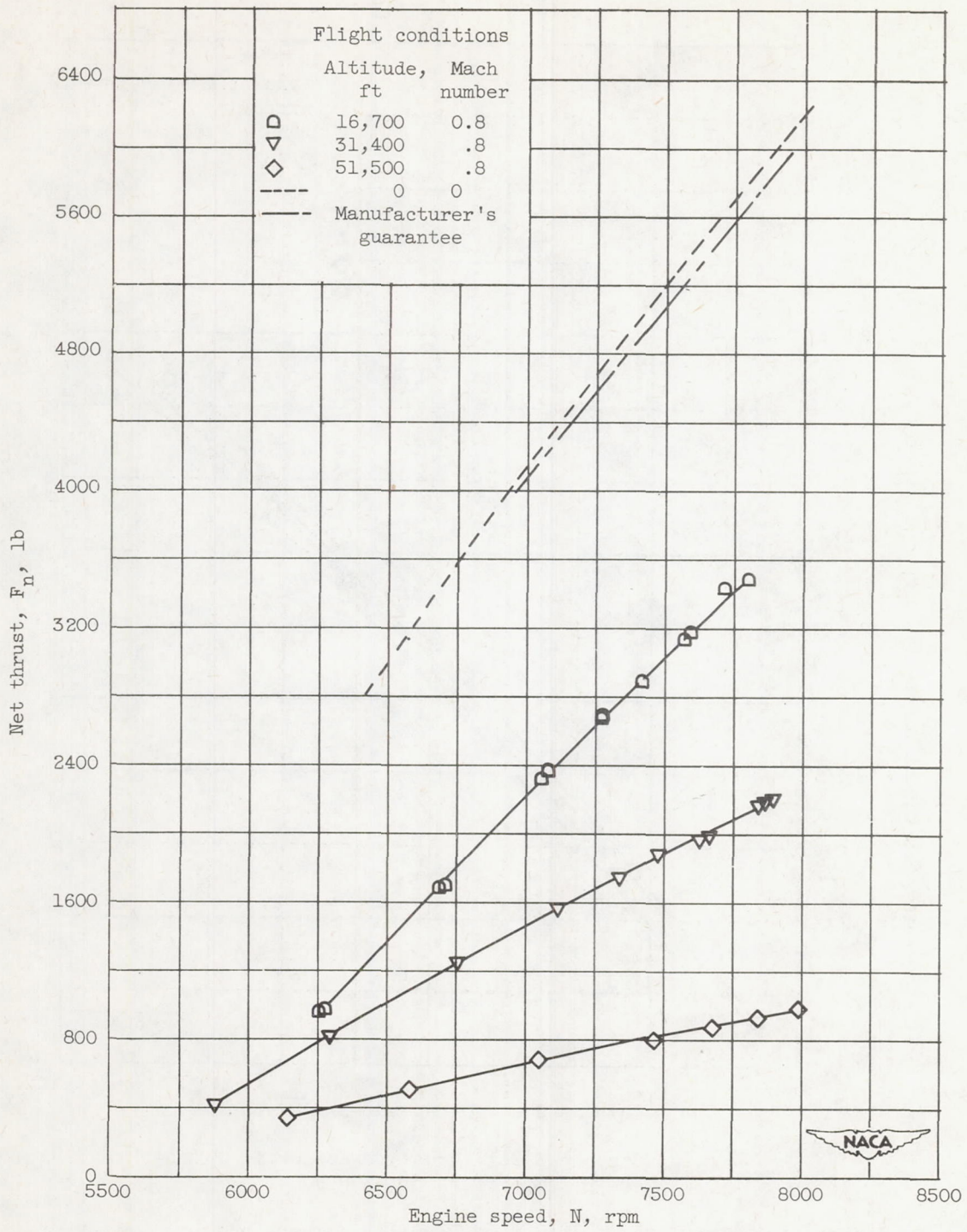
(a) Net thrust.

Figure 15. - Effect of varying altitude on net thrust and net-thrust
specific fuel consumption.
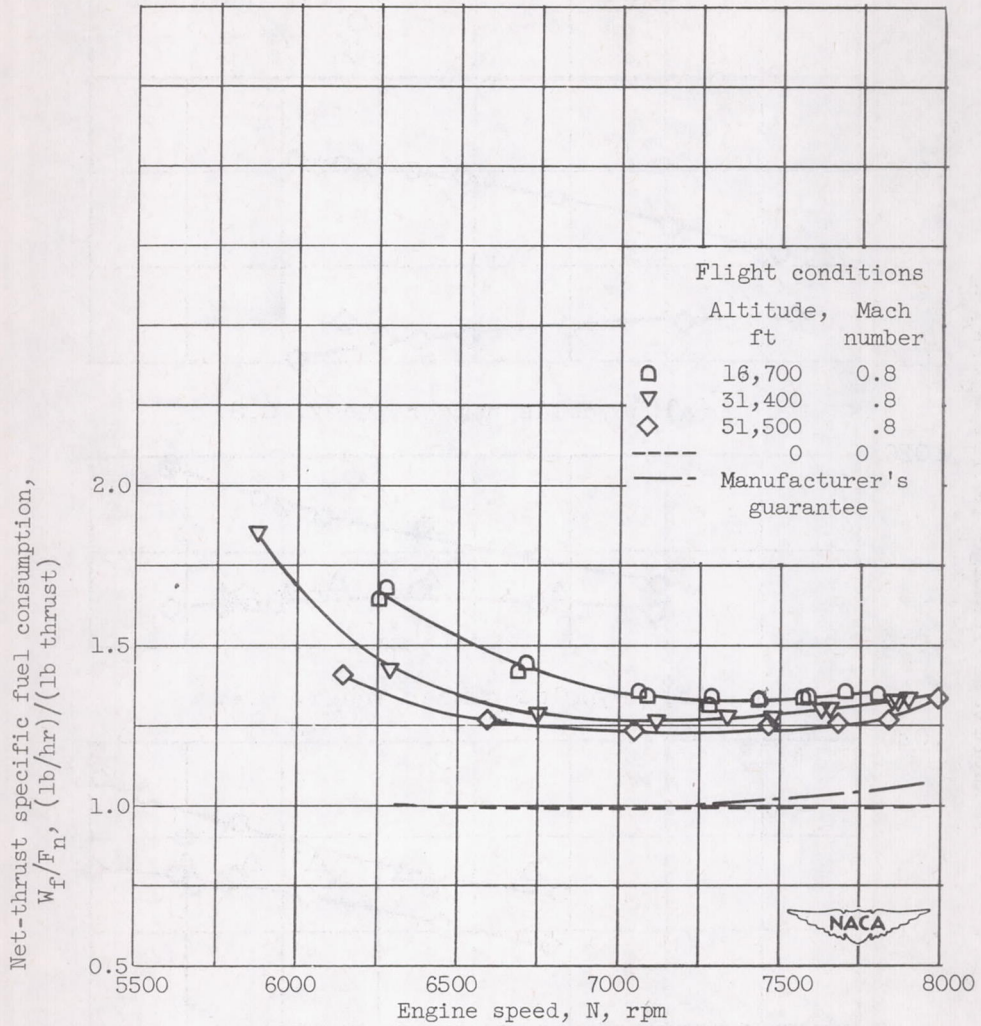
(b) Net-thrust specific fuel consumption.

Figure 15. - Concluded. Effect of varying altitude on net thrust
and net-thrust specific fuel consumption.

(a) Reynolds number index, 0.8.

(b) Reynolds number index, 0.4.

(c) Reynolds number index, 0.2.
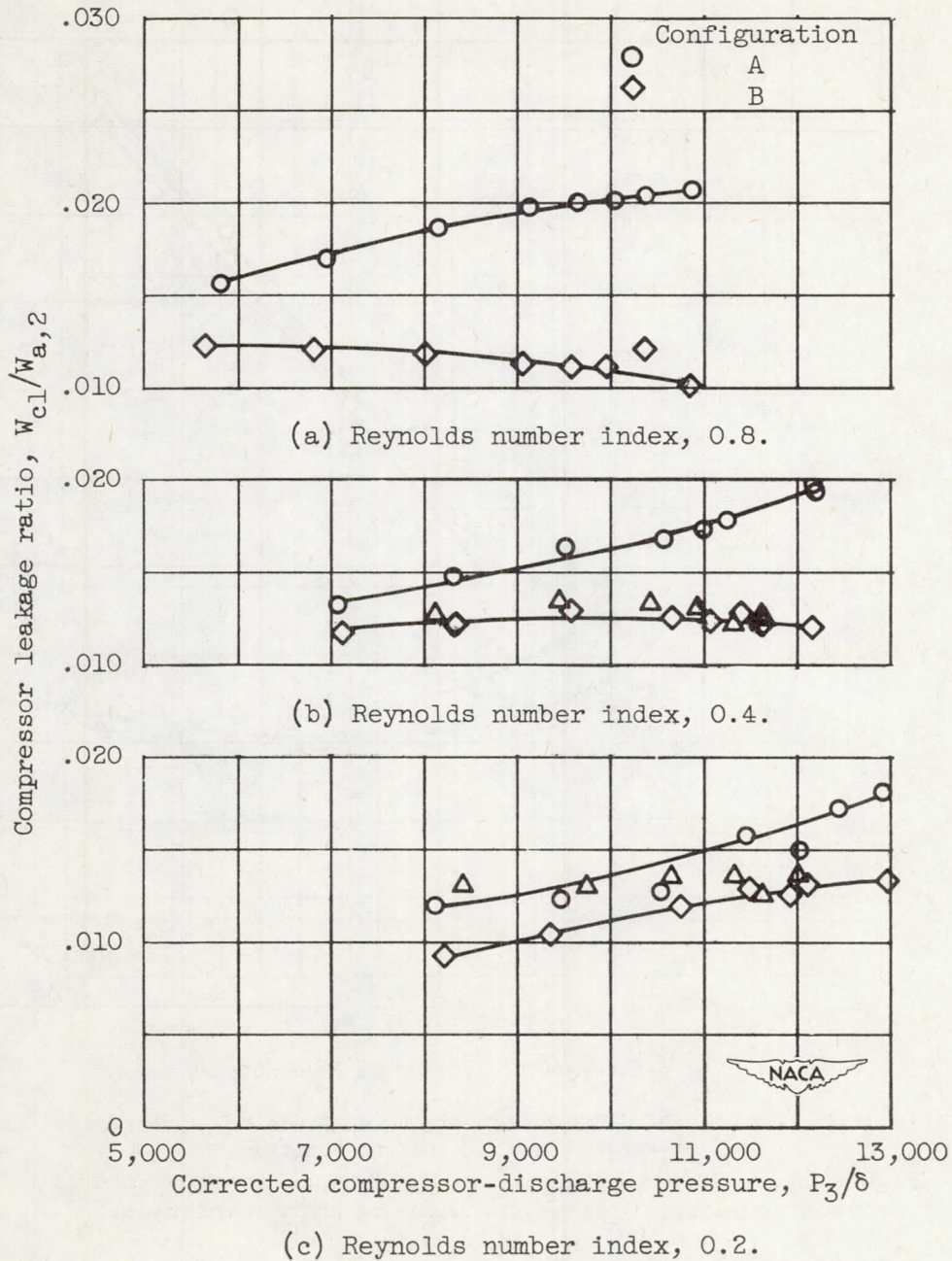
Figure 16. - Effect of improved twelfth-stage seal on
compressor leakage air flow.
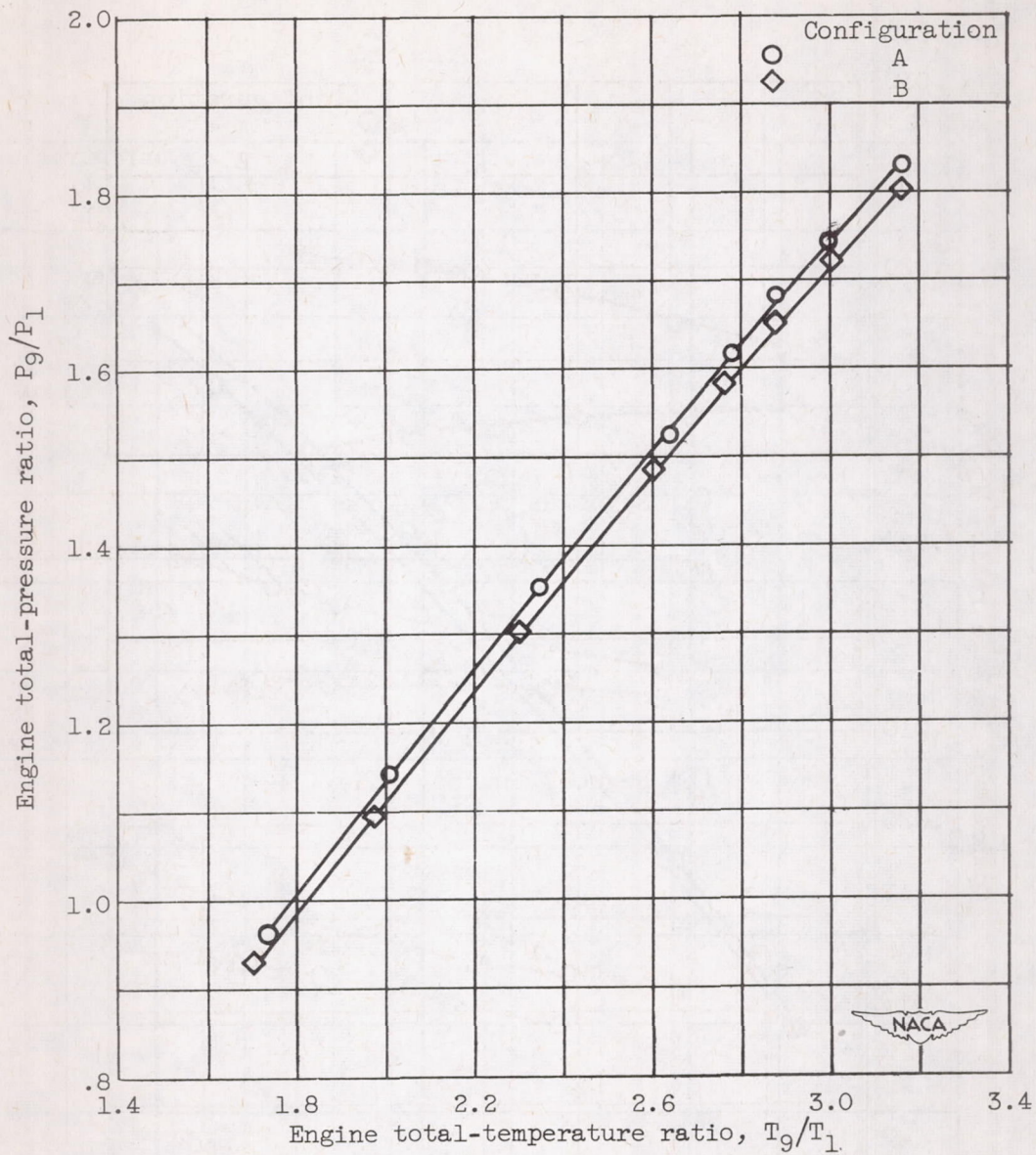
(a) Reynolds number index, 0.8.

Figure 17. - Effect of design modifications incorporated in
configuration B on engine pumping characteristics.
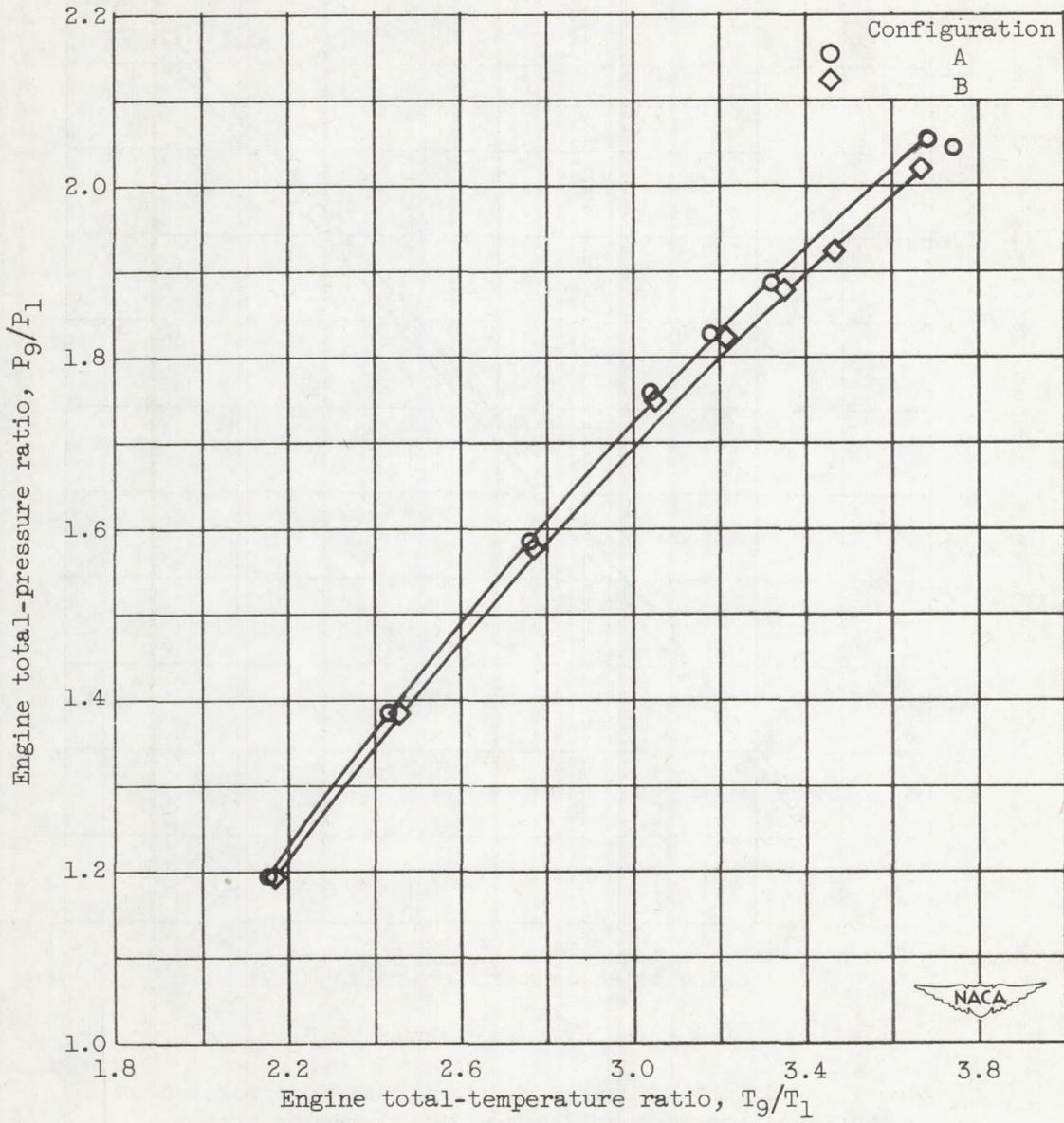
(b) Reynolds number index, 0.4.

Figure 17. - Continued. Effect of design modifications incorporated
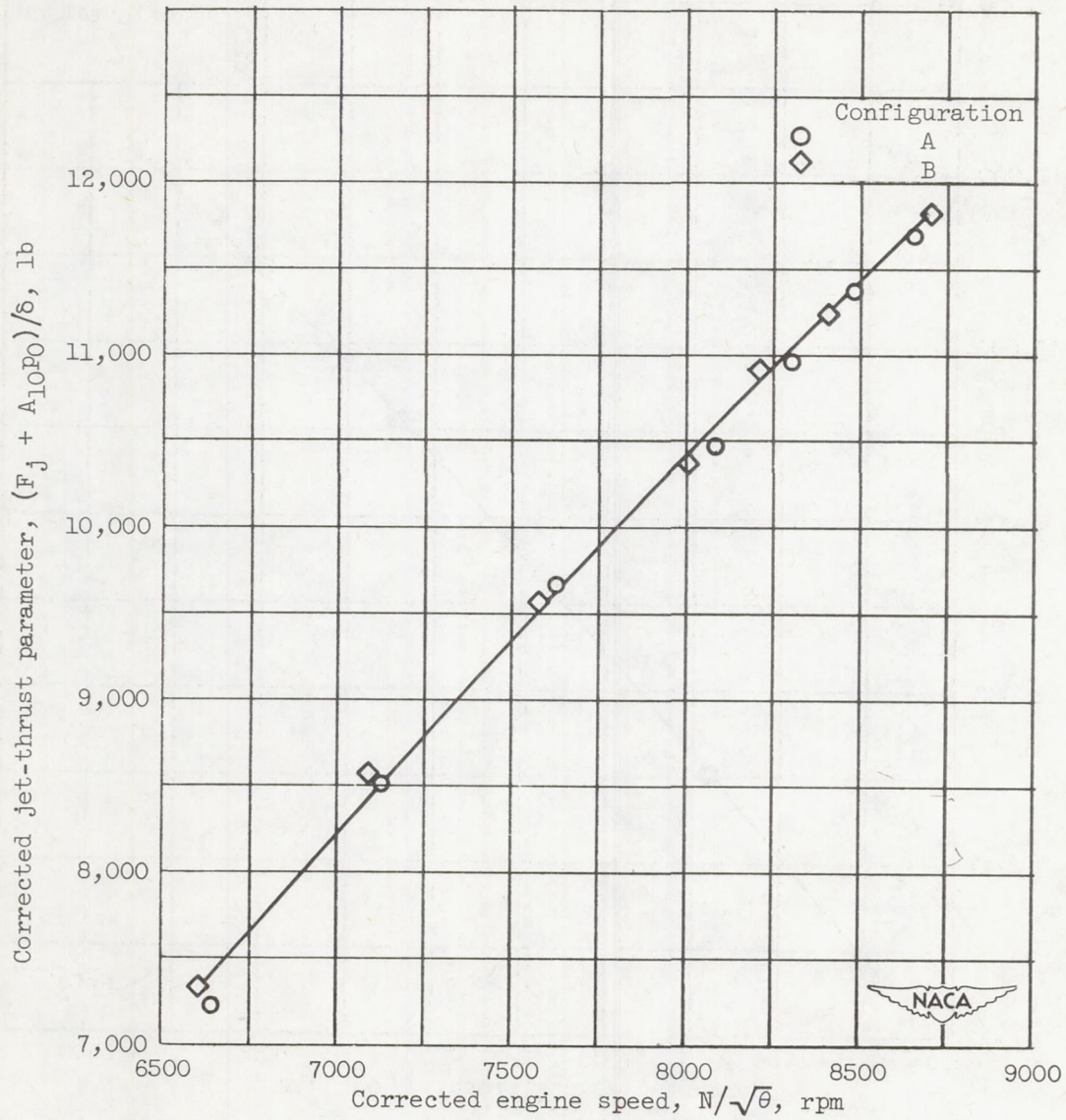in configuration B on engine pumping characteristics.
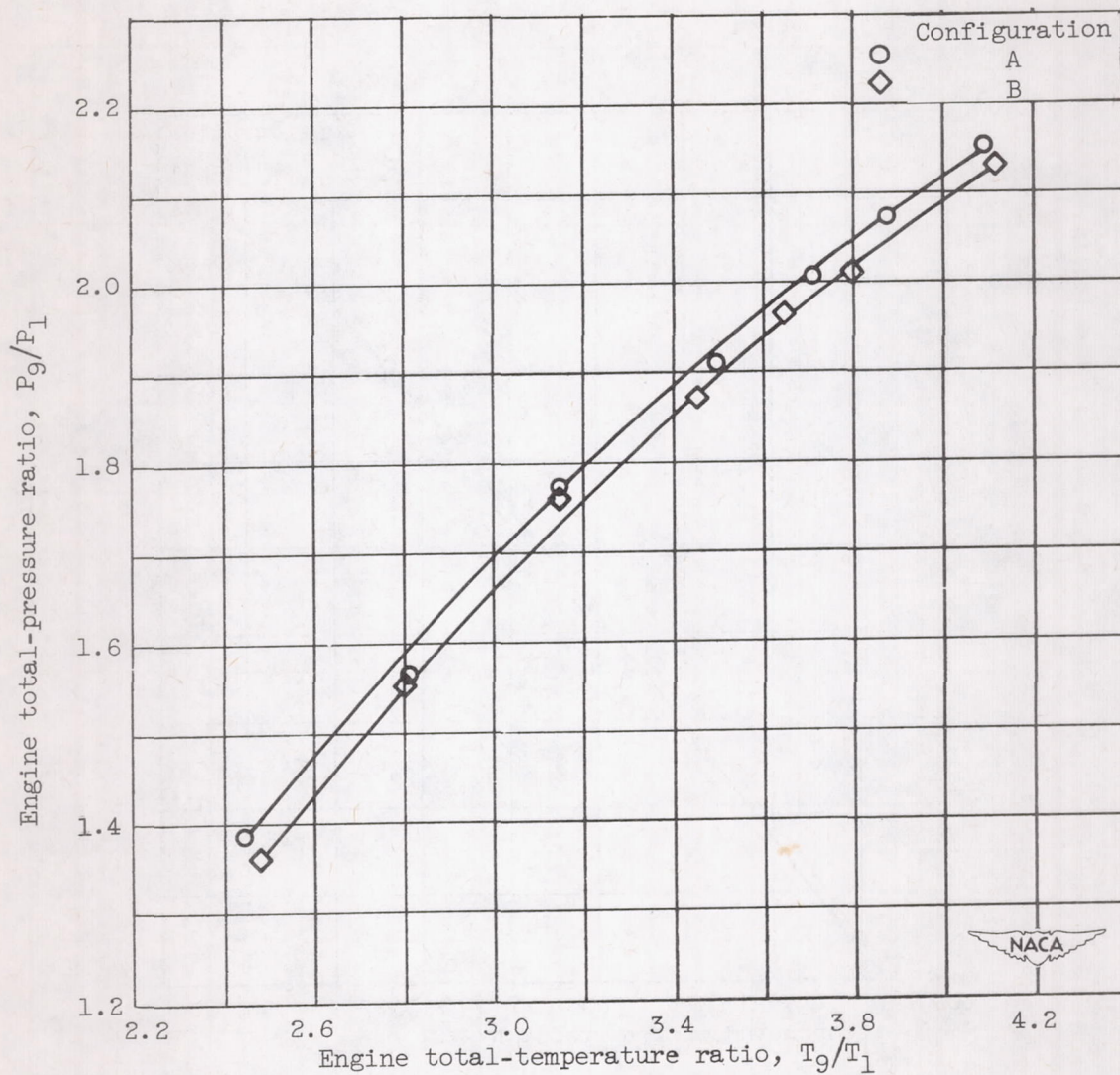
(c) Reynolds number index, 0.2.

Figure 17. - Concluded. Effect of design modifications incorporated
in configuration B on engine pumping characteristics.
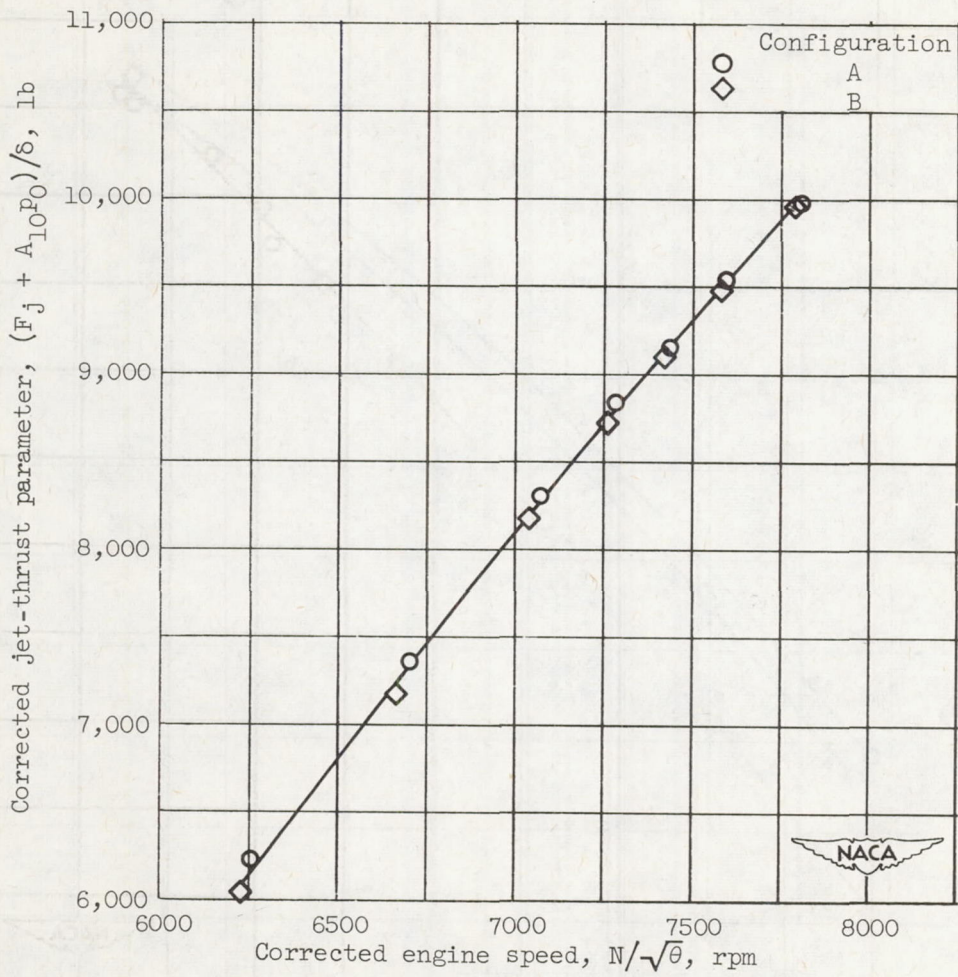
(a) Reynolds number index, 0.8.

Figure 18. - Effect of design modifications incorporated
in configuration B on jet-thrust parameter.
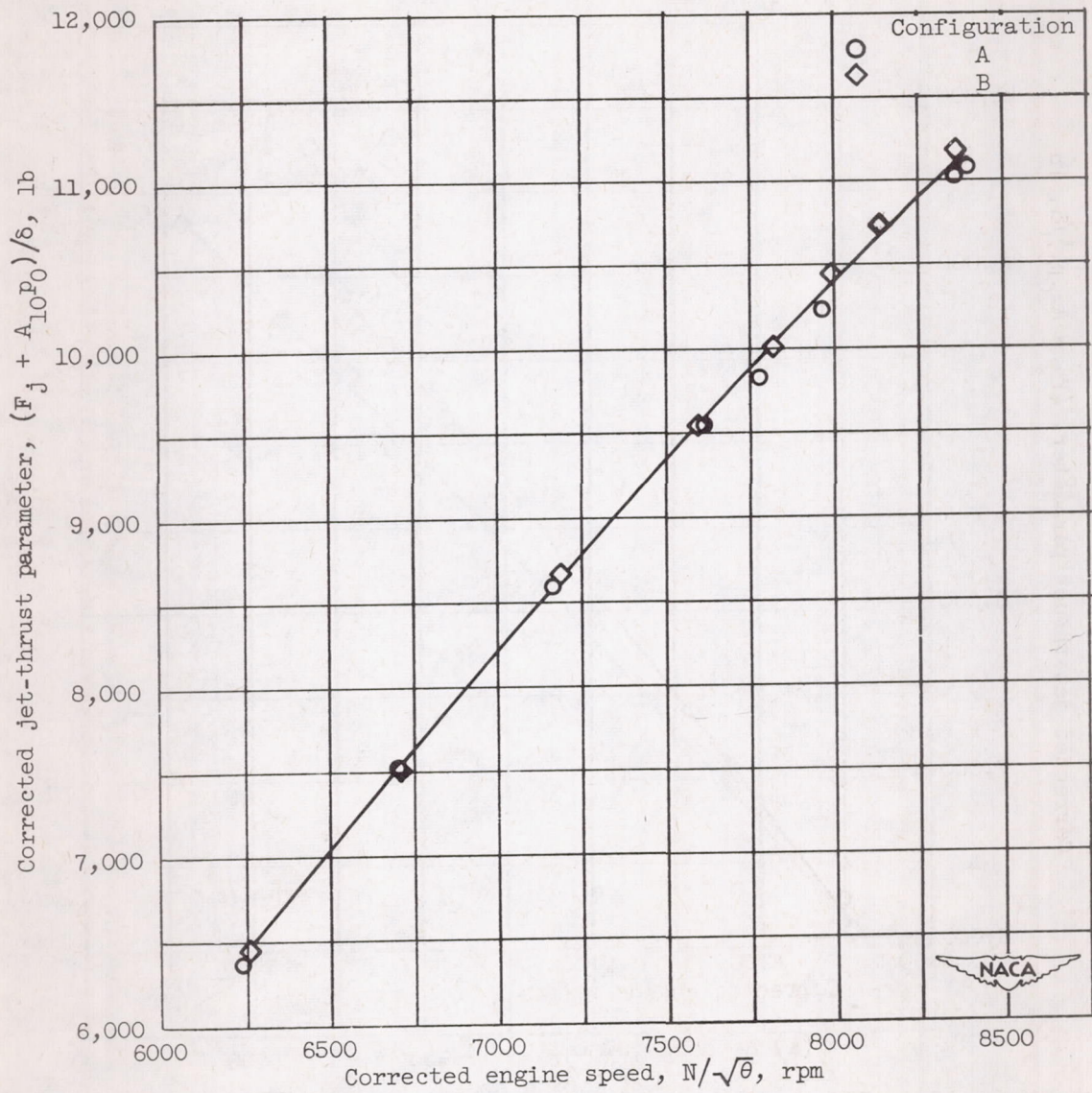
(b) Reynolds number index, 0.4.

Figure 18. - Continued. Effect of design modifications incorporated in configuration B on jet-thrust parameter.

(c) Reynolds number index, 0.2.

Figure 18. - Concluded. Effect of design modifications incorporated
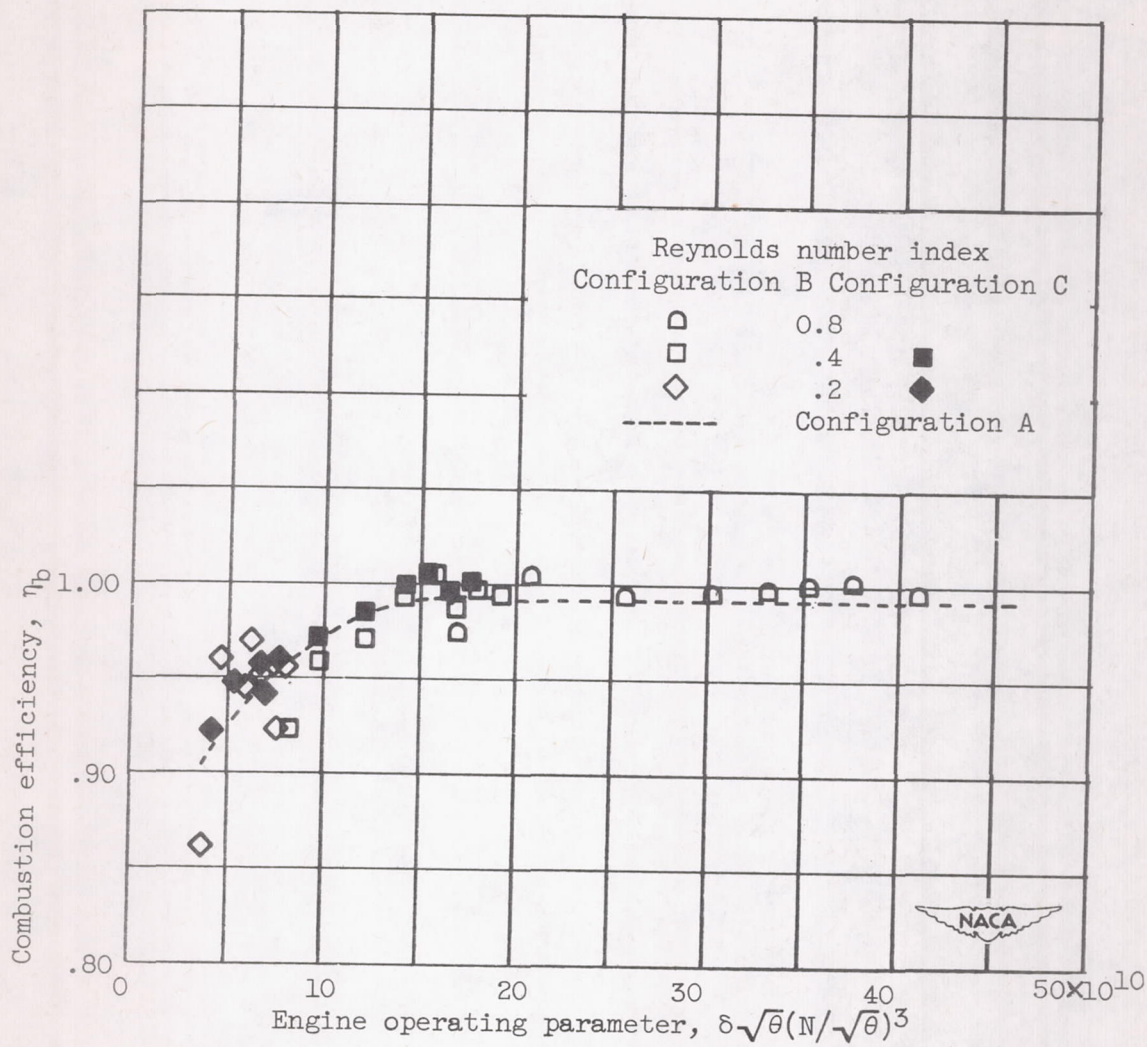in configuration B on jet-thrust parameter.

NACA RM E52L16

Figure 19. - Effect of design modifications incorporated
in configurations B and C on combustion efficiency.